ADVISORY GROUP FOR AERONAUTICAL
RESEARCH AND DEVELOPMENT

REPORT 256

EFFECTS OF UNIT REYNOLDS NUMBER, NOSE BLUNTNESS, AND ROUGHNESS ON BOUNDARY LAYER TRANSITION

by

J. L. POTTER and J. D. WHITFIELD

APRIL 1960

NORTH ATLANTIC TREATY ORGANISATION
64 RUE DE VARENNE, PARIS VII

REPORT 256

NORTH ATLANTIC TREATY ORGANIZATION

ADVISORY GROUP FOR AERONAUTICAL RESEARCH AND DEVELOPMENT

EFFECTS OF UNIT REYNOLDS NUMBER, NOSE BLUNTNESS, AND ROUGHNESS ON BOUNDARY LAYER TRANSITION

by

J. Leith Potter and Jack D. Whitfield

This Report is one in the Series 253-284 of papers presented at the Boundary Layer Research Meeting of the AGARD Fluid Dynamics Panel held from 25-29 April 1960, in London, England

SUMMARY

Conditions encountered in the high Mach number flow regime are shown to profoundly affect the longitudinal extent of the boundary layer from beginning to end of transition, the distribution of fluctuation energy in the laminar layer, and the effectiveness of surface roughness in promoting transition.

A critical layer of intense local energy fluctuations was found at all Mach numbers studied. The existence of such a critical layer is predicted by stability theory. Hot-wire surveys of the laminar, transitional, and turbulent boundary layers are presented to illustrate the critical layer in laminar flow and the subsequent development into the transition process.

The relation between boundary layer transition on flat plates and cones in supersonic flow is explored and a process for correcting data to account for leading edge bluntness is devised. On the basis of a comparison of data corrected for the effects of leading-edge geometry, it is shown that the Reynolds number of transition on a cone is three times that on a vanishingly thin flat plate. Close agreement between data from various wind tunnels is demonstrated. Study of the effect of finite leading edges yields significant illustrations of the influence of unit Reynolds number on boundary layer transition. It is found that this influence is not entirely associated with leading-edge bluntness.

A correlation of the effects of surface roughness on transition is achieved. This treatment includes two- and three-dimensional roughness in both subsonic and supersonic streams. At this time only zero pressure gradients have been studied. The entire range of movement of transition from its position with no roughness up to its reaching the roughness element is describable by the procedure given. Examples of application of the correlation results show excellent agreement with experimental data from a variety of sources. Implications concerning tripping hypersonic boundary layers are discussed.

3b2c2c: 3b2c1a3

532.526.3

SOMMAIRE

Il est démontré que les conditions rencontrées dans l'écoulement à des nombres de Mach élevés ont une influence considérable sur l'étendue longitudinale de la couche limite, du commencement jusqu'à la fin de la transition, sur la répartition de l'énergie de fluctuation dans la couche limite, et sur l'efficacité de la rugosité pour donner lieu à la transition.

Une couche critique de fortes fluctuations d'énergie locale a été constatée pour tous les nombres de Mach étudiés. D'après la théorie de la stabilité une telle couche critique se laisse prédire. Des études de la couche limite laminaire, transitionnelle, et turbulente effectuées à l'aide de fils chauds sont présentées en vue de mettre en évidence la couche critique en écoulement laminaire, avec l'évolution ultérieure du processus de la transition.

Le rapport entre la transition de la couche limite sur des plaques planes et sur des cônes en écoulement supersonique est considéré et une méthode est élaborée permettant de corriger les résultats obtenus pour tenir compte de l'émoussement du bord d'attaque. Sur la base d'une comparaison de résultats corrigés pour tenir compte de l'influence de la géométrie du bord d'attaque, il est démontré que le nombre de Reynolds dans le cas d'un cône est trois fois plus élevé que celui pour une plaque plane mince à s'évanouir. Il existe une concordance étroite entre les résultats obtenus dans diverses souffleries. L'étude de l'influence des bords d'attaque finis fournit des exemples signifiants quant à l'influence exercée par le nombre de Reynolds unitaire sur la transition de la couche limite. Il a été constaté que cette influence n'est pas entierèment liée à l'émoussement du bord d'attaque.

Une corrélation des effets de la rugosité sur la transition a été réalisée, portant sur la rugosité bi-et tridiemensionnelle, aussi bien dans un écoulement subsonique que dans un écoulement supersonique. Seuls les gradients nuls ont été examinés. L'évolution entière de la transition depuis le point où il ne se trouve pas d'aspérité jusqu'au moment d'atteindre l'aspérité se laisse décrire par la procédure indiquée. Des exemples d'application des résultats de la corrélation montrent une correspondance excellente avec les résultats expérimentaux provenant de sources différentes. Sont traitées, en conclusion, les implications concernant l'action des rugosités dans les couches limites hypersoniques.

CONTENTS

	Page
SUMMARY	ii
SOMMAIRE	iii
LIST OF FIGURES	v
NOTATION	vii
1. INTRODUCTION	1
2. EXPERIMENTAL APPARATUS AND TECHNIQUES	2
2.1 Wind Tunnels	2
2.2 Models	3
2.2.1 3-in Diameter Hollow Cylinder (Fig.1)	3
2.2.2 6-in Diameter Hollow Cylinder (Fig.2)	3
2.3 Instrumentation	3
3. THE TRANSITION PROCESS	4
3.1 Definition of the Transition Region	4
3.2 Methods of Transition Detection	5
3.3 Transition Data and Extent of Transition Region	7
3.4 Distribution of Fluctuations and the Critical Layer	8
4. THE EFFECT OF LEADING EDGE GEOMETRY	9
5. THE EFFECT OF SURFACE ROUGHNESS	13
6. CONCLUDING REMARKS	21
ACKNOWLEDGMENTS	22
REFERENCES	23
TABLE 1	26
FIGURES	27
DISTRIBUTION	

LIST OF FIGURES

		Page
Fig. 1	Three-inch diameter, hollow cylinder model	27
Fig. 2	Six-inch diameter, hollow cylinder model	28
Fig. 3	Typical measurements of boundary layer growth	29
Fig. 4	Analysis of spark Schlieren photographs	30
Fig. 5	Isolines of hot-wire output, $\tilde{e^2}$, in X - Y plane	31
Fig. 6	Comparison of methods of transition detection for $M_\infty = 3.5$	32
Fig. 7	Comparison of methods of transition detection for $M_\infty = 5$	33
Fig. 8	Similarity of transition region	34
Fig. 9	Transition results at $M_\infty = 3$ for b = 0.003 inch and b = 0.008 inch	35
Fig. 10	Transition results at $M_\infty = 3.5$ for b = 0.003 inch and b = 0.008 inch	36
Fig. 11	Transition results at $M_\infty = 4$ for b = 0.003 inch and b = 0.008 inch	37
Fig. 12	Transition results at $M_\infty = 4.5$ for b = 0.003 inch and b = 0.008 inch	38
Fig. 13	Transition results at $M_\infty = 5$ for b = 0.003 inch and b = 0.008 inch	39
Fig. 14	Transition results at $M_\infty = 8$ for b = 0.002 inch	40
Fig. 15	Influence of Mach number on transition Reynolds number for U_∞/ν_∞ = 280,000 per inch	41
Fig. 16	Reynolds numbers of the transition region	42
Fig. 17	Comparison of Isolines of hot-wire output for b = 0.003 inch and b = 0.008 inch at $M_\infty = 5$	43
Fig. 18	Hot-wire output near leading edge for b = 0.003 inch and $M_\infty = 5$	44
Fig. 19	Critical layer height as a function of Mach number	45

Page

Fig. 20 Hot-wire output in boundary layer of a smooth-nose body of revolutions 46

Fig. 21 Comparison of hot-wire outputs with and without surface roughness 47

Fig. 22 Unit Reynolds number influence for various bluntness Reynolds numbers 48

Fig. 23 Transition Reynolds number increase due to bluntness Reynolds number increase 49

Fig. 24 Comparison of Brinich and Sands' data and VKF data 50

Fig. 25 Influence of bevel angle with Mach number as a parameter 51

Fig. 26 Influence of bevel angle with bluntness Reynolds number as a parameter 52

Fig. 27 Unit Reynolds number effect for various Mach numbers as $Re_b \rightarrow 0$ 53

Fig. 28 Comparison of estimated and measured transition Reynolds numbers for $M_\infty \simeq 3$ 54

Fig. 29 Comparison of transition data from various wind tunnels and comparison of flat plate and cone transition data 55

Fig. 30 Effective Reynolds numbers of roughness 56

Fig. 31 Correlation of data for single wires on flat plates, $M_\delta \rightarrow 0$, Reference 29 57

Fig. 32 Correlation of data for single row of spheres on flat plates, $M_\delta \rightarrow 0$, Reference 26 58

Fig. 33 Correlation of data for single wires on hollow cylinders, $M_\delta = 3.12$, Reference 36 59

Fig. 34 Correlation of data for single wires on hollow cylinders, $M_\delta = 3.0 - 4.5$, VKF data 60

Fig. 35 Correlation of data for band of grit on flat plate, $M_\delta = 3.0$, Reference 37 (Table 1a) 61

Fig. 36 Correlation of data for single row of spheres on cones, $M_\delta = 1.9 - 3.67$, Reference 24 62

Fig. 37 Correlation of data for single row of spheres on hollow cylinders, $M_\delta = 3.0 - 5.0$, VKF data 63

Page

Fig. 38 Faired correlation curves for single wires on bodies with zero pressure gradient 64

Fig. 39 Faired correlation curves for two types of three-dimensional elements (as noted) on bodies with zero pressure gradient 65

Fig. 40a Application of correlation-wires on cylinders 66

Fig. 40b Application of correlation-wires on cylinders 66

Fig. 40c Application of correlation-wires on plates 67

Fig. 41a Application of correlation-spheres on plates 67

Fig. 41b Application of correlation-spheres on cylinders and cones 68

Fig. 42 An illustration of the increase in roughness size required at hypersonic speeds 68

NOTATION

a	speed of sound
b	leading-edge thickness (Figures 1, 2)
C_D, C_{DW}	see Equation 14
$\tilde{c}_f$	ratio of local skin friction coefficient at beginning of interaction between roughness and boundary layer to the coefficient at a Reynolds number of 10^6
$\tilde{e^2}$	mean-square hot-wire output, arbitrary units
K	constant (see Table 1)
k	height of roughness element
M	Mach number
n	exponent in Equation 9
p	pressure
P_0'	Pitot pressure
Re	Reynolds number

Re_b	$(U/\nu)_\infty b$
Re_k	$U_k k/\nu_k$ (Equation 10)
Re_k^*	$a^* k/\nu^*$ (Equation 12)
Re_k'	$Re_k (M_p/M_k)(p_p/p_\delta)(T_k/T_w)^{0.5 + \omega}$ (Equation 17)
Re_t	Reynolds number of transition
$(Re_t)_{end}$	Reynolds number at onset of fully developed turbulent flow (see Figure 3)
Re_{to}	Reynolds number of transition on a body with no surface roughness
Re_{X_k}	$U_\delta X_k/\nu_\delta$
$Re_{\Delta X}$	$(U/\nu)_\infty \Delta X$
T	temperature
U	velocity
X	longitudinal, wetted distance along surface
ΔX	longitudinal extent of transition region
Y	vertical distance above surface
γ	ratio of specific heats of air
δ	total boundary layer thickness
δ^*	boundary layer displacement thickness
η_r	temperature recovery factor, $= (T_w - T_\delta)/(T_0 - T_\delta)$
τ_j, τ_j'	see Equation 13
θ	bevel angle of lower leading edge (see Figures 1 and 2)
Λ	Pohlhausen parameter
μ	dynamic viscosity of air
ν	kinematic viscosity, μ/ρ
ρ	mass density
ω	exponent in viscosity-temperature relation

Subscripts

c	critical
k	at height k in undisturbed, laminar boundary layer at station X_k
o	stagnation conditions
p	plateau value in region of roughness element
t	at transition
w	body surface
δ	edge of boundary layer
∞	free stream

Superscripts

*	sonic condition

EFFECTS OF UNIT REYNOLDS NUMBER, NOSE BLUNTNESS, AND ROUGHNESS ON BOUNDARY LAYER TRANSITION

J. Leith Potter and Jack D. Whitfield*

1. INTRODUCTION

Among the many interesting and significant incidents in the history of aerodynamics related by Professor von Kármán in his book 'Aerodynamics' [1] is the story of the discovery that transition from laminar to turbulent boundary layer flow accounts for the great reduction in drag coefficient of a sphere at high Reynolds numbers. Subsequent demonstrations of the significance of transition location are abundant, and the aerodynamicist has learned to respect the importance of that factor.

The effects of transition are of special concern to those who are engaged in testing scale models in simulated environments. To appreciate this, one only has to observe typical examples wherein a shift of the location of transition equal to one body diameter caused a thirty per cent change in base pressure, or where a dynamically unstable model was transformed into a state of dynamic stability by adding a boundary layer trip. Therefore, the experimenters in wind tunnels have to investigate factors affecting boundary layer transition and the behavior of aerodynamic quantities which are sensitive to transition location. Progress in this research is essential to the improvement of even routine model tests. We know now that the greatly increased extent of laminar flow likely to be encountered under conditions prevailing at hypersonic Mach numbers causes this subject to assume added importance.

There is no need to dwell on the adversities encountered in experiments designed to yield useful, general results pertaining to transition. However, our experience at the von Kármán Gas Dynamics Facility shows that boundary layer transition is a remarkably consistent and repeatable phenomenon if extraneous factors are rigorously hunted and eliminated. This repeatability even extends to hot-wire anemometer records of mean fluctuation energies throughout transition regions. It also is evident that one frequently cannot deal with transition-sensitive data by choosing some convenient Reynolds number as a correlation parameter. Quite often the physical location of transition is the dominant variable, while the value of Reynolds number is relatively insignificant unless it accurately reflects transition location (cf. Chapman, Kuehn, and Larson[2] or Potter, Whitfield, and Strike[3]).

It is the purpose of this paper to furnish a report of an investigation concerning certain factors affecting transition. Objectives of the investigation were to further clarify the effects of unit Reynolds number and very small degrees of leading edge bluntness and to devise a means for estimating the effect of roughness on boundary layer transition.

The unit Reynolds number, or Reynolds number per unit length, has been singled out as a factor in boundary layer transition because of plentiful evidence that the

---

* *von Kármán Gas Dynamics Facility, ARO, Inc., U.S.A.*

commonly used forms of Reynolds number of transition generally vary with the unit Reynolds number. This occurs in subsonic and supersonic streams, in free flight and in wind tunnels. It is obvious that part of this is due to the relation between unit Reynolds number and roughness, leading edge bluntness, and possibly wind tunnel turbulence. However, it is not clear that there is no more significance to this factor (cf. Whitfield and Potter[4]).

Even small degrees of nose bluntness having negligible effect on measured pressure distributions have a noticeable effect on boundary layer transition. Therefore, if one is to compare data from different models or if one wishes to make practical use of this phenomenon, some general quantitative evaluation is needed.

The urgent requirement for some reliable method for estimating the effect of both two- and three-dimensional roughness at supersonic speeds is recognized. However, it may not be widely known that the problem is far more acute when hypersonic Mach numbers are concerned. It is probably true that fully developed turbulent boundary layers never have been attained on models in some existing hypersonic and hypervelocity test facilities. Of course, this is partly due to the fact that high Mach and Reynolds numbers seldom are attained simultaneously in a wind tunnel.

We will discuss each of these problems in following sections.

2. EXPERIMENTAL APPARATUS AND TECHNIQUES

2.1 Wind Tunnels

The 12 by 12-in. supersonic wind tunnel and the 50-in. diameter hypersonic wind tunnel of the von Kármán Gas Dynamics Facility (VKF) were utilized for the experimental phase of this study.

The 12 by 12-in. supersonic tunnel[5] is equipped with a flexible plate nozzle, which can be positioned within the Mach number range of 1.5 to 5. The Mach number range from 3 to 5 was used in the present study. Although normally used only as an intermittent wind tunnel, special arrangements were made during a portion of the experimental work to permit use of the main compressor plant of the VKF and thus achieve continuous-flow operation. This was necessary during the measurements of surface temperature distributions in order to assure thermal equilibrium. Stagnation pressures from sub-atmospheric to 60 lb/in^2 absolute were available. The air was furnished from an electrically heated, high pressure storage bottle and the stagnation temperature varied from approximately 80 to 120°F, depending on the test Mach number. However, stagnation temperature was nearly constant for any one tunnel run. Air dryness was maintained at approximately 0.8×10^{-4} lb of water per lb of air. The 3-in. diameter model was mounted in a flow field uniform in Mach number to ±0.02.

The 50-in. diameter, continuous-flow hypersonic tunnel is equipped with a Mach number 8, contoured, axisymmetric nozzle. Stagnation pressure from 60 to 800 lb/in^2 absolute were available and the stagnation temperature was maintained at about 900°F, sufficient to avoid air liquefaction. The wind tunnel is further described in Reference 6. The 6-in. diameter hollow cylinder was mounted in a flow yield which was uniform in Mach number to about ±0.3%. Because of changes in boundary layer thickness

due to changing pressure level, the average Mach number varied from about 8.0 at a stagnation pressure of 100 lb/in^2 absolute to about 8.1 at a stagnation pressure of 800 lb/in^2 absolute.

2.2 Models

The basic models were hollow cylinders, with measurements being accomplished on the exterior surface. Two sizes were required; a 3-in. diameter cylinder was used in the 12-in. tunnel and a 6-in. diameter cylinder was used in the 50-in. diameter tunnel. The interior surface finish of all models was about 20 micro-inches root mean square (rms).

2.2.1 3-in Diameter Hollow Cylinder (Fig. 1)

This cylinder was constructed of laminated Fiberglas and epoxy resin over a stainless steel, tubular core. Twenty-one surface thermo-couples and three static pressure tubes were imbedded in the Fiberglas resin skin. A surface finish of 10 to 15 micro-inches rms was obtained on the epoxy resin surface. Four interchangeable noses with an internal angle of 6 deg and with leading edge thicnesses of 0.0015, 0.003, 0.005, and 0.008 in. were tested.

2.2.2 6-in Diameter Hollow Cylinders (Fig. 2)

Two models, an instrumented cylinder and a non-instrumented cylinder, were constructed for the hypersonic experiments. The non-instrumented model was constructed of stainless steel and had a surface finish of 10 micro-inches rms. The instrumented model was constructed with 41 surface thermocouples and 12 static pressure tubes imbedded in hot-sprayed aluminum oxide. The relative porosity of the aluminum oxide makes an accurate estimate of the surface finish difficult. Conventional machine-shop practice will produce readings of 100 to 200 micro-inches rms. However, comparisons of transition locations on the two cylinders agree, indicating the instrumented cylinder to be aerodynamically smooth at Mach number 8.

This model was tested with a leading edge thickness of 0.002 in. and with an internal bevel angle of 11.5 deg.

2.3 Instrumentation

The hot-wire equipment was developed by Kovasznay at Johns Hopkins University and is described in Reference 7. Minor modifications have been made in attempts to improve the signal-to-noise ratio and to permit the automatic recording of data.

Hot-wire surveys of the boundary layer from the laminar region to fully developed turbulent flow were made at selected test conditions. The hot-wire is, of course, sensitive to a combination of variables (velocity, density, and temperature) and the relative sensitivity to fluctuations of these quantities changes as the mean flow changes.

The simplest types of surveys were accomplished by maintaining the hot-wire at a constant current and traversing the wire longitudinally at constant vertical distance above the model surface. This was repeated at various heights. These are referred

to as the 'constant current' traces and were used to construct the isolines of constant hot-wire output presented herein.

The second, and more time-consuming, method consisted of positioning the wire at a given X position and taking data from the hot-wire for several wire currents at each Y position. The sensitivity variations of the wire could then be approximated and the data corrected accordingly. This latter method, referred to as constant temperature, was used only within laminar flow regions. The qualitative distribution of fluctuations within the laminar boundary layer is comparable for the two techniques at moderate wire temperatures, approximately 250^{o}F (see Figure 20). It was found in certain low-density flow conditions that the constant current operation produced an excessive wire temperature as the hot-wire traversed the lower portion of the boundary layer and hence underwent large changes in sensitivity. The constant temperature method was used under such low density conditions.

The hot-wires used in this study were 0.00015-in. diameter and 0.0003-in. diameter by 0.10-in. long tungsten wires for operation to Mach number 5. The Mach number 8 testing was accomplished with platinum-coated tungsten wires of 0.0003-in. diameter and 0.10 in. length. Successful operation with the latter wires in the higher temperature Mach 8 flow was accomplished at moderate wire temperatures (about 1000^{o}F). The general use of these wires in high temperature flow is not recommended since an irreversible resistance rise occurred above 1000^{o}F. Other wire materials are currently being studied to find a wire suitable for higher temperatures.

The surface temperatures, schlieren photographs, and the boundary layer pressure profiles were obtained with conventional wind tunnel instrumentation. The total-head pressure variation along the surface was obtained from a 0.02-in. high by 0.04-in. wide elliptically shaped total-head tube mounted against the surface in such a manner as to allow it to slide on the model surface. This tube was connected to a pressure transducer mounted directly to the probe holder.

3. THE TRANSITION PROCESS

3.1 Definition of the Transition Region

It is well known that transition of the boundary layer from laminar to fully developed turbulent flow occurs over a distance of many boundary layer thicknesses. In a strict sense, then, the concept of a transition point is ambiguous. However, it is common practice to adopt some definition of transition point for purposes of analysis, and it has been shown[3] that the influence of transition on certain transition-sensitive quantities can be accurately evaluated using an effective location which approximates the middle of the transition zone. Experimental studies of various factors influencing the transition process may be accomplished with an arbitrary, but consistent, definition of transition location provided that similarity of the mean transition process is retained.

One of the initial objectives of this research was to examine similarity of the transition region while under the influence of various factors. This was accomplished by examining the relationship between several methods of transition detection and the complete transition region.

Boundary layer growth was used here to define the transition region as shown in the accompanying diagram.

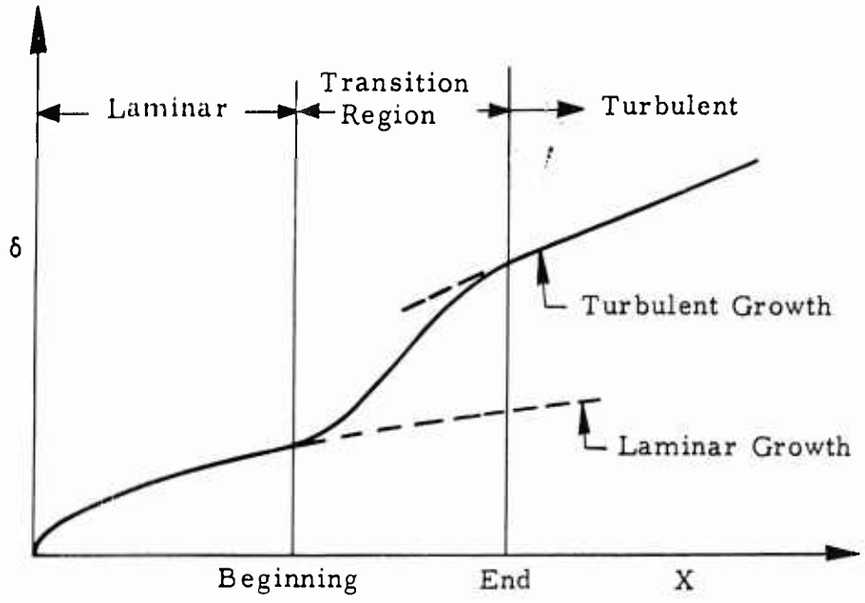

The *beginning of transition* was taken as the point of initial, measurable deviation of the boundary layer thickness from a laminar rate of growth. Such a point is not well defined since it is located by seeking small deviations from an already somewhat arbitrarily defined quantity, boundary layer thickness, δ. Fortunately, it will be seen that this is not a critical point. The *end of transition* was defined as the point where a fully developed turbulent profile was obtained.

3.2 Methods of Transition Detection

The five methods used to detect transition were: (1) change in rate of boundary layer growth, (2) average visual indication from schlieren photographs, (3) maximum surface temperature location, (4) location of maximum output from a hot-wire traversed near the surface, and (5) location of maximum pressure from a total-head tube traversed along the model surface.

The boundary layer growth was obtained from the mean hot-wire resistance variations and from boundary layer pressure profiles. The hot-wire technique consisted of observing the increase in mean hot-wire resistance as the hot-wire entered the boundary layer and thus locating the edge of the boundary layer. Typical measurements of the boundary layer growth are shown in Figure 3 with the previously defined beginning and end of transition noted.

The average schlieren indications of transition were obtained from a numerical average of locations read from a large number (10 to 40) of schlieren photographs taken at each test condition. A typical analysis of these photographs is shown in Figure 4. This analysis is based on 36 spark schlieren photographs. It is apparent

that a large deviation from the average indication may exist in a given photograph. It should be noted that these photographs were taken with a conventional wind-tunnel schlieren system using a spark of short duration, approximately 0.5 microseconds. The data spread obtained from these photographs is due, in a large part, to the uncertainty in reading the photographs and should not be interpreted as a measure of the oscillation of the transition region.

Relatively early in our use of the hot-wire anemometer to detect transition, it became apparent that the transition region was not characterized by a sudden and violent onset of fluctuations but was rather an orderly, developing process which appeared to originate at or near the leading edge. The hot-wire was used to survey the entire boundary layer flow field. Most of these surveys were taken with a wire operated at a constant current. These data are presented here in terms of isoline diagrams of constant hot-wire output, $\widetilde{e^2}$, which is the mean-square signal from the hot-wire equipment. Such a diagram for $M_\infty = 3.5$ is shown in Figure 5. An electronic squaring circuit developed by Kovasznay[7] was used to obtain this mean signal. The 'noise' noted here and in later figures refers to the electronic noise of the hot-wire equipment. The locations shown for the 'noise' level correspond to the condition where the hot-wire signal and electronic noise are approximately equal. These diagrams are very interesting because of the pictorial representations of the transition process. One obvious and salient feature is the relatively intense stratification of fluctuations observed in the laminar region and the early portion of the transition region. The existence of this 'critical layer,' which is indicated by stability theory[8,9], is well known in regard to incompressible flow from the work of Schubauer and Skramstad[10] and has been observed in supersonic flow by Laufer and Vrebalovich[11] and Demetriades[12]. However, these earlier experiments were concerned only with studies of laminar instability so none of the earlier data enabled comparison of the magnitude of fluctuations in the laminar region and those in the transition region. The fact that these disturbances are of the same order injects considerable complication into the interpretation of a transition 'point' from hot-wire traverses at heights above the surface.

In Figure 5 we observe that a maximum hot-wire output from $Y \to 0$ can be located with reasonable precision. The measurement of surface temperature distributions on the same model revealed that this maximum hot-wire signal near the surface corresponds to the maximum surface temperature, as noted in Figure 5. Comparisons of the various methods of detection are shown in Figure 6 for $M_\infty = 3.5$. It may be observed that the similarity between the maximum hot-wire signal and the maximum surface temperature extends into the fully developed turbulent region where the hot-wire signal and the surface temperature become substantially constant. Similar measurements for $M_\infty = 5$ are shown in Figure 7. The same relative relation exists between all the various methods of transition detection.

The similarity of the transition region of variable leading edge bluntness, variable unit Reynolds number, and variable Mach number can be examined by considering the corresponding behavior of the different methods of transition detection. Such a comparison is shown in Figure 8. These data indicate reasonable similarity when the precision of such methods is considered.

3.3 Transition Data and Extent of Transition Region

Measurements of transition locations by the previously described methods are presented in Figures 9 - 13 for two leading edge thicknesses, b = 0.003 in and 0.008 in, for M_∞ = 3 to 5. Figure 14 is presented for b = 0.002 in and M_∞ = 8. These data permit us to study the extent of the transition region as influenced by the variables present.

Determination of transition location by means of wall temperature distribution always corresponded to a condition of equilibrium wall temperature at all Mach numbers. However, since it was very inconvenient to establish this condition for all testing, transition locations determined by other methods in the M_∞ = 3-5 range correspond to slightly non-equilibrium heat transfer conditions. At Mach numbers of 3 to 5, the wall temperature was 0-7% greater than its adiabatic recovery value, and tests indicated no discernible effect on transition location. At Mach number 8, radiation from model to surroundings apparently established an equilibrium wall temperature less than adiabatic recovery. The ratio T_W/T_∞ was ten, whereas the theoretical adiabatic recovery value would have been twelve.

The influence of Mach number on the magnitude of the transition Reynolds number and the extent of the transition region are presented in Figure 15. The tendency of transition Reynolds numbers to increase with increasing Mach number (U/ν constant) in the hypersonic regime has been observed before, but the magnitude of the increase is perhaps surprising.

A study of these data indicates that the transition region, when defined in terms of a transition zone Reynolds number ($Re_{\Delta X} = U_\infty \Delta X/\nu_\infty$), is fairly independent of unit Reynolds number and leading edge geometry. That is,

$$Re_{\Delta X} = f(Re_t, M_\infty) \tag{1}$$

as shown in Figure 16. The transition zone Reynolds number, $Re_{\Delta X}$, is presented versus Reynolds number based on distance to the end-of-transition, $(Re_t)_{end}$, because of the better experimental definition of the end as compared to the beginning of transition at supersonic and hypersonic speeds. Also included in Figure 16 are subsonic data from Silverstein and Becker[13], Schubauer and Skramstad[10], Bennett[14], Feindt[15] and Smith[16]. These subsonic data include data taken under the influence of pressure gradients and varying turbulence levels in the free stream, yet they seem to fit in very well. The supersonic data are all Coles's flat plate data[17] or the hollow cylinders of the present study. Although a significant increase in $Re_{\Delta X}$ is associated with increasing Mach number, the rate of increase of ΔX with Mach number is not as great as the rate of increase in the boundary layer thickness. Or, based on δ at the beginning of transition, we find

$$\text{for} \quad M_\infty \simeq 0, \quad \frac{\Delta X}{\delta} \simeq 150$$

$$\text{for} \quad M_\infty \gtrsim 4, \quad \frac{\Delta X}{\delta} \simeq 80.$$

3.4 Distribution of Fluctuations and the Critical Layer

Boundary layer surveys with the hot-wire were made for several Mach numbers, unit Reynolds numbers, and leading-edge thicknesses, both with and without surface roughness. All of the surveys obtained with a smooth surface had the same characteristic pattern. The influence of a change in leading-edge thickness at $M_\infty = 5$ and $U_\infty/\nu_\infty = 280{,}000$ per inch is illustrated in Figure 17. The influence of the increased leading-edge thickness on the location and extent of the transition region may be noted; otherwise the characteristic pattern is the same.

The flow region near the leading edge and immediately downstream was studied in some detail. This work had a two-fold purpose: (a) the possibility of a leading-edge separation bubble was considered and (b) it was desired to better define the stratification of fluctuations very near the leading edge and their variation with Mach number.

Regarding the first objective, considerable time was spent in probing the leading edge vicinity with hot-wire and pressure probes. No evidence of any flow separation could be detected. It was therefore concluded that any leading-edge separation bubbles were quite small compared to probe size if they existed.

Typical results related to the second objective are presented in Figure 18. The fluctuations were found to exist quite close to the leading edge. Also evident here are the extremely sharp vertical gradients of fluctuation energy existing within the laminar boundary layer. This is seen in both the diagram of isolines of $\widetilde{e^2}$ and the cross-plot of $\widetilde{e^2}$ versus height Y. The cross-plot of hot-wire output, $\widetilde{e^2}$ versus Y, was obtained from constant current operation of the hot-wire and hence contains the effect of marked variation in sensitivity across the boundary layer. Since the sensitivity of the hot-wire to all fluctuations decreases quite rapidly as the wire is moved from the model surface towards the free stream, it can be seen that the fluctuation energy concentration in the critical layer is very pronounced. Laufer and Vrebalovich[11] have shown, in a classic experimental treatment of the stability of a supersonic laminar boundary layer, that this critical layer is the result of disturbances which have developed into a wave motion with a definite wave velocity and amplitude variation, as expected from the stability theory. A similar result has been shown by Demetriades[12] for a laminar, hypersonic boundary layer.

An interesting result of the present experimental study of the critical layer for various unit Reynolds numbers, leading-edge thicknesses, and Mach numbers is that the height of the critical layer can be represented reasonably well in terms of boundary layer thicknesses and Mach number, or

$$Y_c/\delta = f(M_\infty) \qquad (2)$$

This relationship is given by Figure 19, where the present data are compared with subsonic data from Klebanoff and Tidstrom[18] and the earlier mentioned data from Laufer and Vrebalovich and Demetriades.

The origin of the natural disturbances in the boundary layer is, of course, a question of considerable interest. The present results infer, as do the results of Laufer and Vrebalovich, that these disturbances exist all the way forward to the

leading edge. The possibility of significant leading edge separation bubbles has been eliminated. However, both of these experiments were conducted on two-dimensional models with sharp leading-edges. A brief experiment was conducted to examine the possibility that these disturbances might be produced only by the sharp two-dimensional leading edge. The front of the 3-in diameter hollow cylinder was closed with a smooth nose to form a body of revolution. This nose was constructed in the form of a cone-cylinder. The cone apex was rounded off with a spherical radius of 0.5 in tangent to the cone and the cone-cylinder junction was faired smooth with approximately a 3-in radius; thus no sharp edges existed. The results of a hot-wire survey at constant X are shown in Figure 20. The reduced local unit Reynolds numbers produced by the strong nose shock resulted in laminar flow over the available test length of this model. These surveys were taken at an aft station for easier detection of a critical layer. Evidence of a critical layer is clear.

Laufer and Vrebalovich suggested that free-stream turbulence, acting as a forcing function, causes an interaction between the shock wave and the boundary layer, and this in turn produces disturbances in the boundary layer. Having determined that the disturbances and their distribution in the boundary layer are not peculiar to very sharp leading edges nor due to separation at the leading edge, the VKF study indirectly supports their hypothesis.

Some interesting observations were made which appear to be related to the outward displacement of the critical layer. For Mach number 5, it was found that roughness elements inserted into the region of near calm in the lower portion of the laminar boundary layer produced virtually no effect on the distribution of fluctuation patterns downstream until the top of the roughness element approached the level where fluctuations were found in the boundary layer on the smooth body. This calm region of the laminar boundary layer at high supersonic speeds apparently is a region of high stability in which disturbances do not tend to be highly amplified. Of course, this also is related to the low local unit Reynolds number near the surface.

An example of surveys behind roughness elements (1/16-in diameter spheres) of a height greater than the undisturbed boundary layer thickness is shown in Figure 21. For comparison the smooth surface case also is shown. Such cases as this represent the only departures observed from the characteristic pattern of isolines shown for the smooth model. These data suggest that similarity of the natural transition process is not maintained behind large roughness elements. This, in turn, suggests that measurements should be made in a region well removed from the roughness element if it is desired to simulate turbulent flow due to natural transition. It should also be noted that large roughness elements can produce flow distortions extending outside the natural boundary layer which will persist well downstream of the roughness location. When such large roughness elements are used, the distortion of the flow external to the boundary layer may be so great as to affect quantities normally not influenced by the boundary layer. Since large roughness usually is required at locally hypersonic Mach numbers, the problem of tripping the boundary layer is particularly difficult in this flow regime.

4. THE EFFECT OF LEADING EDGE GEOMETRY

Bluntness at the leading edge of an aerodynamic body has an important effect on transition and has been studied by several investigators. Brinich and Sands[19] have

published one of the more recent experimental studies of leading edge bluntness. Their studies were conducted with a stream Mach number of 3.1.

Bertram suggested in Reference 20 that the unit Reynolds number effects (e.g., an increase in Re_t with increasing U_∞/ν_∞) in supersonic flow could be due to the finite leading edges always present. Bertram plotted Brinich's and Sands's data in the form of transition Reynolds number ($Re_t = U_\infty X_t/\nu_\infty$) versus bluntness Reynolds number ($Re_b = U_\infty b/\nu_\infty$ where b = leading edge thickness) to illustrate the similar influence of increasing U_∞/ν_∞ or increasing Re_b on the transition Reynolds number, Re_t. Examination of these plots and other data reveals a systematic behavior not accounted for by this method of correlation.

The present studies were undertaken to extend the available data on the effects of small degrees of leading edge bluntness to higher Mach numbers and to examine closely the possible relationships between bluntness effects and unit Reynolds number effects. The present experimental studies were conducted with a hollow cylinder model. The results and analysis are based on transition locations derived from the maximum hot-wire signal, $\widetilde{e^2}$, with the probe traversed near the surface. This has been shown to be directly compatible with transition locations derived from maximum surface temperatures, as used by Brinich and Sands in Reference 19.

Attempts to correlate the present data in terms of a ratio of transition locations given by Brinich and Sands as

$$\frac{(X_t)_b}{(X_t)_{b \to 0}} = f(Re_b) \tag{3}$$

revealed systematic deviations, depending on how the variation in Re_b was obtained. The transition distance ratio was observed to be a function of U_∞/ν_∞ and b as well as their product, or

$$\frac{(X_t)_b}{(X_t)_{b \to 0}} = f(U_\infty/\nu_\infty, b) \tag{4}$$

A study of Brinich's and Sands's data for small degrees of bluntness also reveals small but similar effects. This can be illustrated by cross-plotting the data versus U_∞/ν_∞ with Re_b as a parameter. Such cross-plots are shown in Figure 22. These data are plotted on log-log scales and the curves are observed to be slightly convergent as U_∞/ν_∞ increases rather than the parallel curves required for constant ratios of transition distances.

Regarding these cross-plots with Re_b as a parameter, two other trends of significance may be noted: (1) Re_t increases with increasing U_∞/ν_∞ for Re_b = constant and (2) there is a marked difference in the magnitude of Re_t between the two sets of data. Item (1) provides the answer to one of the questions leading to these studies - namely, is the unit Reynolds number effect due entirely to bluntness? Clearly it is not. This and Item (2) will be discussed later in this report.

A close inspection of Figure 22 indicates, for a given set of data, a nearly constant incremental change in Re_t for a given increase in Re_b. This suggests a relationship of the form

$$(Re_t)_b - (Re_t)_{b \to 0} = f(Re_b) \quad (5)$$

The VKF data are presented in Figure 23 in this manner. The correlation is seen to be quite reasonable for the small bluntness Reynolds numbers of the present study. The indicated influence of Mach number is surprising, since a decreasing influence of bluntness is noted from $M_\infty = 3$ to 3.5 as opposed to an increasing influence for $M_\infty > 3.5$. The later comparison of these data with other data will indicate an interrelationship of factors influencing these results; hence the interrelation of Mach number and bluntness implied by Figure 23 is not conclusive.

The data of Brinich and Sands[19] were reduced in a like manner and compared to the present data in Figure 24. Brinich's and Sands's data for $M_\infty = 3.1$ indicate nearly twice the influence of bluntness in comparison to the present data. Two possible reasons for differences in these data are (1) differences in leading-edge geometry noted in Figure 24 and (2) different wind tunnels. Comparison of some transition data from a 10-deg cone in the VKF 12-in Tunnel and transition data from Brinich and Sands on a 10-deg cone taken during their bluntness study do not reveal significant differences. However, it was shown in Figure 22 that an appreciable difference in the absolute magnitude of Re_t existed between the hollow cylinder models.

Assuming, for the moment, that similar results would be obtained from the two wind tunnels for a given model, the explanation of these data was sought in the differences in leading-edge geometry.

Laufer and Marte[21] tested a flat plate with a bottom or internal bevel angle of 24 deg in the Jet Propulsion Laboratory's 20-in wind tunnel (JPL-20 in). These results are compared with Brinich's and Sands's data and the VKF data in Figure 25. Assuming now that three wind tunnels (VKF 12-in tunnel, NASA Lewis 12-in tunnel, and JPL 20-in tunnel) would produce similar results on a given model, a rather strong influence due to the bevel angle appears to be present.

An explanation of the apparent interrelations between bluntness Reynolds number and the bevel angle is not known. However, consideration of the local subsonic flow produced by a finite leading edge bluntness points to the possibility of an influence of the bevel on the stagnation point location. Attempts to estimate the possible movement of the stagnation point have not been made but, if such a movement occurs, then a change in the shock-induced shear layer adjacent to the model surface may occur[22]. Leading edge vibrations are another possible source of the effect of the bevel angle. However, it seems unlikely that the influences on such vibrations due to changing U_∞/ν_∞ or tunnel density level would be almost exactly the same as varying the physical leading edge thickness to produce a given change in the bluntness Reynolds number, Re_b. This latter possibility is discounted for lack of proof at this time, and the extrapolated Re_t values to $\theta = b = 0$ are referred to as the 'aerodynamically' flat plate data.

Based on the assumption that the three sets of data are directly comparable, sufficient information is at hand to estimate the combined effects of leading edge bluntness and the bevel angle for $M_\infty \simeq 3$. A typical plot for U_∞/ν_∞ = constant with Re_b as a parameter is shown in Figure 26. Such cross-plots for other U_∞/ν_∞ values indicate that, although the level of all the curves increases as U_∞/ν_∞ increases,

the inter-relation between Re_b and θ is substantially independent of U_∞/ν_∞. The data of Figure 26 indicate

$$(Re_t)_{\theta, b} = (Re_t)_{\substack{\theta = 0 \\ b = 0}} + f(Re_b, \theta) \tag{6}$$

Using linear relationships for the case of small degrees of bluntness, one writes

$$(Re_t)_{\theta, b} = (Re_t)_{\substack{\theta = 0 \\ b = 0}} + \frac{\partial Re_t}{\partial Re_b} Re_b + \frac{\partial Re_t}{\partial \theta} \theta + \frac{\partial^2 Re_t}{\partial Re_b \, \partial \theta} Re_b \theta \tag{7}$$

From Figure 26 and other similar plots, these constants are evaluated and it is found that

$$(Re_t)_{\theta, b} = (Re_t)_{\substack{\theta = 0 \\ b = 0}} + 160\, Re_b + 36500\, \theta + 55 Re_b \theta \tag{8}$$

where θ is in degrees and

$$(Re_t)_{\substack{\theta = 0 \\ b = 0}} = f(U_\infty/\nu_\infty) \simeq \text{constant } (U_\infty/\nu_\infty)^n \tag{9}$$

The latter condition is found from the consideration of other U_∞/ν_∞ values, as mentioned earlier. The Re_t values for an 'aerodynamically' flat plate (i.e., $\theta = b = 0$) at $M_\infty = 3$ are shown in Figure 27. Direct extrapolation of the measured data to $Re_b = 0$ for $M_\infty = 3$ to 5 is shown for comparison to illustrate the U_∞/ν_∞ influence.

The unit Reynolds number effect is found to be present to varying degrees in all the experimental data and even in the aerodynamically flat plate case. Elimination of the effect of leading edge bluntness as the basic cause of the unit Reynolds number effect adds indirect support to the analysis by Whitfield and Potter[4]. This analysis indicates that the phenomenon may be due to the varying energy levels of the different frequencies which are amplified at different unit Reynolds numbers. The possibility that free-stream turbulence is associated with the unit Reynolds number effect remains. Suitable free-flight transition data would help to resolve this question. Although free-flight data showing increasing Re_t with increasing $(U/\nu)_\delta$ exist, the data are not complete enough to permit analysis of possible extraneous factors.

The experimental data used in this analysis may be summarized by comparison with Equation (8). This comparison is given in Figure 28 for many U_∞/ν_∞ and b values. The use of linear relationships for the effect of Re_b and θ is seen to allow an accurate estimate of Re_t up to about 3×10^6. Also included in Figure 28 are data obtained by Chapman, Kuehn, and Larson[2] on a flat plate in the NASA Ames Tunnel No. 1. These data were not used in the analysis to evaluate the constants in the above relation but are seen to agree quite well with the equation given.

The preceding analysis has been based on the assumption that data from the three wind tunnels are directly comparable. Although it was stated earlier that cone transition data were available, the discussion of these results was delayed, since it

was also desired to compare the estimated Re_t for an 'aerodynamically' flat plate (i.e. $\theta = b = 0$) to Re_t for a sharp cone. Comparison of the test facilities and results obtained for the 'aerodynamically' flat plate and the cone is shown in Figure 29. Fluid properties for this comparison are based on conditions at the outer edge of the boundary layer. Since most of the cone data were available for $M_\delta = 2.7$, Brinich's and Sands's[19] cone data and the 'aerodynamically' flat plate were corrected to $M_\delta = 2.7$ using the Mach number effect for transition on a cone found by Laufer and Marte[21]. Data from the JPL 12-in tunnel also are included to illustrate the similarity of the U_δ/ν_δ effect on Re_t for a cone and an 'aerodynamically' flat plate. The agreement between the wind tunnels is seen to be reasonable and the factor between Re_t on a cone and the 'aerodynamically' flat plate is approximately 3. This is a significant result and it is interesting to note that Battin and Lin[23] predicted that the minimum critical Reynolds number of stability theory would be in the same ratio for the cone and plate.

The apparent strong interdependence of factors defining the leading edge of a flat plate or hollow cylinder model prevents us from drawing conclusions regarding the detailed influence of Mach number on leading edge effects; hence the influence of Mach number on the 'aerodynamically' flat plate cannot be precisely evaluated at this time. None-the-less, we believe the considerations presented here are of some importance in this connection.

5. THE EFFECT OF SURFACE ROUGHNESS

Previous studies of this subject have been reported in references too numerous to mention here. Among the more recent analyses of the subject is that published by Dryden[25] who dealt with low speed flows. He found that the ratio of the Reynolds numbers of transition with and without roughness, Re_t/Re_{t_0}, was well represented as a function of k/δ_k^*, the ratio of roughness height to the displacement thickness of the undisturbed boundary layer at the station of roughness. The correlation held only for transition locations, X_t, less than or equal to X_{t_0} and greater than X_k, where X_{t_0} corresponds to the case of no roughness and X_k is the station where roughness is attached. The accompanying sketch illustrates some of the nomenclature used in this discussion.

Further experimental testing of Dryden's parameter was reported by Klebanoff, Schubauer, and Tidstrom[26], who found that k/δ_k^* served admirably for single, two-dimensional elements but was totally ineffective as a correlation parameter when the roughness consisted of a single row of spheres. The latter investigators suggested that the three-dimensional roughness seemed to have little effect on transition when the quantity Re_k was less than some critical value, and that the location of transition moved almost precipitously to a point near the station where roughness was attached when Re_k slightly exceeded this critical value.

The parameter is defined as

$$Re_k = U_k k/\nu_k \qquad (10)$$

where U_k/ν_k = unit Reynolds number in undisturbed boundary layer corresponding to conditions at height k and location X_k

k = height of roughness.

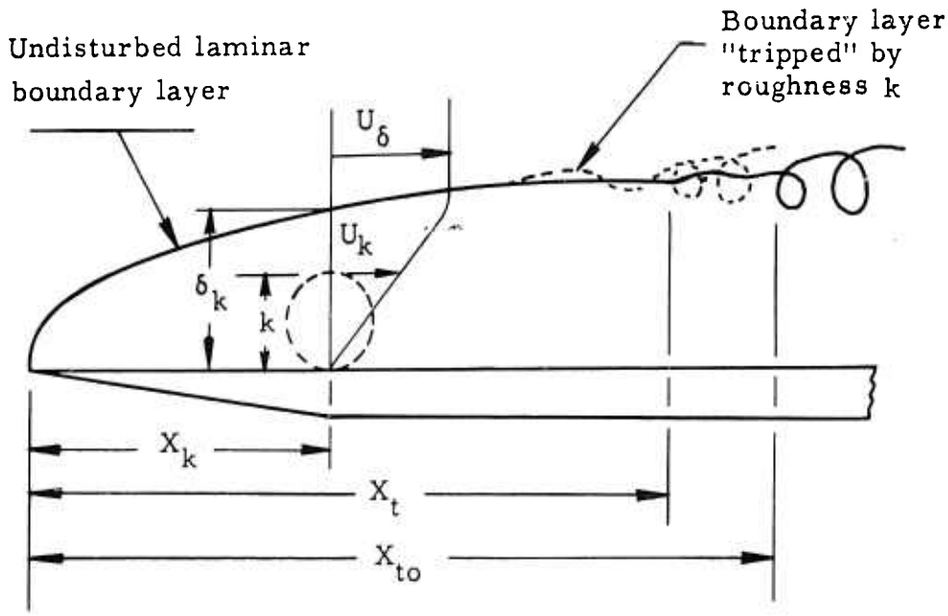

A critical Reynolds number equivalent to $\sqrt{(Re_k)}$ appears to have been suggested originally by Schiller[27]. However, the concept of a nearly stepwise shift of transition from its undisturbed location, X_{to}, to the roughness station, X_k, was proved erroneous as a general rule by the data of Fage[28] and numerous later investigators. The more recent view has credited this critical behavior to three-dimensional roughness, while considering that two-dimensional roughness produces a more gradual effect on the mean location of transition. It will be observed when viewing recent data that even three-dimensional roughness does not always produce an instantaneous shift of X_t.

Tani, Hama, and Mituisi[29] published a paper in which they described a roughness correlation parameter based on G.I. Taylor's parameter for transition caused by free-stream turbulence. This accomplished a correlation of their data for the case of single, two-dimensional elements on a flat plate in low speed flow. Unaware of this work which was not widely known in the United States, one of the present authors[30] also undertook to derive a roughness parameter from the Pohlhausen boundary layer profile parameter, λ, after the manner of Taylor's early analysis of free-stream turbulence. Tani et al, arrived at their parameter by replacing certain terms in Taylor's parameter by appropriate roughness characteristics. The analysis by Potter was done by setting the problem in functional form and empirically determining the functions from published data. Again, only the single, two-dimensional element on a flat plate in low speed flow was considered. It was Gibbings[31] who called attention to the fact that both analyses gave results that could be reduced to identical functional forms and differed only by a constant. This slight difference in the value

of the constant was due to the use of different experimental data. Although neither expression was originally given in this form, both can be expressed as

$$(U_\delta k/\nu_\delta)(X_t/X_k)^{1/2} = \text{constant} \tag{11}$$

Another interesting point is that the left side of Equation (11), based on flat plate flow, is proportional to either

$$(U_\delta X_t/\nu_\delta)^{1/2}\ (k/\delta_k)$$

or

$$(U_\delta X_t/\nu_\delta)^{1/2}\ (k/\delta_k^*)$$

where k/δ_k^* is the parameter proposed by Dryden. Since both analyses assumed that roughness contributed the only effective disturbances to the laminar boundary layer, it was not expected that they would do very well as X_t approached X_{t_0} or X_k. However, the values for $U_\delta k/\nu_\delta$ when $X_t \to X_{t_0}$ or $X_t \to X_k$ were rather good approximations for subsonic, two-dimensional flow.

We should note that Winter, Scott-Wilson, and Davies[32] gave values of $U_\delta k/\nu_\delta$ for wires which would fix transition at the wire location. Their data included cases wherein the free-stream Mach number was as high as 3. They recommended $U_\delta k/\nu_\delta = 700$ for Mach numbers up to 0.9, from whence $U_\delta k/\nu_\delta$ increased exponentially up to about 5200 at the limit of their data slightly above $M_\delta = 3$. The scatter of data used to define Re_k was very great, but they were forced to use available results from different models having various pressure distributions.

Recently Smith and Clutter[16] have conducted tests in a low speed wind tunnel to obtain further data on the effects of roughness. They recommended values of Re_k representing maximum sizes of roughness permissible without appreciable effect on transition location. Later, the same authors[33,34] recommended values of a Reynolds number, Re_k^*, to represent the limits $X_t \to X_{t_0}$ and $X_t \to X_k$. This Reynolds number is defined as

$$Re_k^* = a^* k/\nu^* \tag{12}$$

where ν^* is based on T^* and p_δ, the superscript * denoting sonic conditions. Smith and Clutter suggested that Re_k^* must exceed approximately 100 for roughness to have effect in very low speed flows, and approximately 300 to 400 in flows where compressibility effects are important. In order to bring X_t near X_k, they suggested $Re_k^* \simeq 400$ to 900 for all Mach numbers for both wire and spherical roughness elements. In order to make Re_k^* for low speed flow to fall in this range they had to define it as $2Re_k$. They offer justification for this in Reference 34. Gibbings[31] recently has given a criterion for the occurrence of transition at a wire roughness. For incompressible, low turbulence, flat plate flow, he suggests $(U_\delta k/\nu_\delta)_{M=0} = 826$. He also derives an expression for the relation between X_t and X_k when transition is downstream of a wire, namely

$$\frac{d(\eta'/\eta)}{d[X_t/X_k - 1]} = 1/3 \tag{13}$$

where

$$\eta' = \frac{(U_\delta k/\nu_\delta)_w}{(Re_{X_k})^{1/2}}$$

$$\eta = \frac{(U_\delta k/\nu_\delta)}{(Re_{X_k})^{1/2}}$$

and the subscript w denotes the case of transition at the wire. Effects of compressibility are represented by increasing the required value of $U_\delta k/\nu_\delta$ according to Equation (14),

$$(U_\delta k/\nu_\delta) = (U_\delta k/\nu_\delta)_{M=0} \left[\frac{1}{1 - C_{DW}/C_D}\right] \tag{14}$$

where $C_D = 0.75$

C_{DW} = estimated wave drag coefficient discussed in Reference 31

At this point it seems appropriate to remark on the emergence of either $U_\delta k/\nu_\delta$ or $U_k k/\nu_k$ in many analyses, even when the starting points of the analyses appeared completely different. The former parameter is independent of roughness location when $dp/dX = 0$, but the second form of Reynolds number, which we denote by Re_k, is a function of position of roughness as well as height. Furthermore, the use of Re_k is compatible with a compressibility correction factor based on M_k, the Mach number at the height k in the boundary layer, which would offer more flexibility than a factor based on M_δ. Therefore, we have chosen to use a roughness effectiveness parameter which we shall denote by Re_k' where

$$Re_k' = Re_k \; f(M_k) \tag{15}$$

for the correlation to be described.

Continuing toward formulation of our correlation procedure, we suggest that a suitably general term representing location of transition is the Reynolds number based on boundary layer thickness at transition. This is proportional to $(U_\delta X_t/\nu_\delta)^{1/2}$. In order to eliminate extraneous factors insofar as possible, we choose to divide the above transition Reynolds number by its corresponding value when $k = 0$ at the same unit Reynolds number. When $dp/dX = 0$, this ratio is $(X_t/X_{t0})^{1/2}$. Since our parameter Re_k' must be calculated at a station X_k rather than X_t, it is possible that the effectiveness of the roughness varies accordingly to the distance between roughness and transition. This possibility is strongly suggested by the type of analysis which considers that Pohlhausen's parameter reaches a certain value at transition[29,30] and it also seems quite in keeping with boundary layer stability theory. It is logical that this effect would vary with magnitude of the disturbance created by the roughness. This reasoning leads to selection of the quantity representing relative positions of transition and roughness,

$$\sqrt{(X_t/X_{t0})} - \sqrt{(X_k/X_{t0})}(Re_k'/\text{constant})$$

for all flows with $dp/dX = 0$. The constant, which we denote by K, represents the value of Re_k' where $X_t = X_k$.

The next matter is the function of Mach number, $f(M_k)$, which is intended to account for the very complicated process occurring when a partially supersonic shear flow encounters a roughness element. Smith and Clutter suggest reducing Re_k to Re_k^* as given by Equation (12). This is based on the assumption that sonic flow will always exist near the top of a roughness element when M_k exceeds unity, and may be expressed as

$$Re_k^* = (Re_k/M_k)\left(\frac{(\gamma + 1)/2}{1 + (\gamma - 1)\, M_k{}^2/2}\right)^{0.5 + \omega} \tag{16}$$

when it is assumed that

$$T_0 = \text{constant}$$

$$\rho^* = \rho_k(T_k/T^*), \qquad p_k = p^* = p_\delta$$

$$\mu^* = \mu_k(T^*/T_k)^\omega$$

As noted earlier, Gibbings also has offered a compressibility factor which is indicated in Equation (14).

The present authors have investigated yet another approach which they believe has a reasonably sound basis. Specifically, we use the results of studies of separated flows published by Chapman, Kuehn, and Larson[2] to estimate the plateau pressure, p_p, near a two-dimensional roughness element when $M_k > 1$.

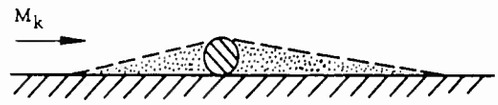

a. Roughness element

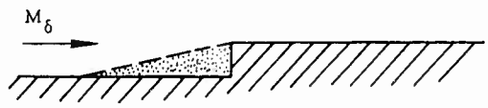

b. Assumed model for flow approaching and at top of roughness element

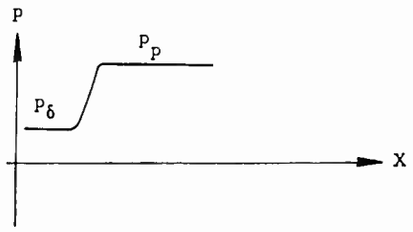

c. Typical pressure distribution corresponding to (b), after Ref. 2

We assume the compression is isentropic insofar as the relations between pressure and Mach number are concerned. Inasmuch as the flow is separated around the roughness element, which is itself generally in close contact with the model wall, we assume wall temperature T_w is the appropriate temperature determining density and viscosity. This leads to a roughness Reynolds number

$$Re'_k = Re_k \, (U_p/U_k)(\rho_p/\rho_k)(\mu_k/\mu_p) = U_p k/\nu_p$$

i.e. a Reynolds number based on roughness height and plateau flow conditions. If it is assumed that

$$T_0 = \text{constant}$$

$$\rho_p = \rho_k(p_p/p_k)(T_k/T_w), \qquad p_k = p_\delta$$

$$\mu_p = \mu_k(T_w/T_k)^\omega, \qquad \omega = \text{function of temperature}$$

then

$$Re'_k = Re_k(M_p/M_k)(p_p/p_\delta)(T_k/T_w)^{0.5 + \omega} \tag{17}$$

The really significant term in Equation (17) is the temperature ratio. The product of Mach number and pressure terms is approximately unity. Assuming, for simplicity, that the term $\sqrt{(\tilde{c}_f)}$ used in Reference 2 can be neglected in the determination of p_p since the effect on Re'_k will be small, and further approximating by assuming $T_w = T$ (adiabatic wall) $\simeq 0.9\ T_0$, we then arrive at the expression of the form

$$Re'_k = Re_k \, f(M_k)$$

namely

$$Re'_k \simeq Re_k(M_p/M_k)(p_p/p_\delta)\left(\frac{1.11}{1 + (\gamma - 1)M_k^2/2}\right)^{0.5 + \omega} \tag{18}$$

When $M_k \leqslant 0.75$, it is assumed that $T_w = T_0$ and $Re'_k \simeq Re_k$. The value of Re_k is most easily determined for flows where $dp/dx = 0$ by utilizing the charts prepared by Braslow and Knox[35]. Figure 38 of Reference 2 is used to obtain p_p, and a table of flow functions may be used to find M_p corresponding to isentropic compression from p_δ to p_p. As noted earlier, a further approximation may be written for $M_k \geqslant 0.75$ and $T_w = 0.9\ T_0$:-

$$Re'_k \simeq Re_k \left(\frac{1.11}{1 + (\gamma - 1)M_k^2/2}\right)^{0.5 + \omega} \tag{19}$$

Both Equations (18) and (19) are plotted in Figure 30, where Equation (16) also is shown. Lacking information on the shear flow around three-dimensional roughness, we are forced to apply Equation (17) to both types of roughness. This may be partially excused on the basis that the temperature term is dominant and presumably would be the same for both two- and three-dimensional roughness. While we have not yet completed a thorough study of the matter, it appears that our correlation procedure is almost equally good whether based on Re^*_k or Re'_k.

For the remainder of our discussion we shall use Re'_k, as defined by Equation (18) with $\omega = 1.00$. This is equivalent to Equation (19) with $\omega = 0.85$ in the entire range of the data used herein. We do not believe an attempt at greater precision is justifiable at this time. In Figures 31-37 the method of correlation proposed here is tested by a collection of the most recently published data. Both two- and three-dimensional roughness are included, and Mach numbers from near zero up to five are represented. All data are for bodies having no pressure gradients. The data include cases where k/δ_k ranges from 1/10 to nearly 4. The bodies represented are flat plates, hollow cylinders, and cones. The values of Re_k required to bring X_t near X_k exceed 20,000 in some of the supersonic flow data.

Boundary layer trips consisting of a single row of three-dimensional elements obviously admit another variable, namely the lateral spacing of the spheres. Earlier experimenters have found that the lateral spacing is not a significant factor within rather wide limits. Klebanoff, Schubauer, and Tidstrom[26] investigated spacings of 1/8, 1/4, and 1/2 in or 2, 4, and 8 sphere diameters, finding no appreciable effect. Van Driest and McCauley[24] investigated spacings of 1/32, 1/16, 1/8, and 3/16 in without observing an important effect. (The latter spacings are not given in terms of diameters in Reference 24). Spacing of spherical elements was 1/8 in for all the VKF tests. With these results in mind, no consideration was given to lateral spacing in the present correlation.

The spherical roughness elements tested by Van Driest and McCauley[24] and by the present researchers were in some cases mounted on thin, two-dimensional bands which encircled the models. Those used by the former were approximately 0.0012 in thick and 0.25 in wide. The VKF tests utilized bands 0.006 in thick and 0.1875 in wide. The roughness height, k, in all the following has been taken as sphere diameter plus band thickness. In the VKF experiments, k was determined by directly measuring the roughness height on the models.

Values of X_{t_0} were not determined during the tests reported by Klebanoff et al[26], so a constant Reynolds number of transition on the smooth plate had to be assumed in order to calculate X_{t_0} values. There may be some misrepresentation in Figure 32 because of this, although it is believed small on the basis of a private communication from the experimenters. In this case, then, the use of X_{t_0} as a reference quantity merely normalizes the abscissa and does not serve to eliminate extraneous effects as it does on the other figures. This is not intended to imply that the scatter on Figure 32 is entirely due to this factor, though it may be responsible to some degree.

We have attempted to show representative experimental data from recent, more extensive tests of bodies without pressure gradients. It should be noted that not all data from every source represented in Figures 31 - 37 have been plotted, simply because of the vast quantity of data involved. Selection of data to be shown here has been on a random basis, with no effort to include only data favorable to our correlations.

It will be noted that the constant divisor of Re'_k is varied as in Table 1 for different situations.

It is interesting that the scatter of points in the correlations is insensitive to the constant over broad ranges. However, the constant does determine the value of Re'_k where the correlation predicts $X_t = X_k$. Since the correlation method makes it

possible to deal with the entire range of X_t from X_{t0} to X_k, the characteristic 'knee' where the variation of X_t changes slope and begins to approach X_k asymptotically is reproduced in curves drawn by means of our correlation. Most earlier analyses of the problem were based on the simplifying assumption that $X_t = X_k$ at a point which would approximate point A in the accompanying diagram.

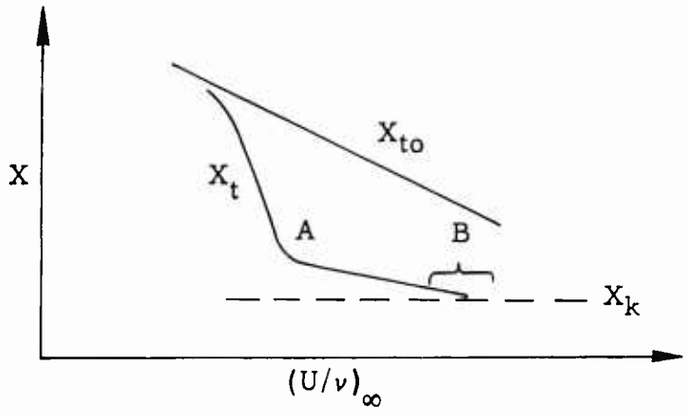

While such an approximation often is satisfactory, it can lead to large errors in some cases. By the present method, one usually will estimate the point $X_t = X_k$ much nearer the experimental result, because wide variations in the constant divisor in our parameter cause only small relative errors. This result is due to the effect of the constant being strongest in the region B of the diagram.

The correlated data have been used to establish working curves. These curves, which result from fairing smooth curves through the data points on Figures 31 - 37, are shown in Figures 38 and 39. All the supersonic, wire trip data are represented by a single curve. However, separate curves are required in order to accommodate the supersonic, sphere trip data for cones and hollow cylinders. At this time, we do not know if this indicates fundamentally different reaction to roughness on axisymmetric and effectively two-dimensional bodies such as the hollow cylinder. The flat plate with distributed grit compares most closely with the cone model data, but there is reason to believe that distributed grit is a more effective trip than a single row of spheres. One reason is that grit of a nominal size will include a number of grains larger than nominal size. Therefore, we probably should not consider the grit and spheres equivalent. Again, it should be remarked that undue significance should not be given to the constant divisors, K. They do to some extent represent the relative effectiveness of the different types of roughness and seem to vary as Mach number changes from low subsonic to supersonic. But it was pointed out earlier that relatively wide variations from the particular values used have little importance because of the way K is used here.

Systematic data relating to other types of roughness elements in supersonic, zero pressure gradient flows have not come to the attention of the authors. It may prove necessary to define some 'effective' Re_k' for elements not having such simple geometry as wires, spheres, or grit bands.

Another point deserving mention is the effect of the particular $f(M_k)$ used to determine Re_k'. The curves representing supersonic data on Figure 39 may be made to

fall more closely together if another $f(M_k)$ is used, but at the moment we lack firm justification for choosing another function. Figure 37, which includes data covering Mach numbers from three to five for one model in one wind tunnel, shows no systematic effect of Mach number which would indicate another choice of $f(M_k)$. Perhaps subsequent research will reveal more on this matter.

To demonstrate the accuracy of the correlation in estimating transition location, a few, randomly chosen examples of the use of the correlation are shown in Figures 40 and 41. Considering the great complexity of the problem we believe the results are extremely encouraging.

A final illustration of the use of the correlation is given in Figure 42. There it is shown that k/δ_k for the condition $X_t = X_k$ increases approximately as the first power of M_δ at hypersonic Mach numbers. The required roughness height, k, would increase roughly as M_δ^3 for otherwise constant conditions. This seems to demonstrate the futility of trying to bring transition near the leading edges of bodies in most wind tunnels when M_δ is hypersonic, since the flow external to the boundary layer would be badly distorted by the roughness. However, some relief is offered by the fact that most hypersonic bodies are quite blunt; hence local Mach numbers near the noses often are relatively low. In some cases this advantage will be partially cancelled by the 'inviscid' shear layers on such bodies, which will in turn cause local Re_k values to decrease. It should be noted that highly cooled walls produce conditions making Re_k' greater than given by Equation (18).

6. CONCLUDING REMARKS

Although this is an interim report of continuing research, several significant results have been found from the studies to date. Such results are briefly summarized:-

1. Detailed similarity has been noted in the transition processes for subsonic, supersonic, and hypersonic flows.

2. A marked increase in the magnitude of transition Reynolds numbers has been found in flows at hypersonic Mach numbers. An apparent interrelationship of factors influencing transition does not permit, at present, an isolation of the Mach number influence, per se.

3. The extent of the transition region is shown to increase with increasing transition Reynolds numbers at Mach numbers from zero to eight. It increases with Mach number if transition Reynolds number is constant. Quantitative results are given for the case of flow with zero pressure gradient.

4. A critical layer of intense fluctuation energy concentration in the boundary layer flow was observed at all Mach numbers studied. This result is in agreement with published results[10, 11, 12] and is to be expected from stability theory. However, it is noted that the magnitudes of maximum local fluctuation energies are comparable to those found in fully developed turbulent flow. The distance of this layer from the surface increases with Mach number.

5. Transition Reynolds numbers are estimated for a vanishingly thin, 'aerodynamically' flat plate based on an evaluation of leading-edge geometry effects. Data from several wind tunnels are shown to produce very similar results on this basis. Measured cone transition Reynolds numbers are shown to be three times the estimated values for 'aerodynamically' flat plates.

6. Elimination of the influence of leading edge geometry on flat plates, hollow cylinders, and sharp cones leaves an unexplained increase of transition Reynolds number as unit Reynolds number increases. This occurs in different wind tunnels and in free flight. There is no proof that this is due to tunnel turbulence.

7. Parameters which enable the correlation of experimental data on boundary layer transition due to the surface roughness are presented. Both two- and three-dimensional roughness in both subsonic and supersonic streams are treated with equal success. Correlations of a variety of data are shown for bodies with no pressure gradient, and the method is applied to several representative problems to demonstrate its accuracy. Not only the extremes of roughness effectiveness, but the entire relation of transition location and effective roughness size can be estimated.

8. Results of the research show that laminary boundary layers on bodies with hypersonic boundary layers will be difficult to trip at best, and the necessary roughness sizes frequently will create serious flow distortions extending well outside the boundary layer. In the case of large Mach numbers, required size of roughness is shown to increase approximately exponentially with M_δ on bodies with no pressure gradient when wall temperature equals adiabatic recovery temperature and unit Reynolds numbers are equal. A cooled wall requires less roughness for otherwise equal conditions.

ACKNOWLEDGMENTS

The authors wish to acknowledge contributions to this research from their colleagues at the von Kármán Gas Dynamics Facility. Among the many who assisted in the furtherance of this work, special recognition is due to J.C. Donaldson and M. Kinslow for their obtaining and reducing the hot-wire anemometer data, to W.M. Crouch who was responsible for the hot-wire electronics, and R.D. Fisher, Jr., for his meticulous attention to preparation of the hot-wire probes.

REFERENCES

1. von Kármán, T. — *Aerodynamics.* Cornell University Press, Ithaca, New York, 1954.

2. Chapman, D.R. et alii — *Investigation of Separated Flows in Supersonic and Subsonic Streams with Emphasis on the Effect of Transition.* NACA TN 3869, March 1957.

3. Potter, J.L. Whitfield, J.D. Strike, W.T. — *Transition Measurements and the Correlation of Transition Sensitive Data.* Arnold Engineering Development Center TR-59-4 (AD 208775), February 1959.

4. Whitfield, J.D. Potter, J.L. — *The Unit Reynolds Number as a Parameter in Boundary Layer Stability.* Arnold Engineering Development Center TN-58-77, October 1958.

5. Anderson, A. — *Summary Report on Calibration of Tunnel E-1, a 12-Inch Mach 5 Supersonic Wind Tunnel.* Arnold Engineering Development Center TN-58-8, March 1958.

6. Sivells, J.C. — *Operational Experience with a 50-Inch Diameter Mach 8 Tunnel.* Paper presented at joint meeting of the STA-AGARD Wind Tunnel and Model Testing Panel, Marseilles, France, September 1959.

7. Kovasznay, L.S.G. — *Development of Turbulence-Measuring Equipment.* NACA Report 1209, 1954.

8. Rayleigh, Lord — *On the Instability of Certain Fluid Motions.* Proceedings of the London Mathematical Society, 11, 57(1880) and 19, 67(1887); (Scientific Papers I, 474 and III, 17); see also Scientific Papers IV, 203 (1895) and VI, 197(1913).

9. Schlichting, H. — *Boundary Layer Theory.* McGraw-Hill, New York, 1955.

10. Schubauer, G.B. Skramstad, H.K. — *Laminar-Boundary-Layer Oscillations and Transition on a Flat Plate.* NACA Report 909, 1948.

11. Laufer, J. Vrebalovich, T. — *Stability of a Supersonic Laminar Boundary Layer on a Flat Plate.* California Institute of Technology Jet Propulsion Laboratory Report No. 20-116, December 1958.

12. Demetriades, A. — *An Investigation of the Stability of the Hypersonic Laminar Boundary Layer.* California Institute of Technology GALCIT Memorandum No. 43, May 1958.

13. Silverstein, A. Becker, J.V. — *Determination of Boundary Layer Transition on Three Symmetrical Airfoils in the NACA Full Scale Wind Tunnel.* NACA Report 637, 1938.

14. Bennett, H.W. — *An Experimental Study of Boundary Layer Transition.* Kimberly-Clark Corporation, Neenak, Wisconsin, September 1953.

15. Feindt, E.G. — *Untersuchungen über die Abhängigkeit des Umschlages Laminar-Turbulent von der Oberflächenrauhigkeit und der Druckverteilung.* Jahrbuch der Schiffbautechnischen Gesellschaft, 50.Band 1956.

16. Smith, A.M.O.; Clutter, D.W. — *The Smallest Height of Roughness Capable of Affecting Boundary-Layer Transition in Low-Speed Flow.* Douglas Aircraft Company, Report No. ES 26803, August 1957.

17. Coles, D. — *Measurements in the Boundary Layer on a Smooth Flat Plate in Supersonic Flow, Part III. Measurements in a Flat-Plate Boundary Layer at the Jet Propulsion Laboratory.* California Institute of Technology Jet Propulsion Laboratory Report No. 20-71, June 1953.

18. Klebanoff, P.S.; Tidstrom, K.D. — *Evolution of Amplified Waves Leading to Transition in a Boundary Layer with Zero Pressure Gradient.* NASA TN D-195, September 1959.

19. Brinich, P.F.; Sands, N. — *Effect of Bluntness on Transition for a Cone and a Hollow Cylinder at Mach 3.1* NACA TN 3979, May 1957.

20. Bertram, M.H. — *Exploratory Investigation of Boundary-Layer Transition on a Hollow Cylinder at a Mach Number of 6.9.* NACA Report 1313, 1957.

21. Laufer, J.; Marte, J.E. — *Results and a Critical Discussion of Transition-Reynolds-Number Measurements on Insulated Cones and Flat Plates in Supersonic Wind Tunnels.* California Institute of Technology Jet Propulsion Laboratory Report No. 20-96, November 1955.

22. Moeckel, W.E. — *Some Effects of Bluntness on Boundary Layer Transition and Heat Transfer at Supersonic Speeds.* NACA Report 1312, 1957.

23. Battin, R.H.; Lin, C.C. — *On the Stability of the Boundary Layer over a Cone.* Journal of the Aeronautical Sciences, Vol. 17, July 1950, p. 453.

24. van Driest, E.R.; McCauley, W.D. — *The Effect of Controlled Three-Dimensional Roughness on Boundary Layer Transition at Supersonic Speeds.* North American Aviation, Inc. Aero-Space Laboratory, Air Force Office of Scientific Research TN-58-176 (AD-152209) November 1958.

25. Dryden, H.L. — *Review of Published Data on the Effect of Roughness on Transition from Laminar to Turbulent Flow.* Journal of the Aeronautical Sciences, Vol. 20, July 1953, p. 447.

26. Klebanoff, P.S. Schubauer, G.B. Tidstrom, K.D. — *Measurements of the Effect of Two-Dimensional and Three-Dimensional Roughness Elements on Boundary Layer Transition.* Journal of the Aeronautical Sciences, Vol. 22, November 1955, p. 803.

27. Schiller, L. — *Handbuch der Experimentalphysik.* Vol. 4, Part 4, Leipzig, 1932, p. 189.

28. Fage, A. — *The Smallest Size of a Spanwise Surface Corrugation which Affects Boundary Layer Transition on an Airfoil.* ARC R. & M. 2120, 1943.

29. Tani, I. Hama, F.R. Mituisi, S. — *On the Effect of a Single Roughness Element on Boundary Layer Transition.* Reports of the Institute of Science and Technology, University of Tokyo, Vol. 8, No. 3, May 1954.

30. Potter, J.L. — *Subsonic Boundary Layer Transition Caused by Single Roughness Elements.* Journal of the Aeronautical Sciences, Vol. 24, February 1957, p. 158.

31. Gibbings, J.C. — *On Boundary Layer Transition Wires.* ARC 20,593, FM 2754, 3 December 1958.

32. Winter, K.G. Scott-Wilson, J.B. Davies, F.V. — *Methods of Determination and of Fixing Boundary Layer Transition on Wind Tunnel Models at Supersonic Speeds.* Royal Aircraft Establishment TN Aero 2341, September 1954.

33. Smith, A.M.O. Clutter, D.W. — *The Smallest Height of Roughness Capable of Affecting Boundary Layer Transition.* Journal of the Aeronautical Sciences, Vol. 26, April 1959, p. 229.

34. Smith, A.M.O. Clutter, D.W. — *Analysis of Further Data on the Effect of Isolated Roughness on Boundary Layer Transition in Supersonic Flow.* Journal of the Aeronautical Sciences, Vol. 27, January 1960, p. 70.

35. Braslow, A.L. Knox, E.C. — *Simplied Method for Determination of Critical Height of Distributed Roughness Particles for Boundary Layer Transition at Mach Numbers from 0 to 5.* NACA TN 4363, September 1958.

36. Brinich, P.F. — *Boundary Layer Transition at Mach 3.12 with and without Single Roughness Elements.* NACA TN 3267, December 1954.

37. Jones, R.A. — *An Experimental Study at a Mach Number of 3 of the Effect of Turbulence Level and Sandpaper-Type Roughness on Transition on a Flat Plate.* NASA Memorandum 2-9-59L, March 1959.

TABLE 1

Tentative Values of Constant in the Quantity

$$\sqrt{(X_t/X_{to})} - \sqrt{(X_k/X_{to})}\ (Re'_k/K)$$

Type of Data	*Values of Constant, K*
$M_\delta \rightarrow 0$, 2-Dimensional*	300
$M_\delta \rightarrow 0$, 3-Dimensional**	600
$M_\delta = 3.0 - 5.0$, 2-Dimensional*	4500
$M_\delta = 1.9 - 5.0$, 3-Dimensional***	3000

* Includes wires only
** Includes single row of spheres only
*** Includes single row of spheres and distributed grit only

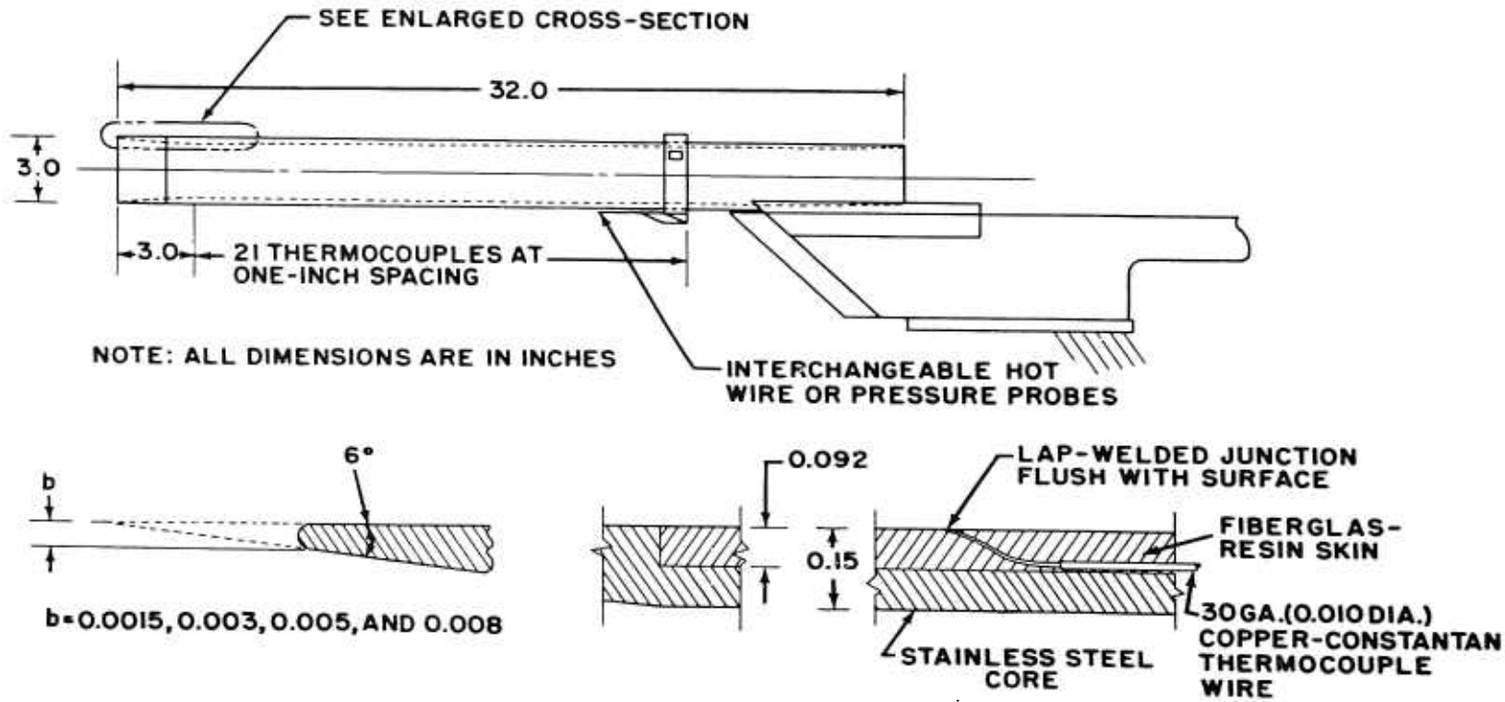

Fig. 1 Three-inch diameter, hollow cylinder model

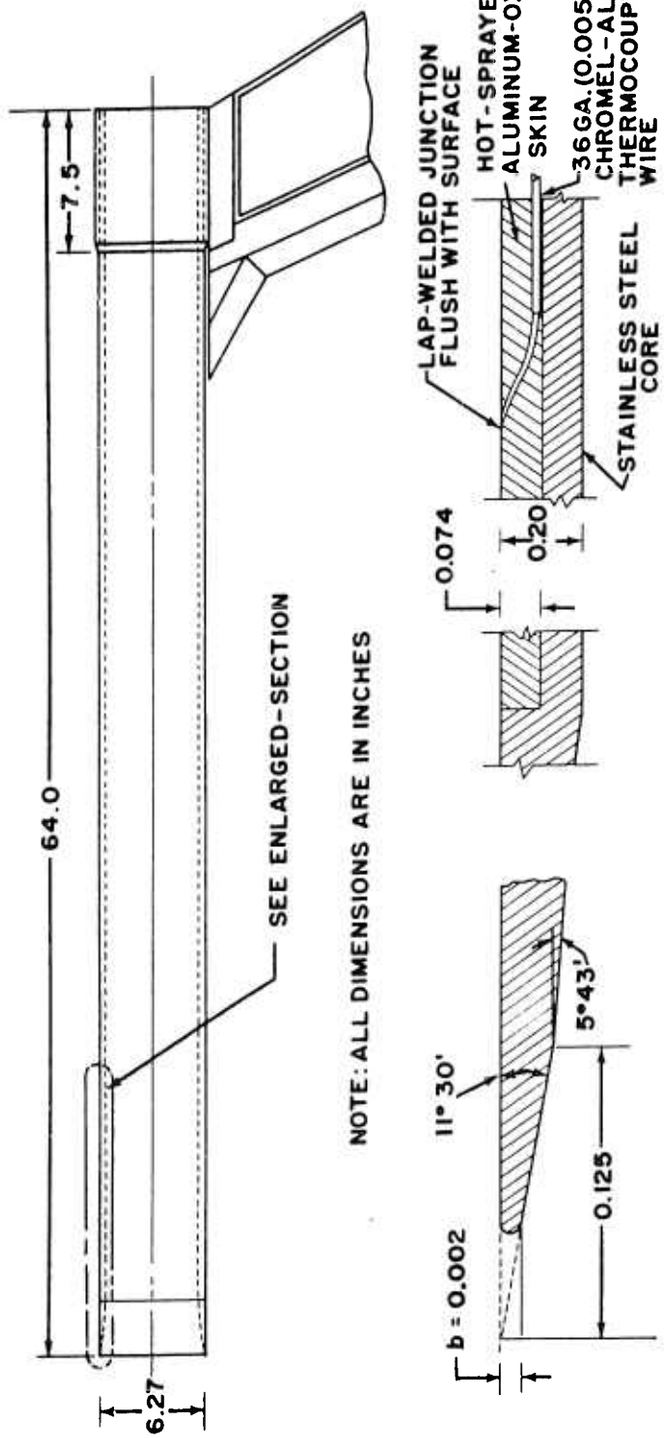

Fig. 2 Six-inch diameter, hollow cylinder model

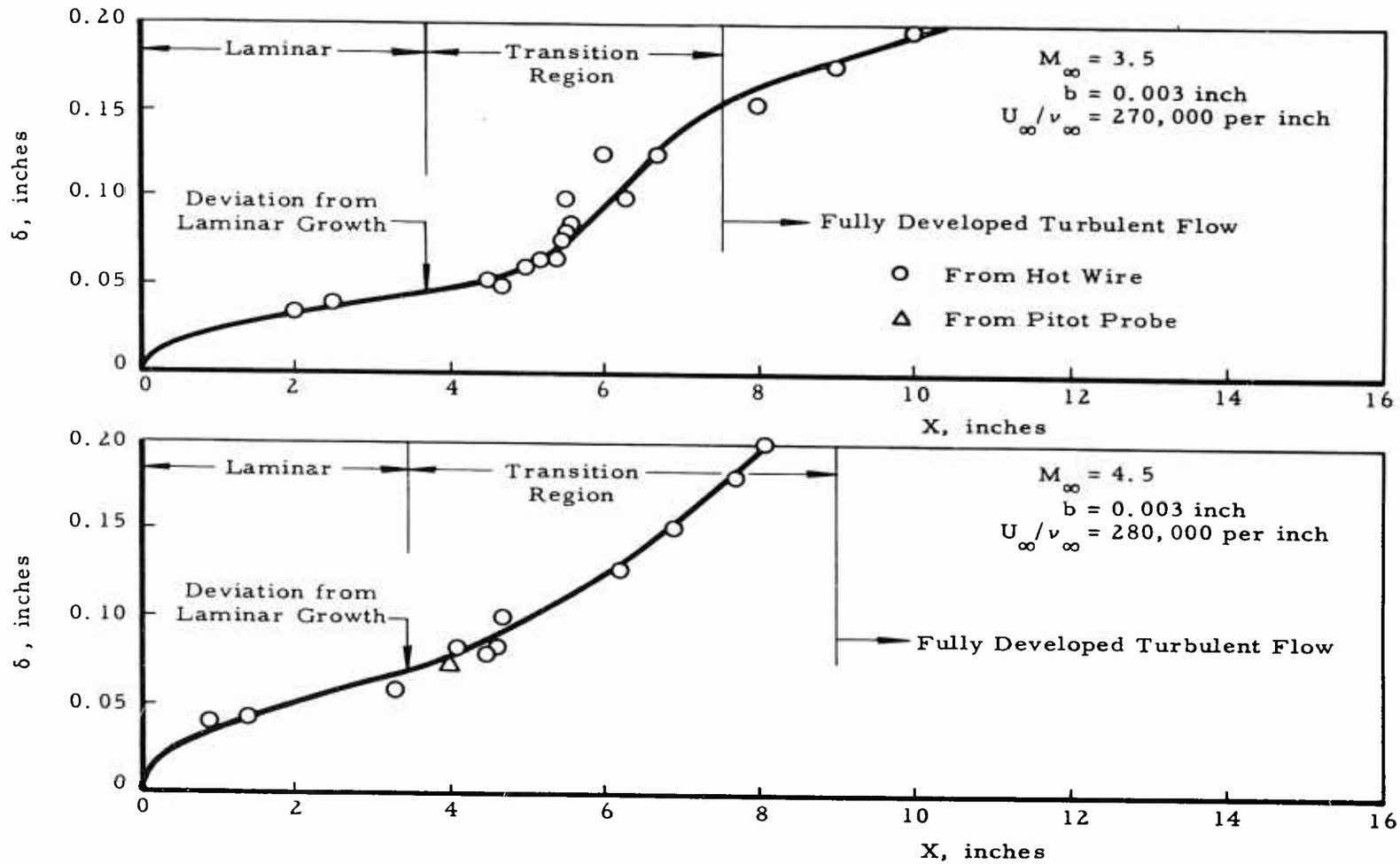

Fig. 3 Typical measurements of boundary layer growth

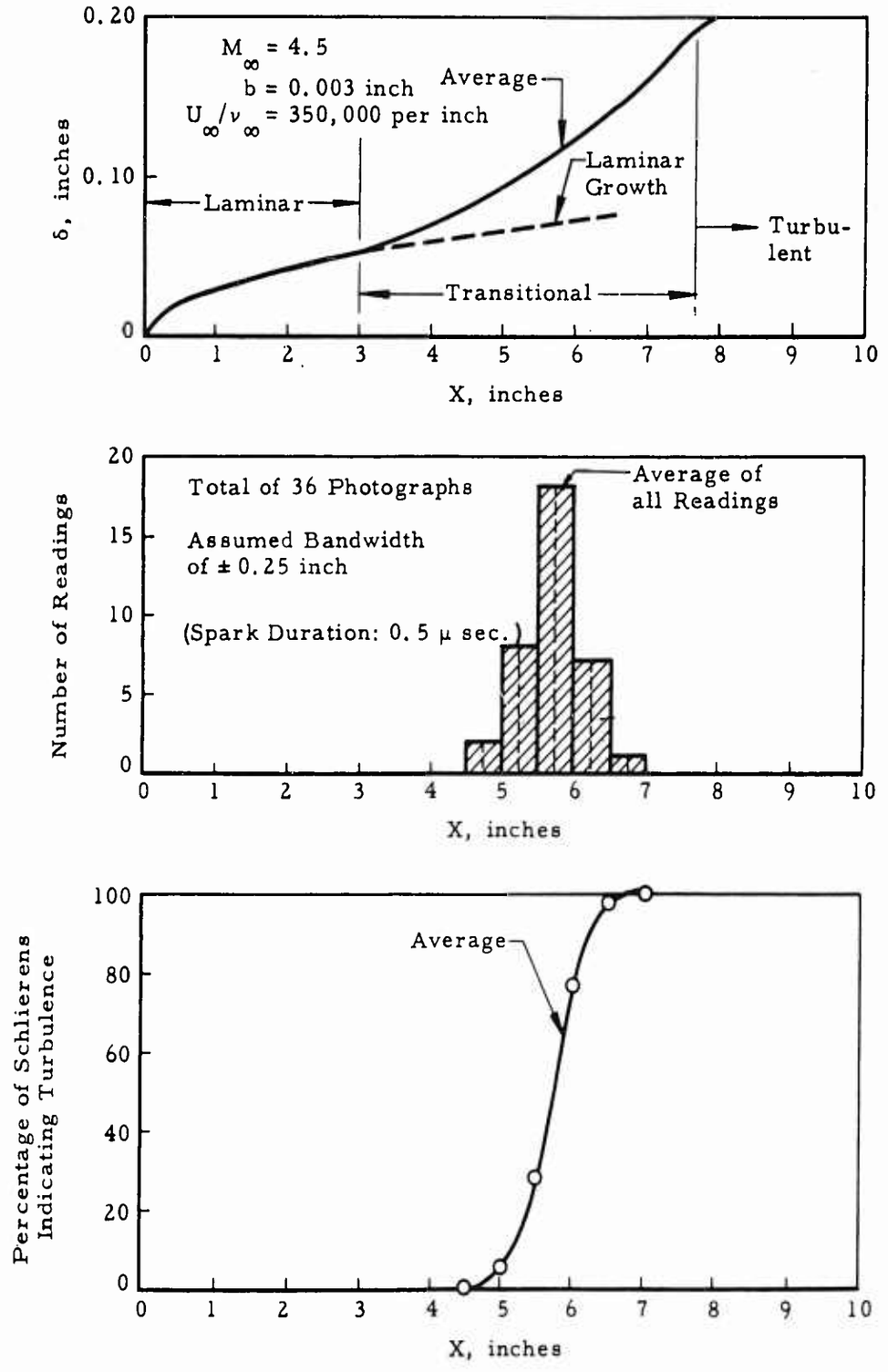

Fig. 4 Analysis of spark Schlieren photographs

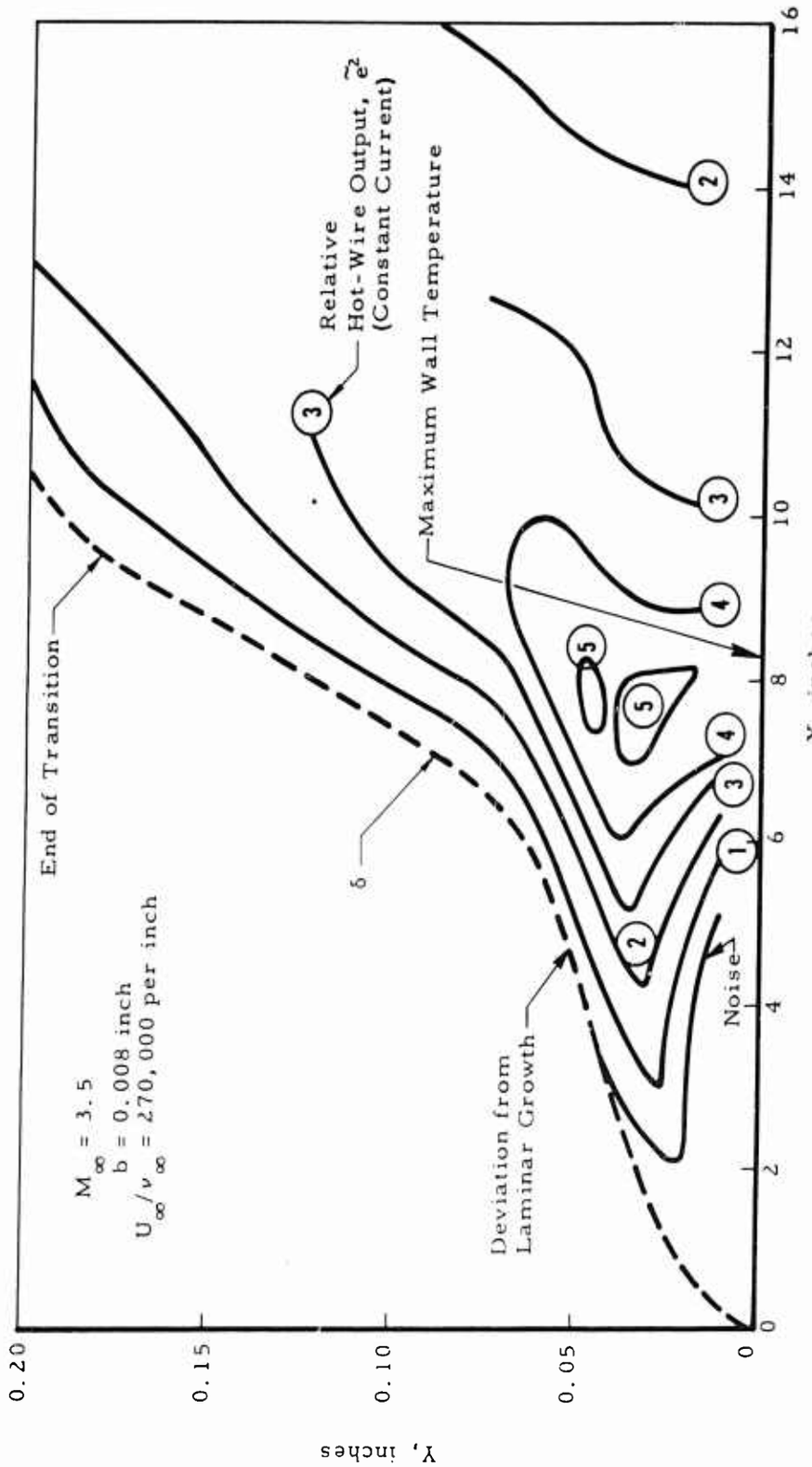

Fig. 5 Isolines of hot-wire output, $\tilde{e}^2$, in X - Y plane

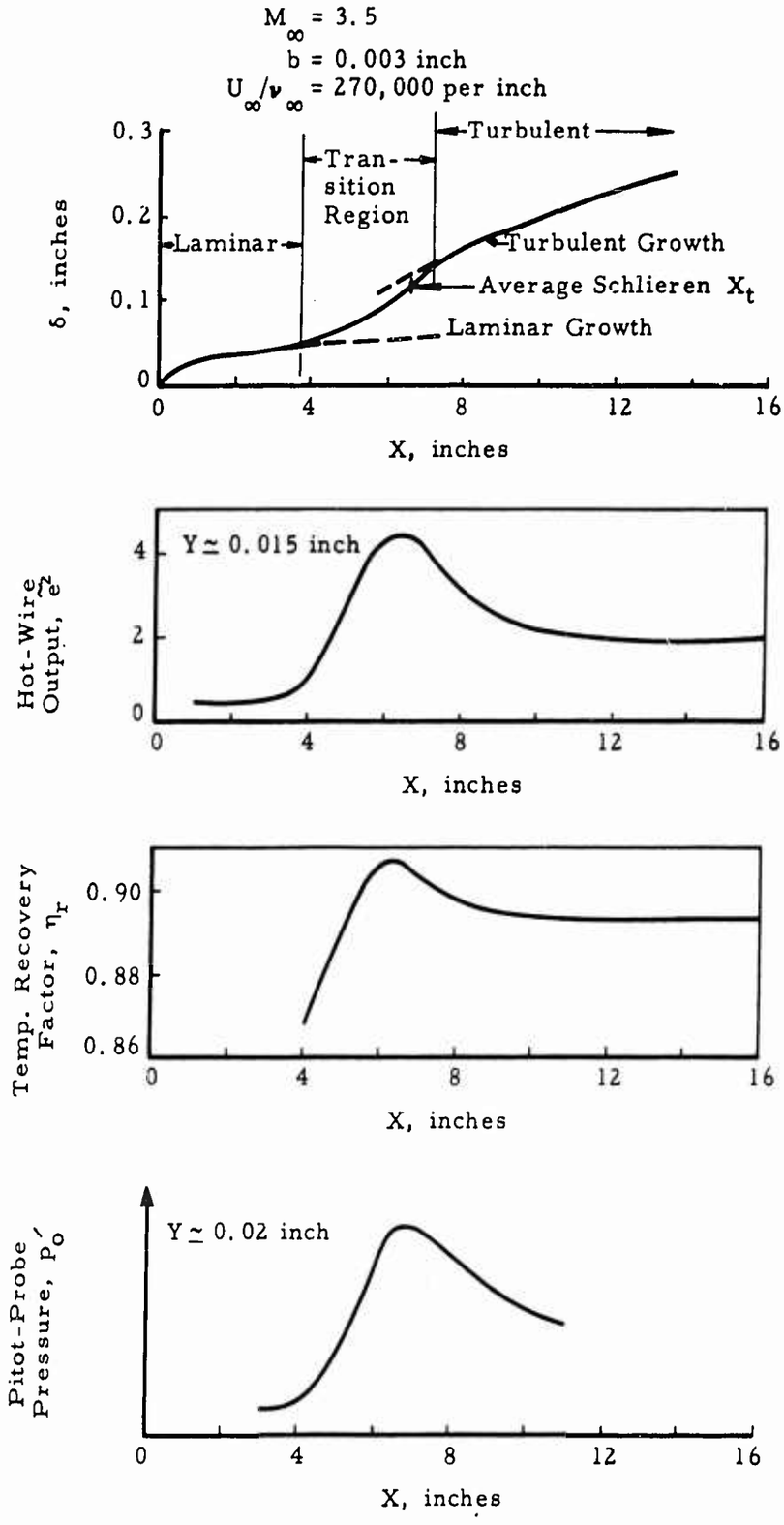

Fig.6 Comparison of methods of transition detection for M_∞ = 3.5

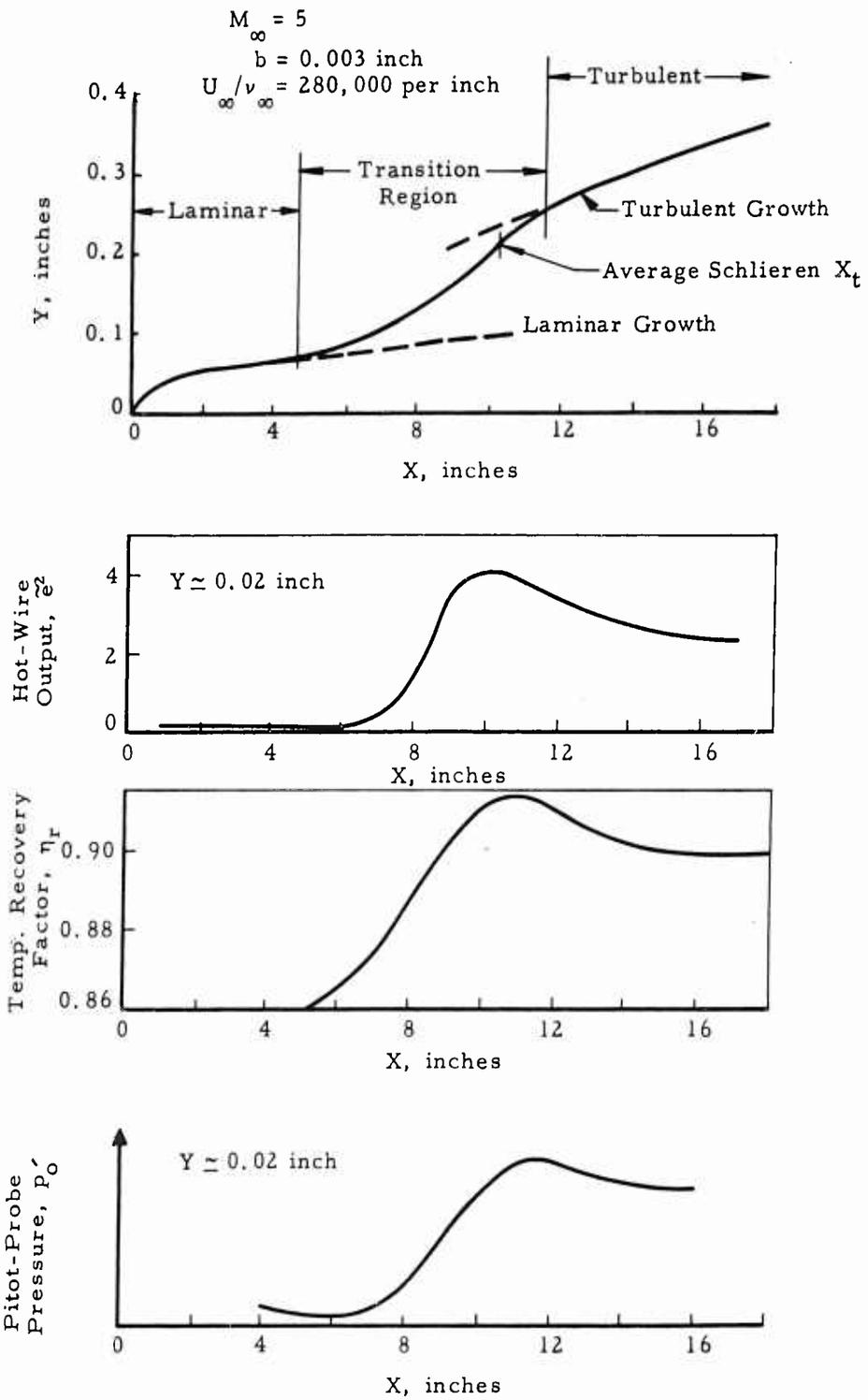

Fig. 7 Comparison of methods of transition detection for $M_\infty = 5$

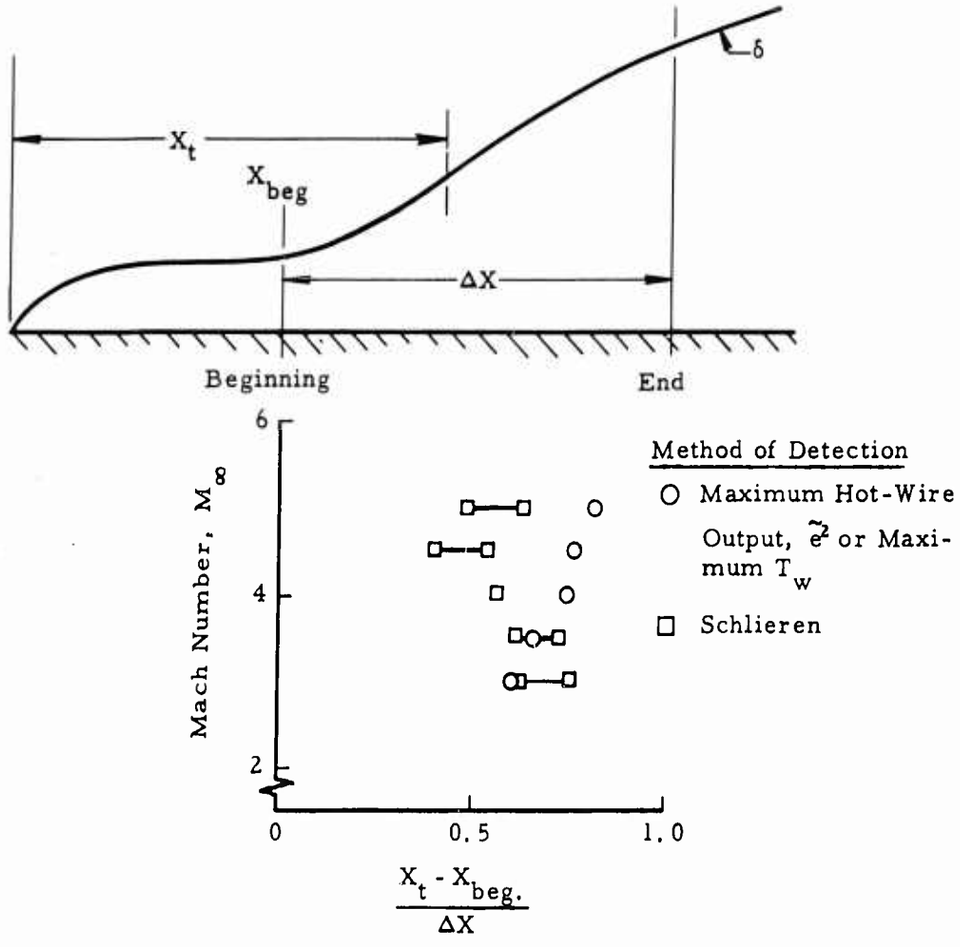

Fig. 8 Similarity of transition region

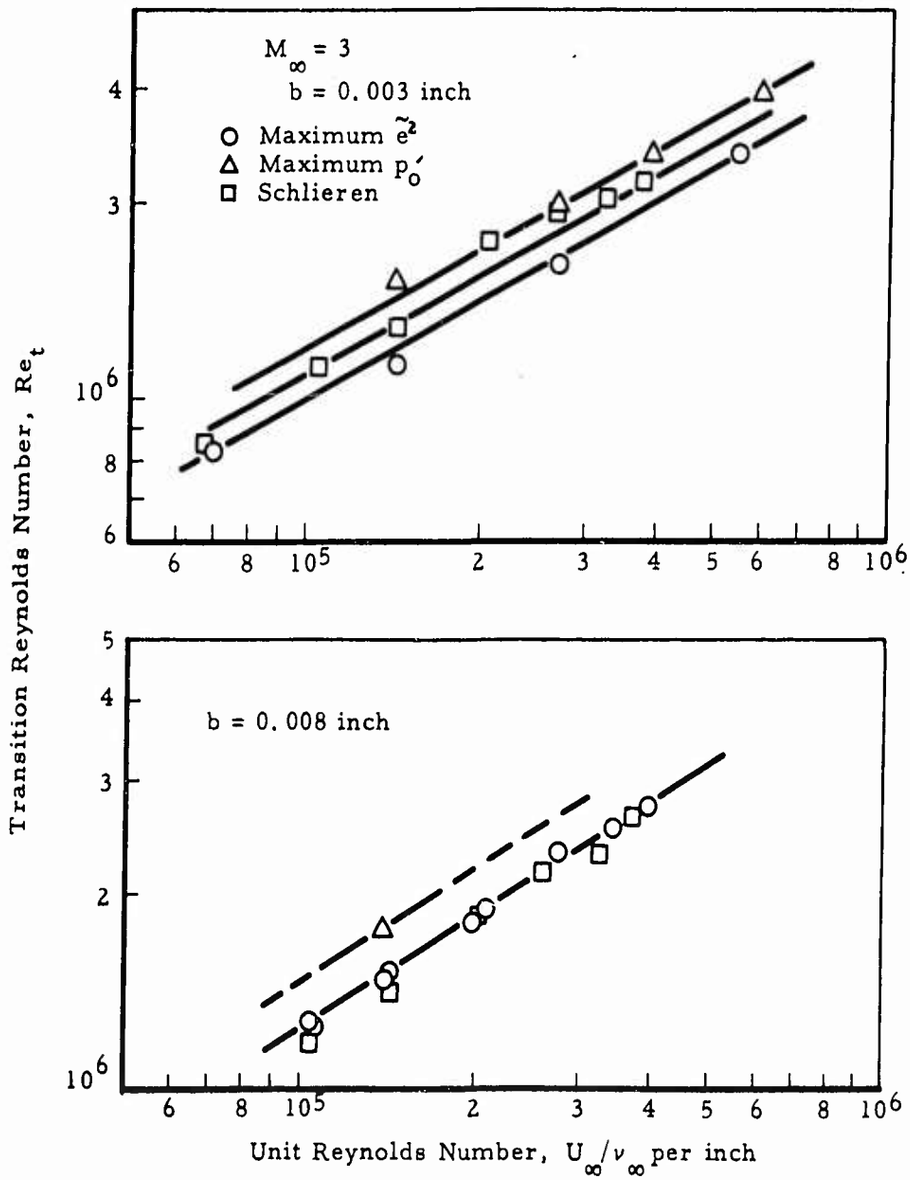

Fig.9 Transition results at M_∞ = 3 for b = 0.003 inch and b = 0.008 inch

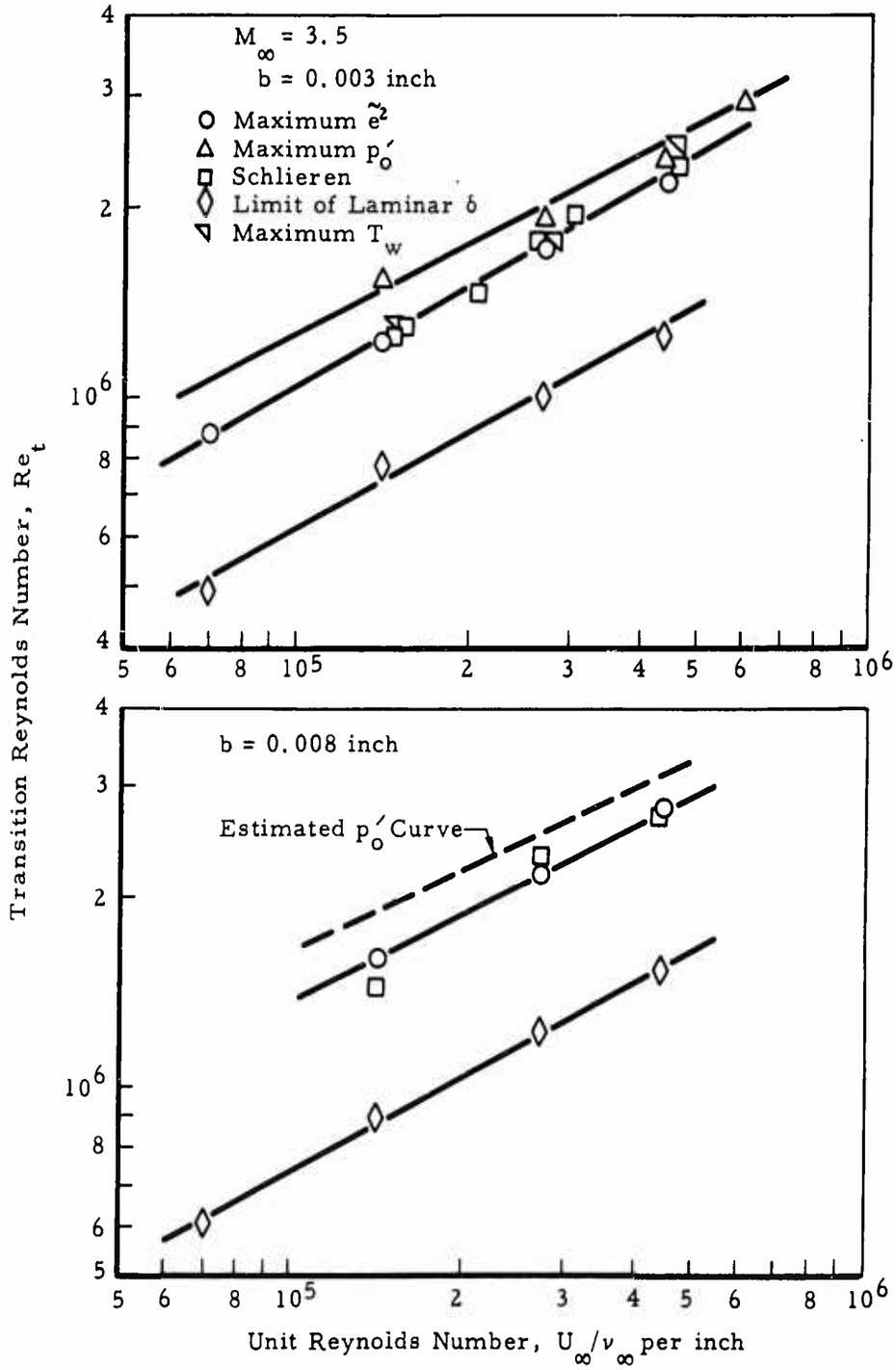

Fig. 10 Transition results at M_∞ = 3.5 for b = 0.003 inch and b = 0.008 inch

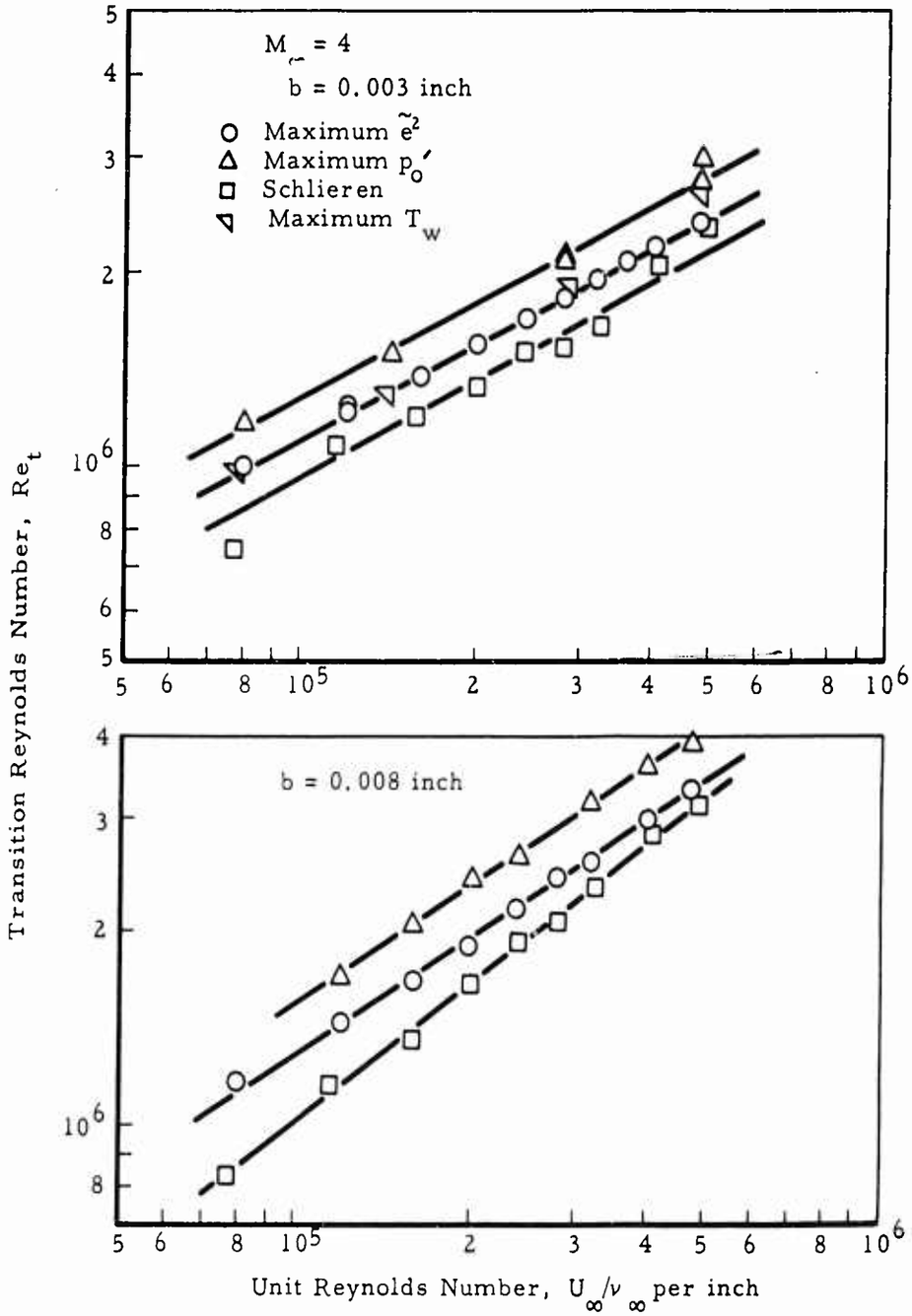

Fig. 11 Transition results at $M_\infty = 4$ for b = 0.003 inch and b = 0.008 inch

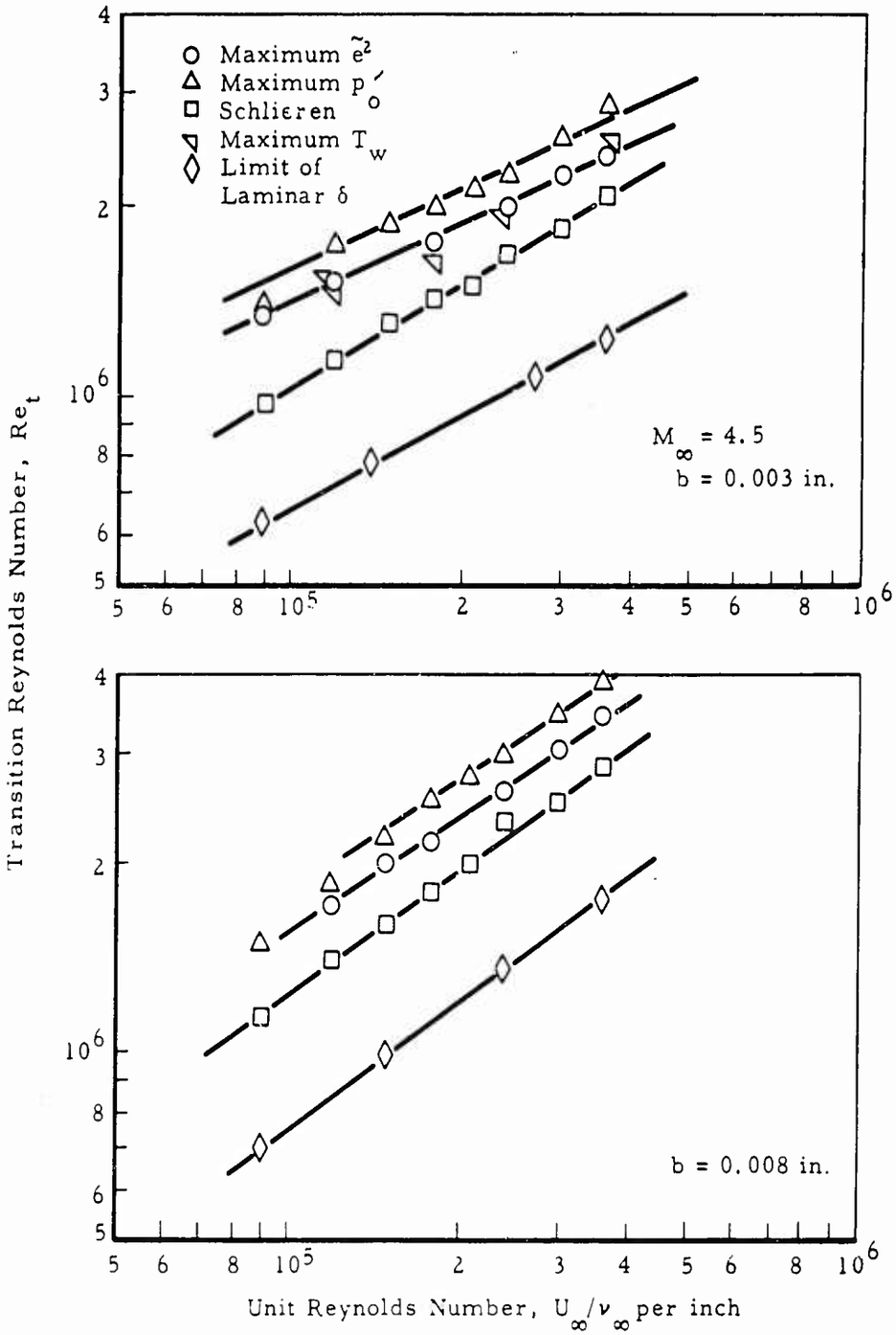

Fig. 12 Transition results at M_∞ = 4.5 for b = 0.003 inch and b = 0.008 inch

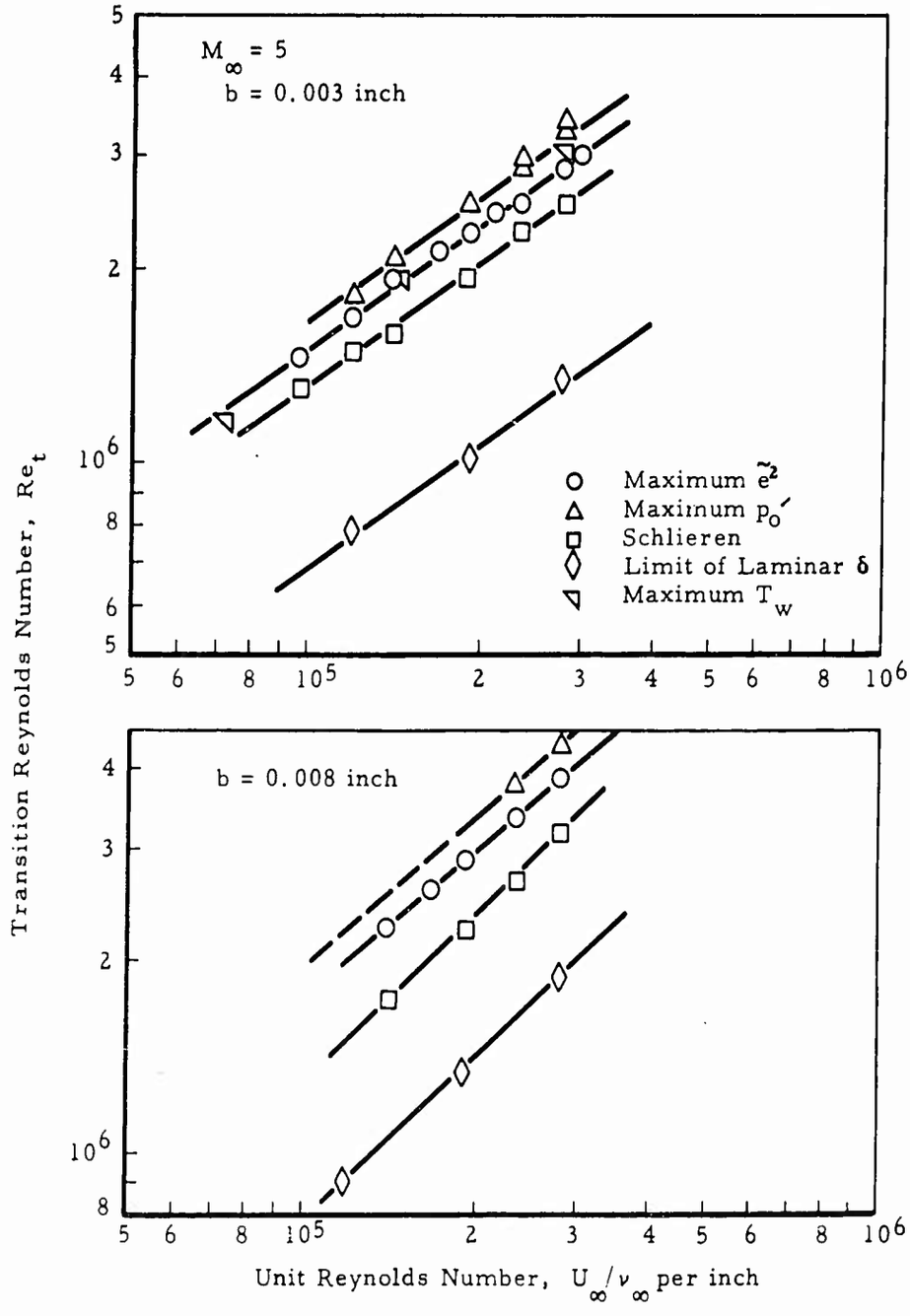

Fig. 13 Transition results at $M_\infty = 5$ for b = 0.003 inch and b = 0.008 inch

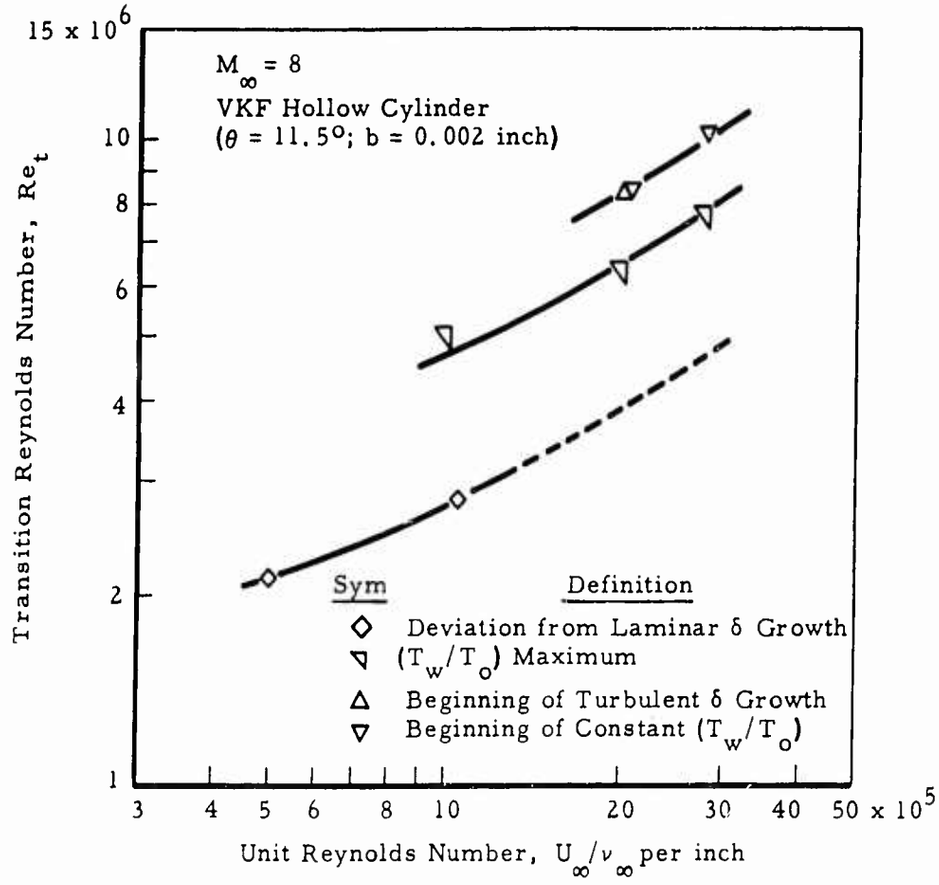

Fig. 14 Transition results at M_∞ = 8 for b = 0.002 inch

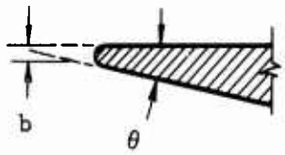

Hollow Cylinder Leading Edge

Open Symbols - 12-in. Tunnel; VKF ($\theta = 6^{\circ}$, b = 0.003 inch)
Solid Symbols - 50-in. Tunnel; VKF ($\theta = 11.5^{\circ}$, b = 0.002 inch)

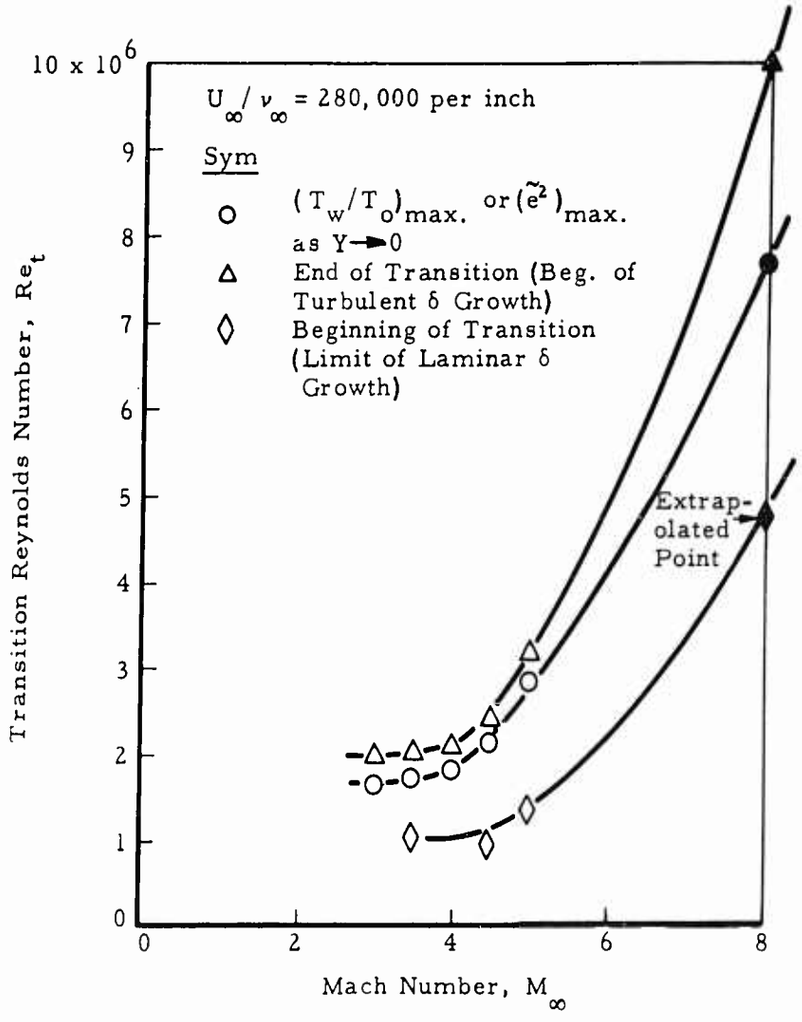

Fig. 15 Influence of Mach number on transition Reynolds number for U_{∞}/ν_{∞} = 280,000 per inch

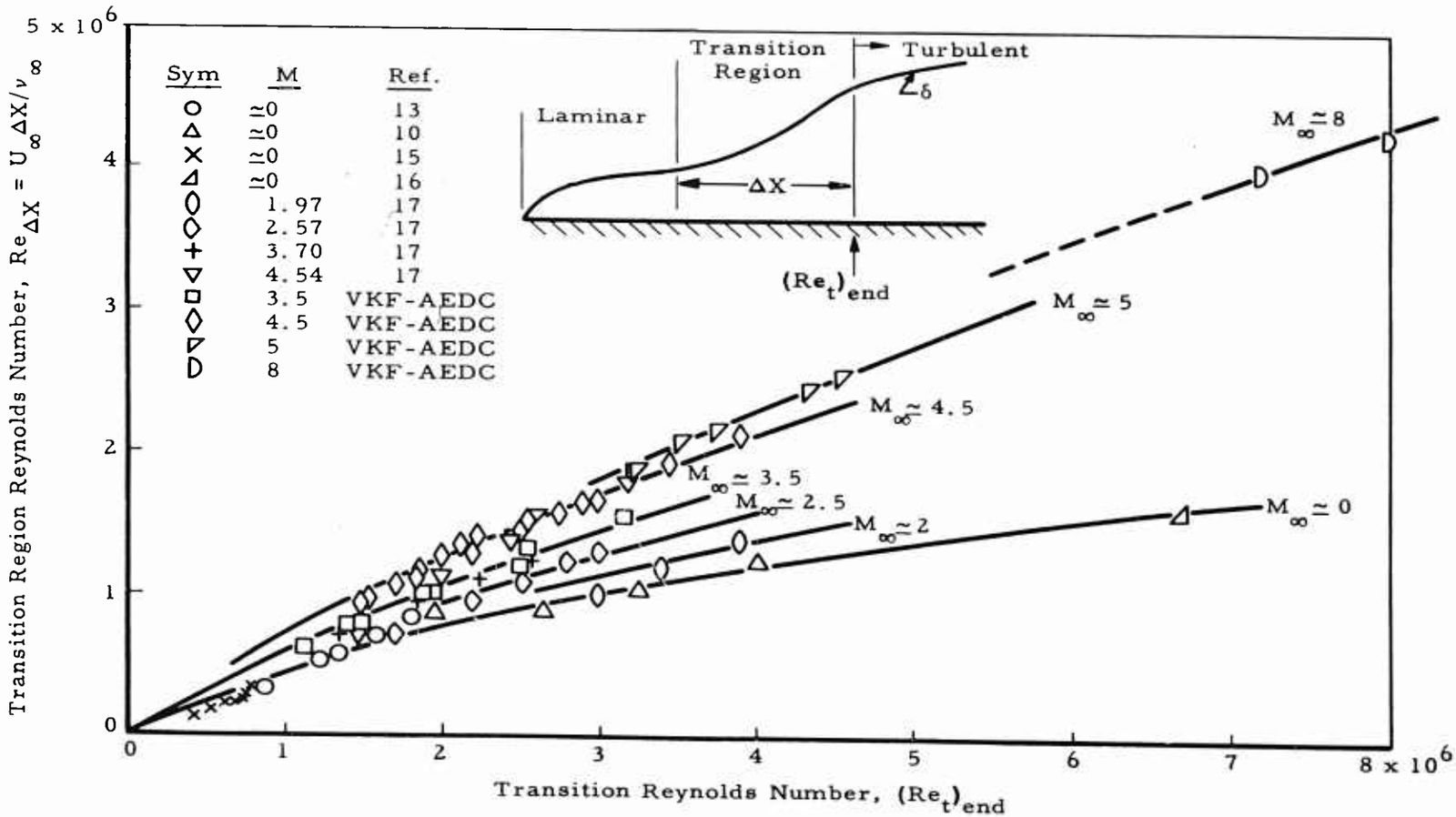

Fig. 16 Reynolds numbers of the transition region

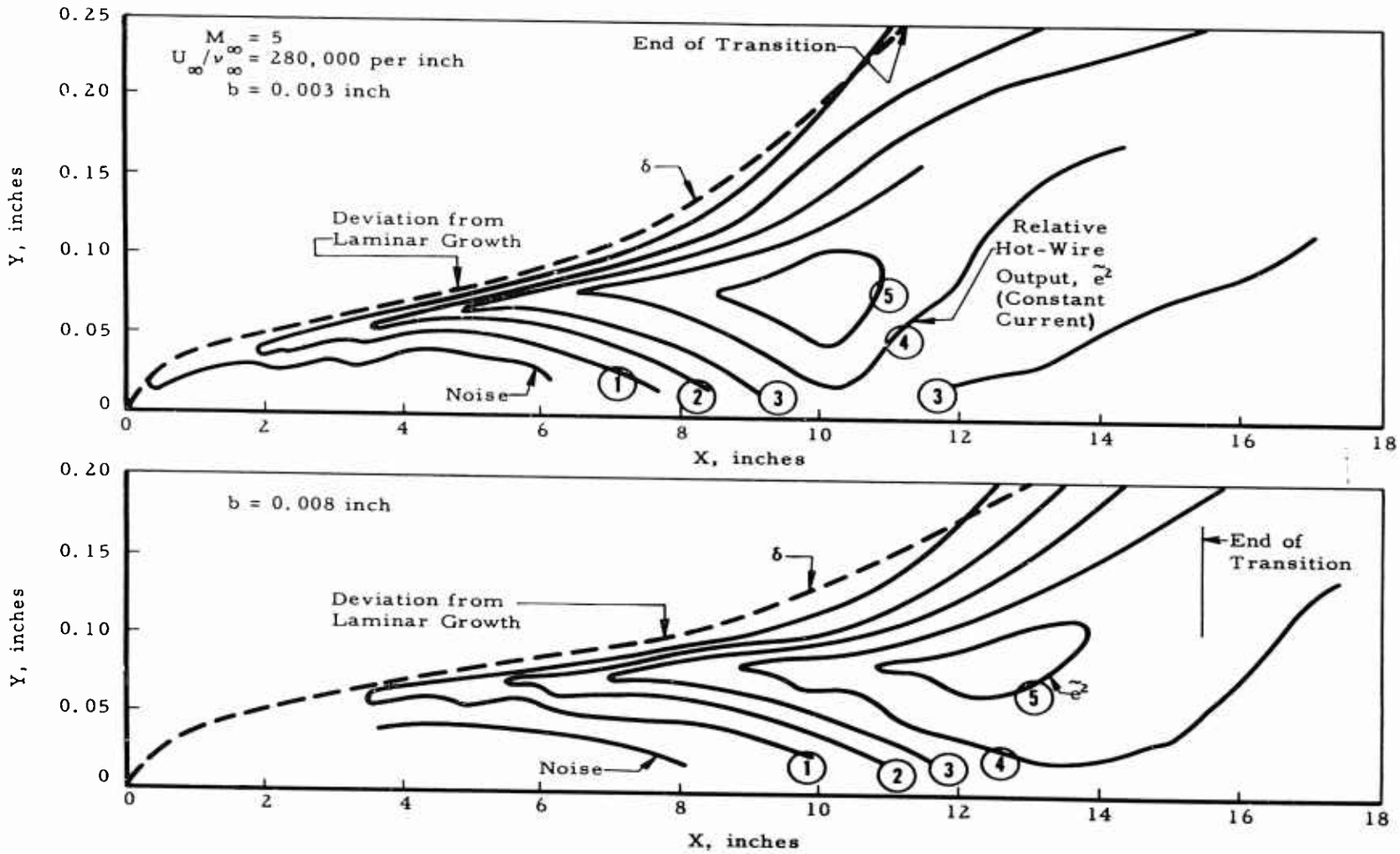

Fig. 17 Comparison of Isolines of hot-wire output for b = 0.003 inch and b = 0.008 inch at M_∞ = 5

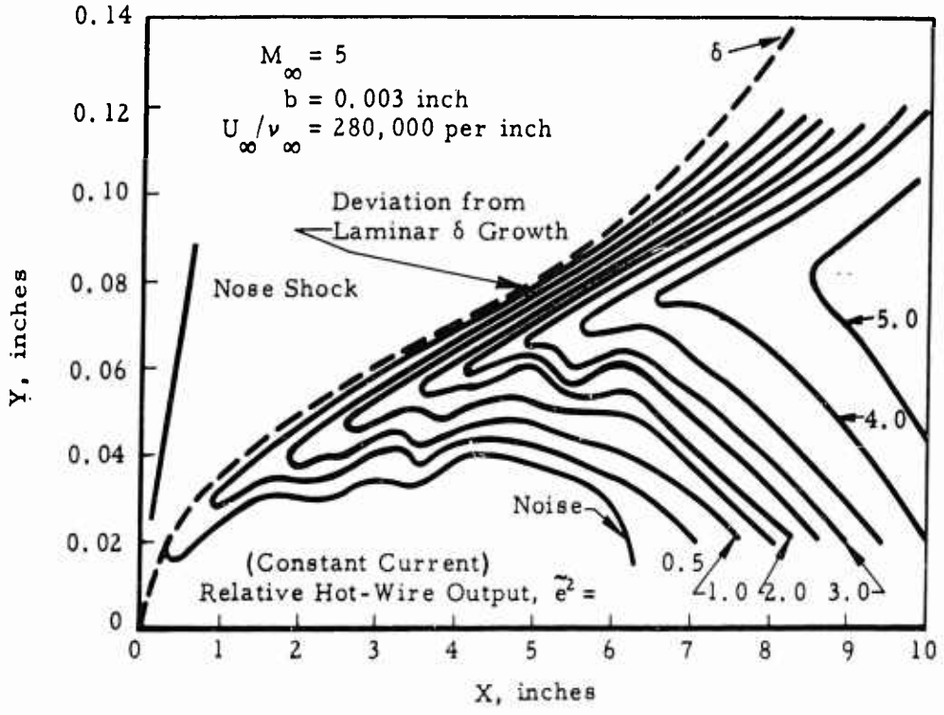

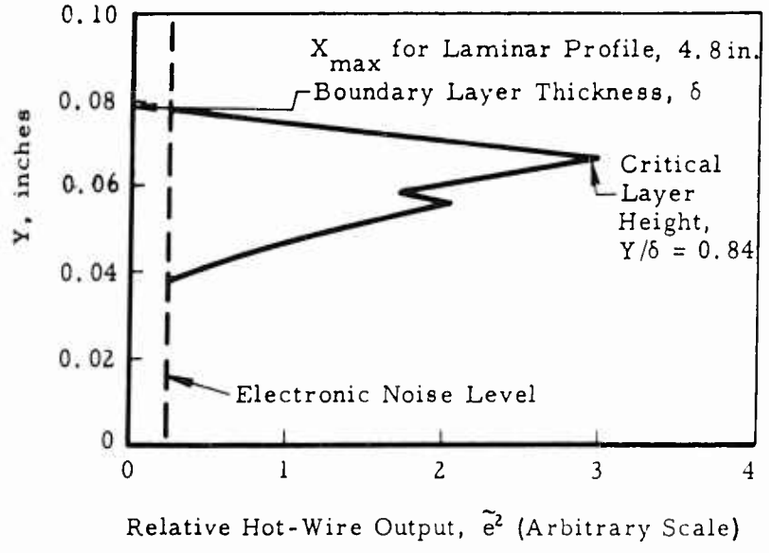

Fig. 18 Hot-wire output near leading edge for b = 0.003 inch and M_∞ = 5

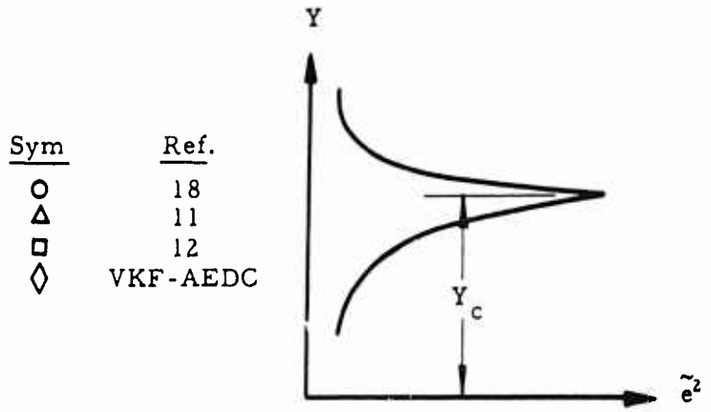

Definition of Critical Height, Y_c

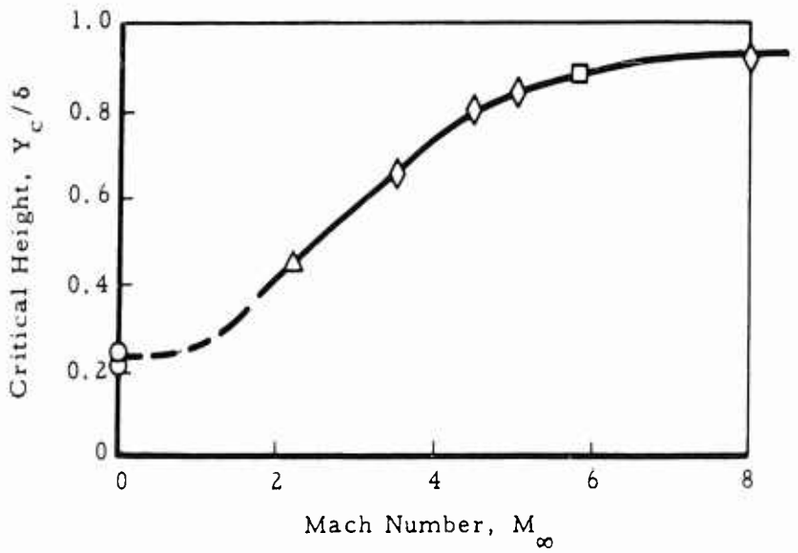

Fig. 19 Critical layer height as a function of Mach number

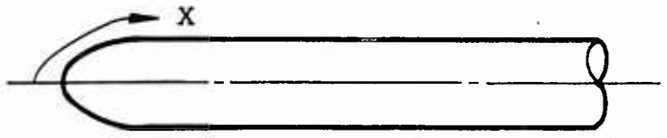

$M_\infty = 4.5$
X = 18 inches
U_∞/ν_∞ = 280,000 per inch

O- Constant Hot-Wire Current
---Estimated for Constant Wire Temperature

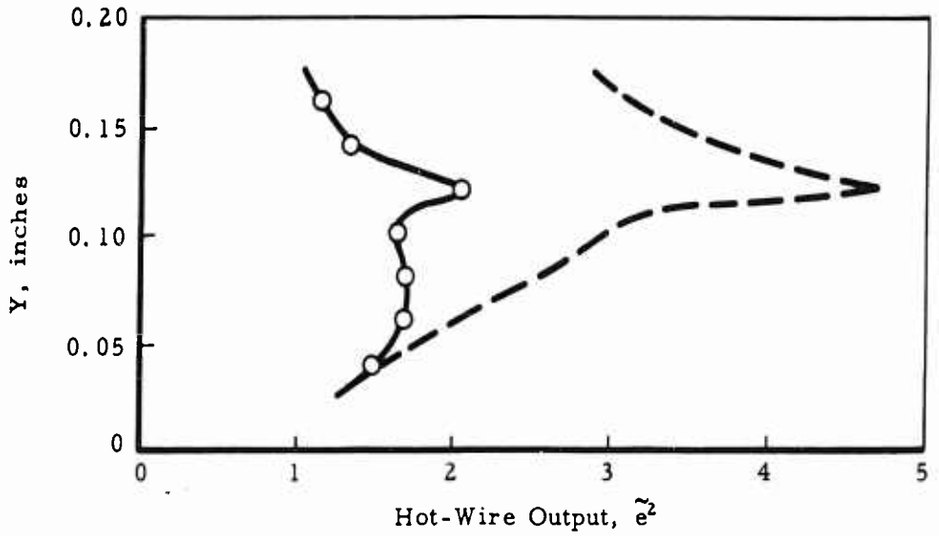

Fig. 20 Hot-wire output in boundary layer of a smooth-nose body of revolution

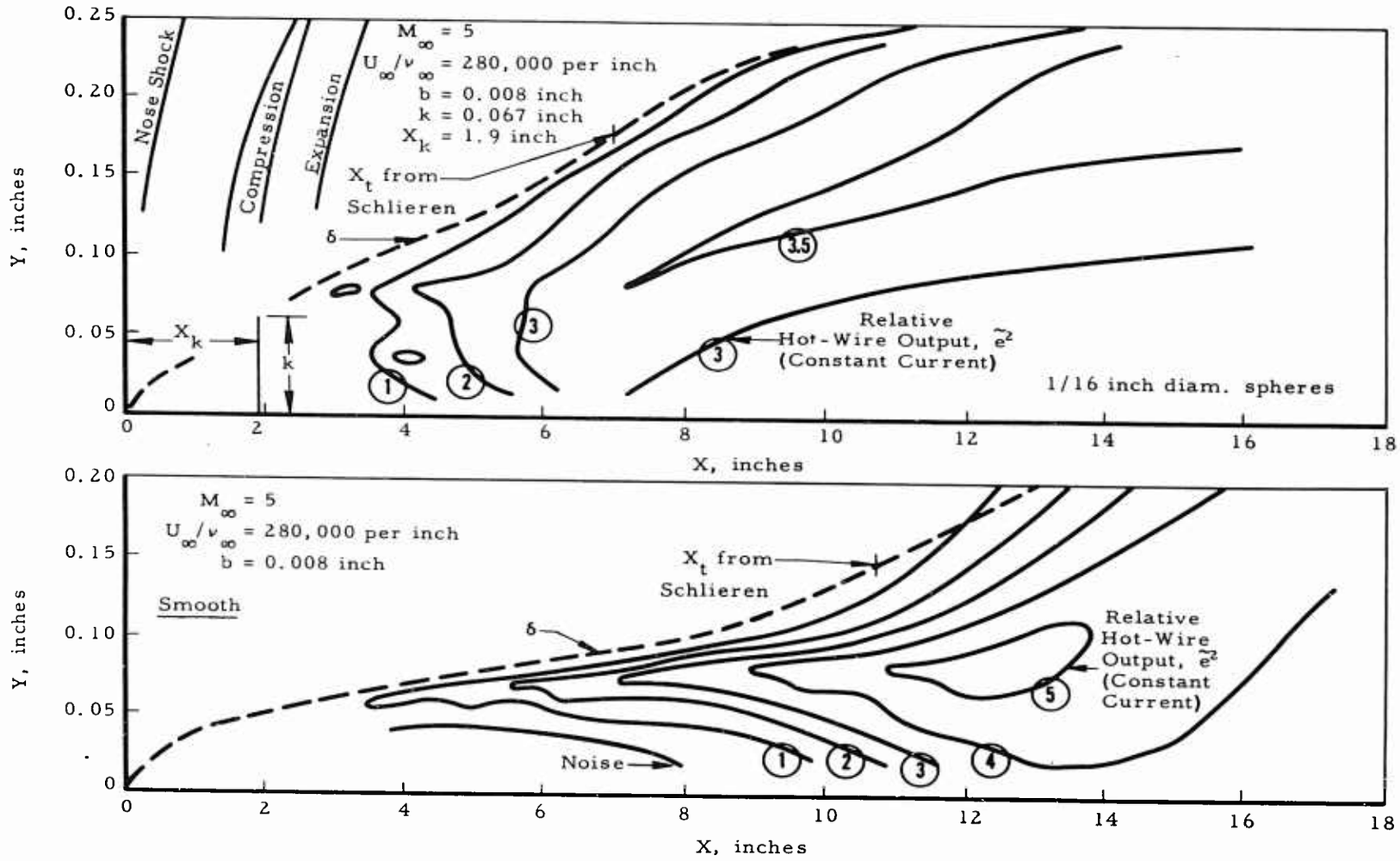

Fig. 21 Comparison of hot-wire outputs with and without surface roughness

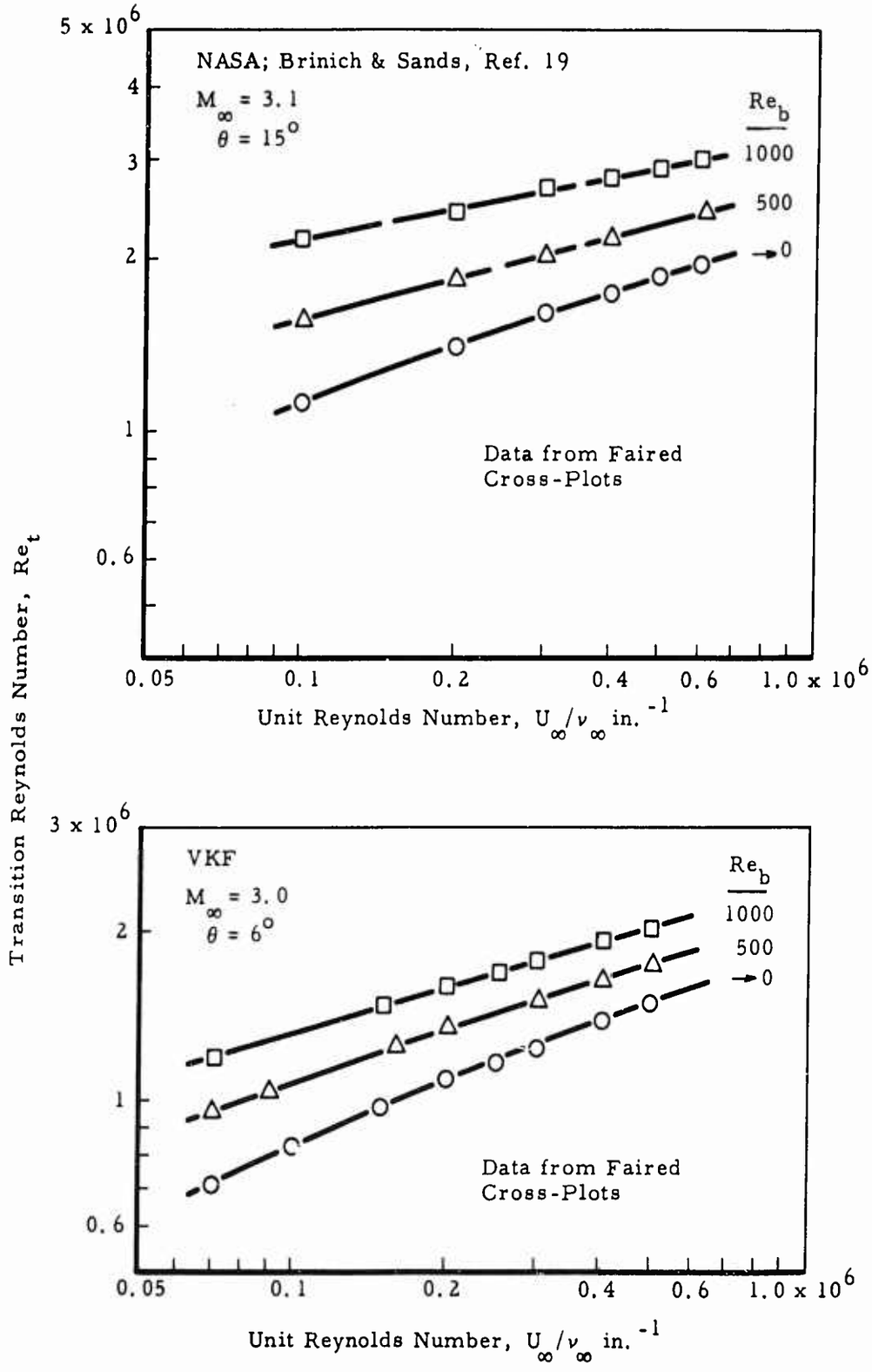

Fig. 22 Unit Reynolds number influence for various bluntness Reynolds numbers

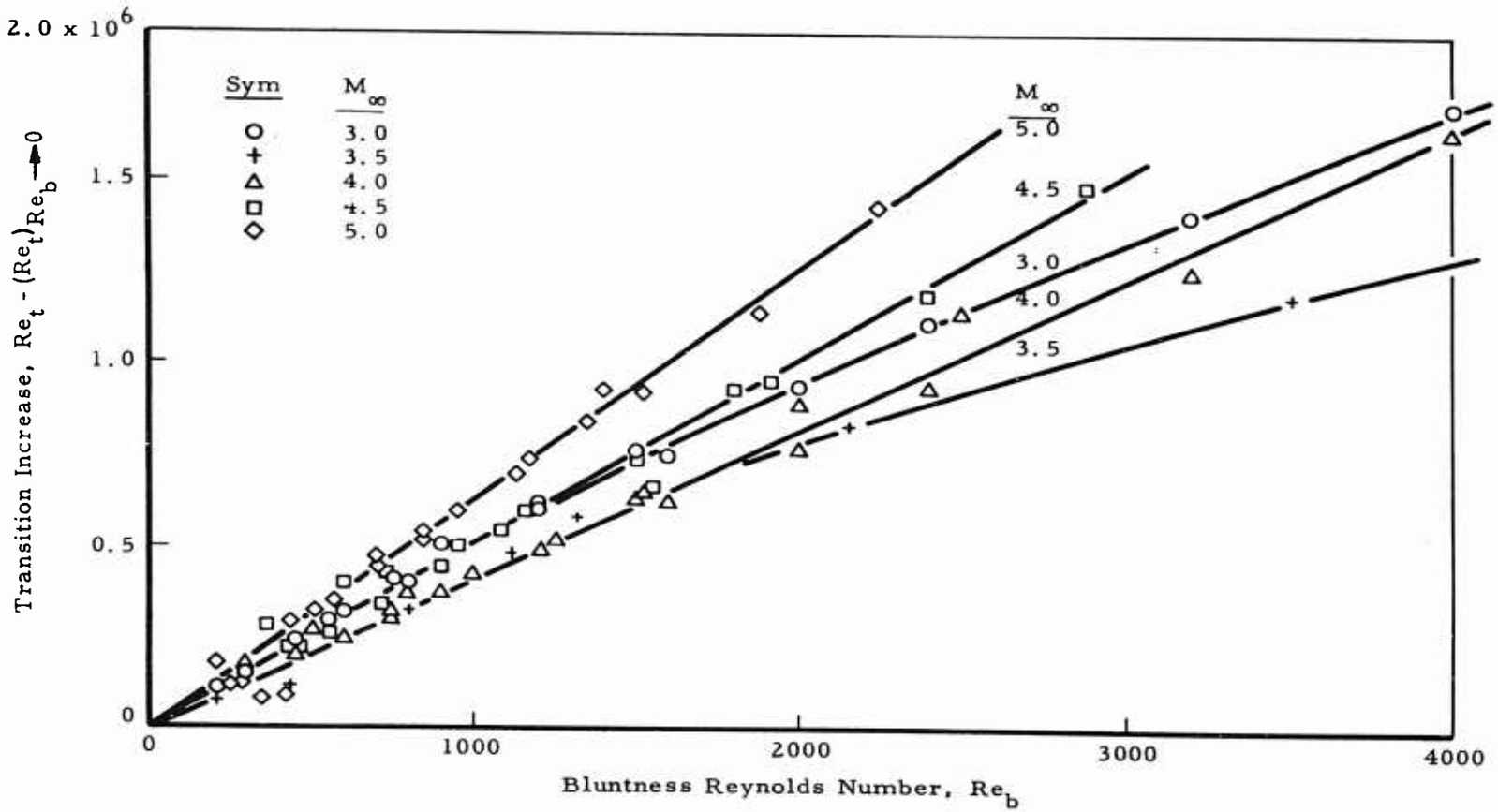

Fig. 23 Transition Reynolds number increase due to bluntness Reynolds number increase

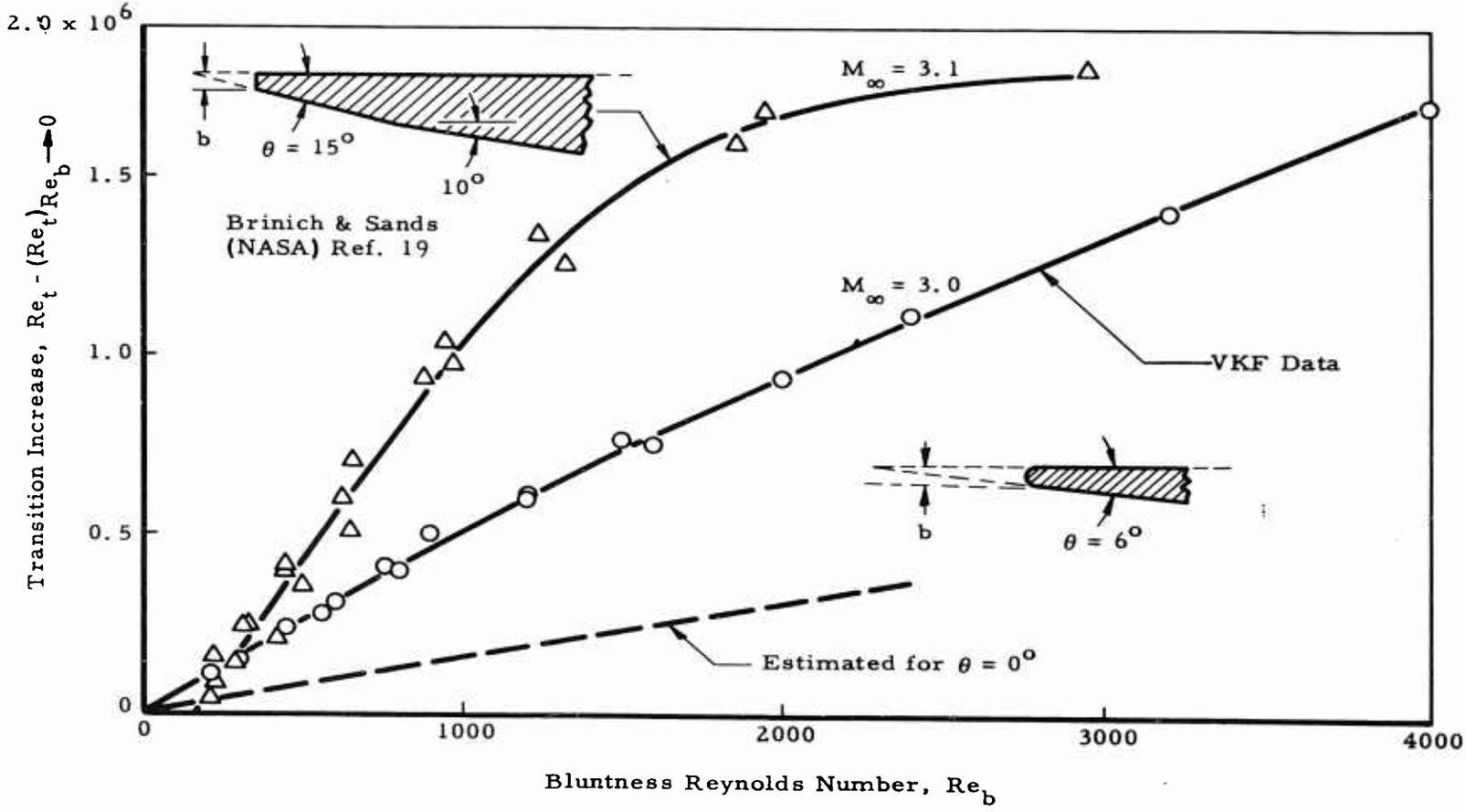

Fig. 24 Comparison of Brinich and Sands' data and VKF data

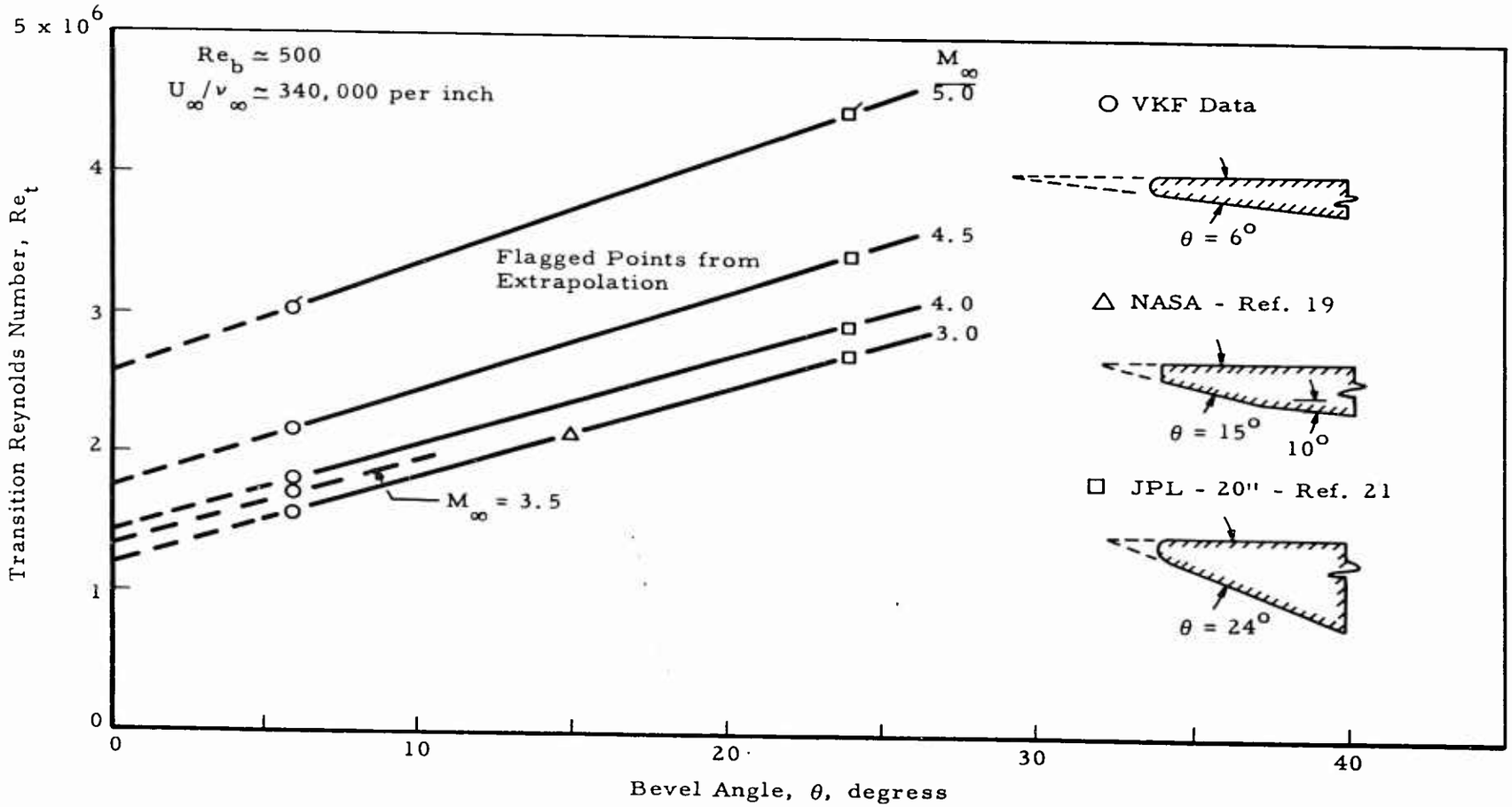

Fig. 25 Influence of bevel angle with Mach number as a parameter

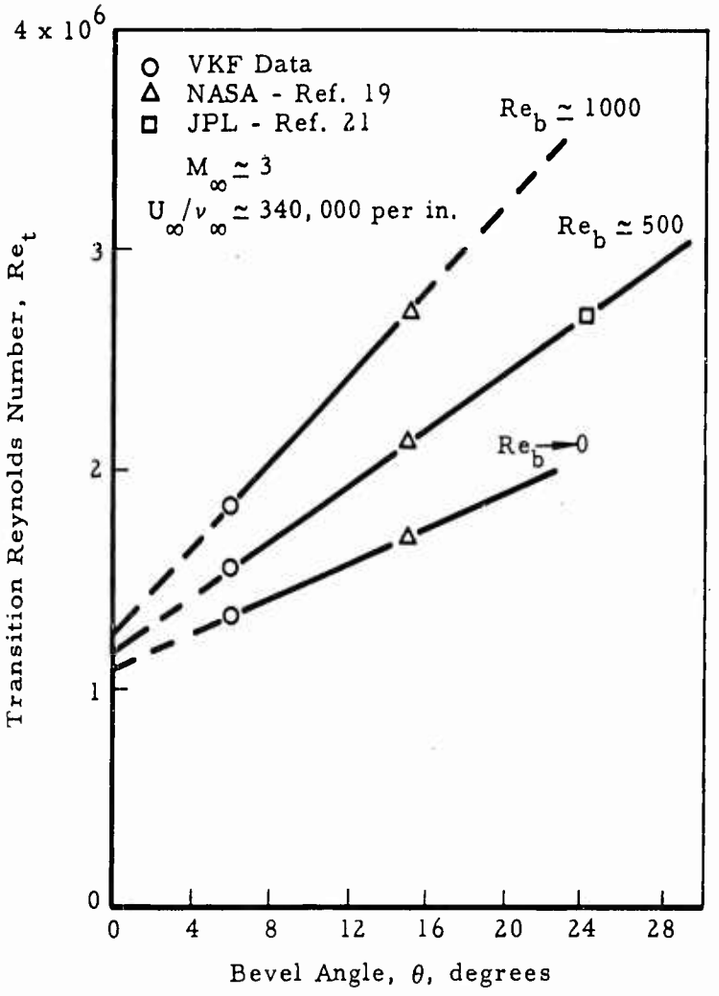

Fig. 26 Influence of bevel angle with bluntness Reynolds number as a parameter

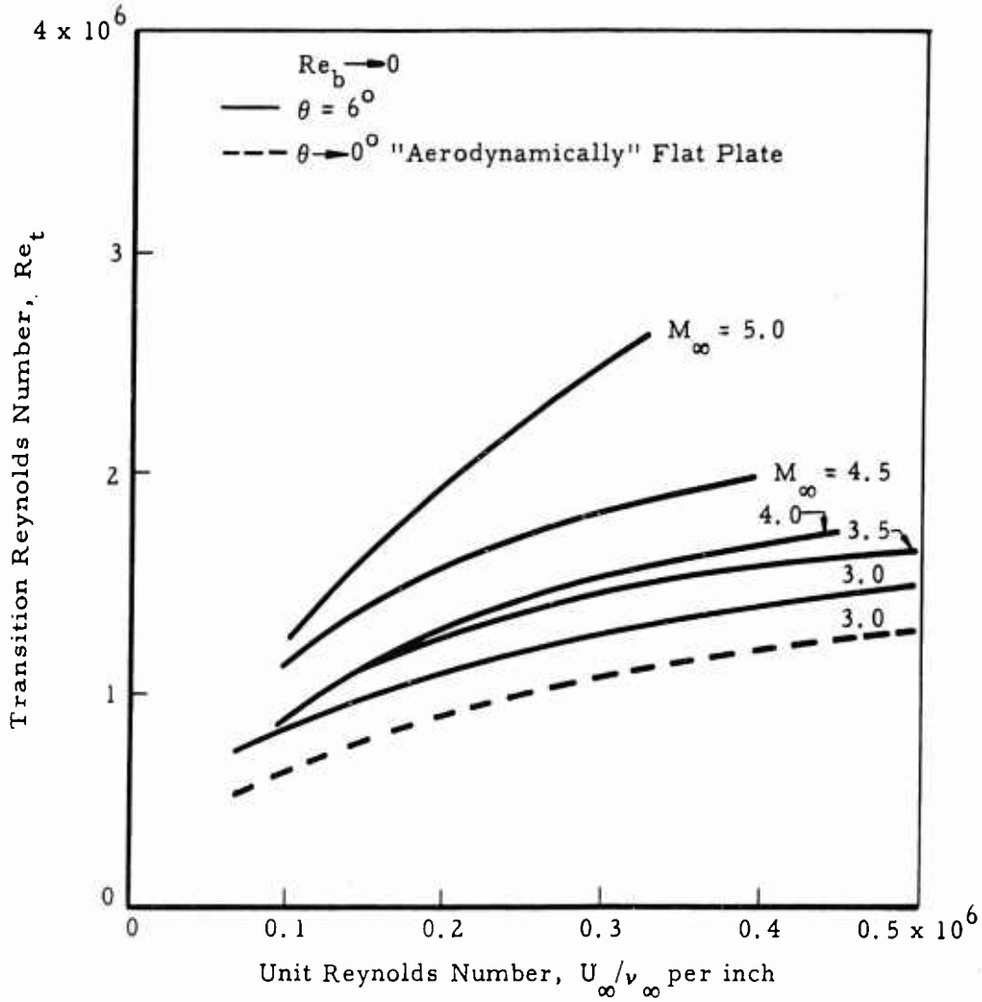

Fig. 27 Unit Reynolds number effect for various Mach numbers as $Re_b \rightarrow 0$

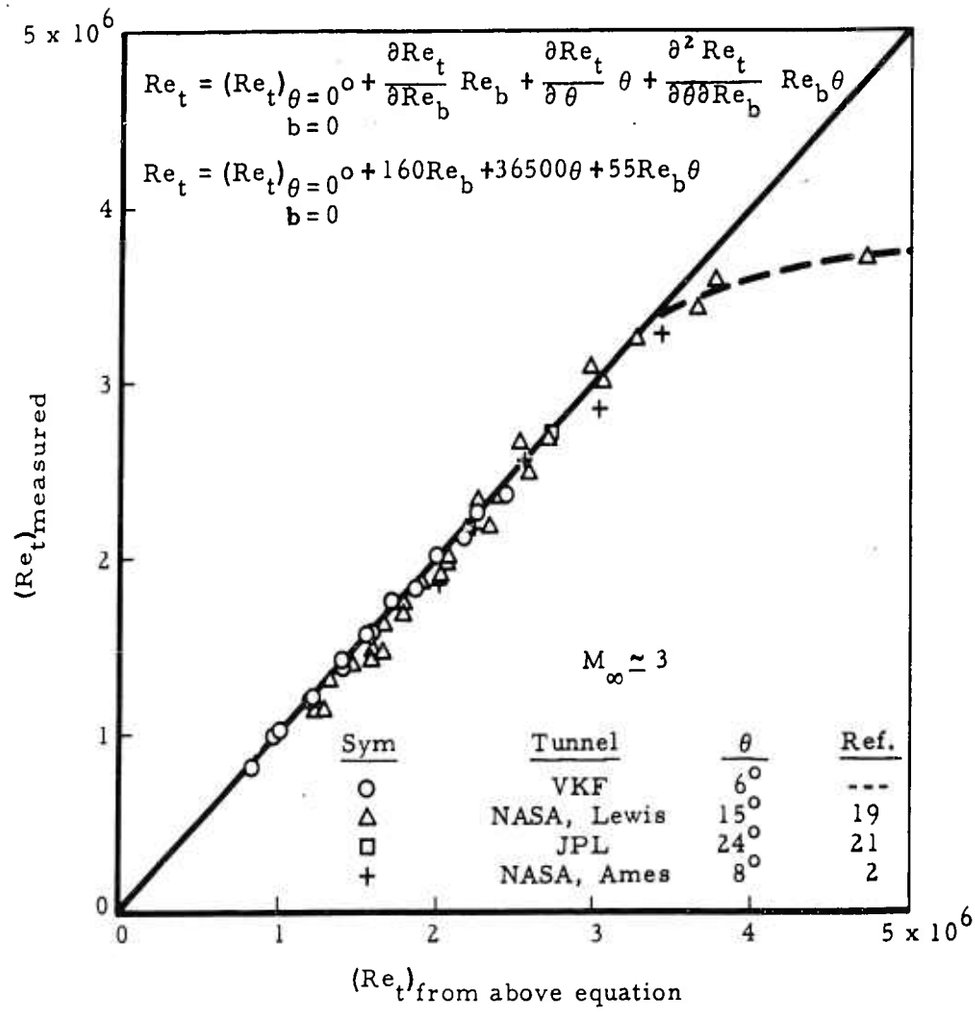

Fig. 28 Comparison of estimated and measured transition Reynolds number for $M_\infty \simeq 3$

Sym	Tunnel	Method	M_δ	Remarks	Ref.
○	VKF - 12"	Max. T_w/T_δ	2.7	10° Cone	—
△	JPL - 20"	Max. T_w/T_δ	2.7	5° Cone**	21
□	JPL - 12"	Max. T_w/T_δ	2.7	10° Cone	24
◇	JPL - 12"	Schlieren	2.7	10° Cone	24
◁	NASA (Lewis 12")	Max. T_w/T_δ	3.0	10° Cone	19
◣	——	Max. T_w/T_δ	*		

* Corrected to $M_\delta = 2.7$ **From Faired Curve

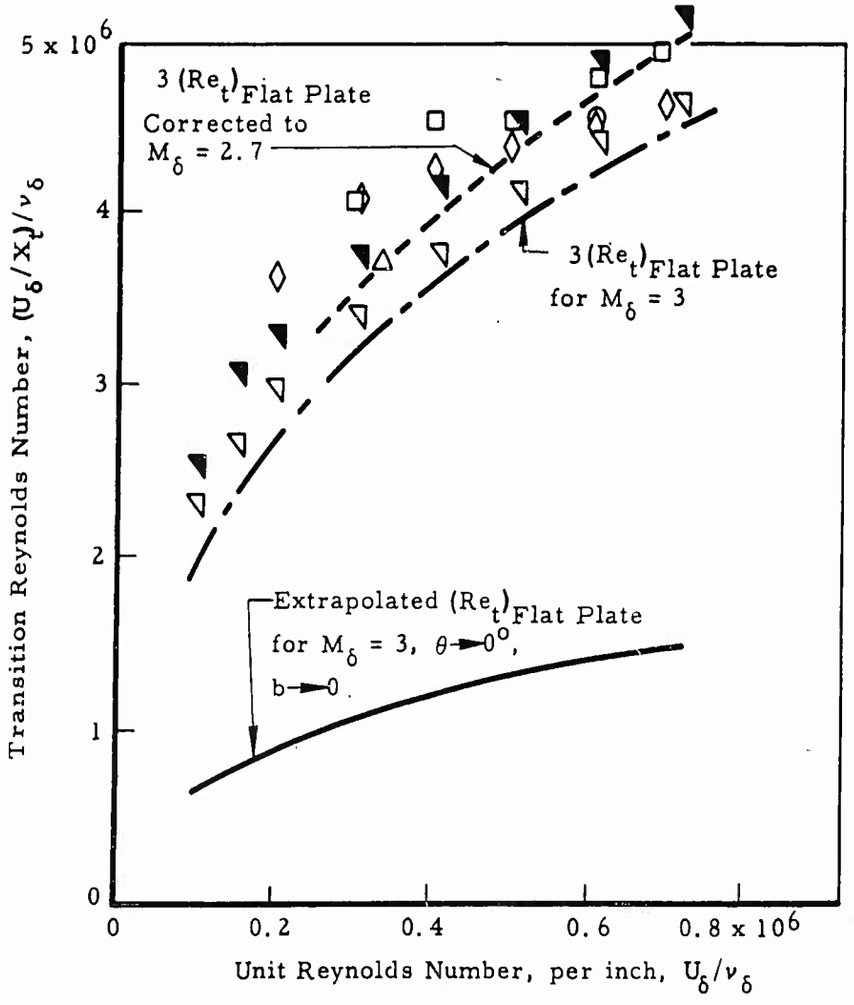

Fig. 29 Comparison of transition data from various wind tunnels and comparison of flat plate and cone transition data

$$Re'_k \text{ or } Re^*_k = Re_k \times f(M_k)$$

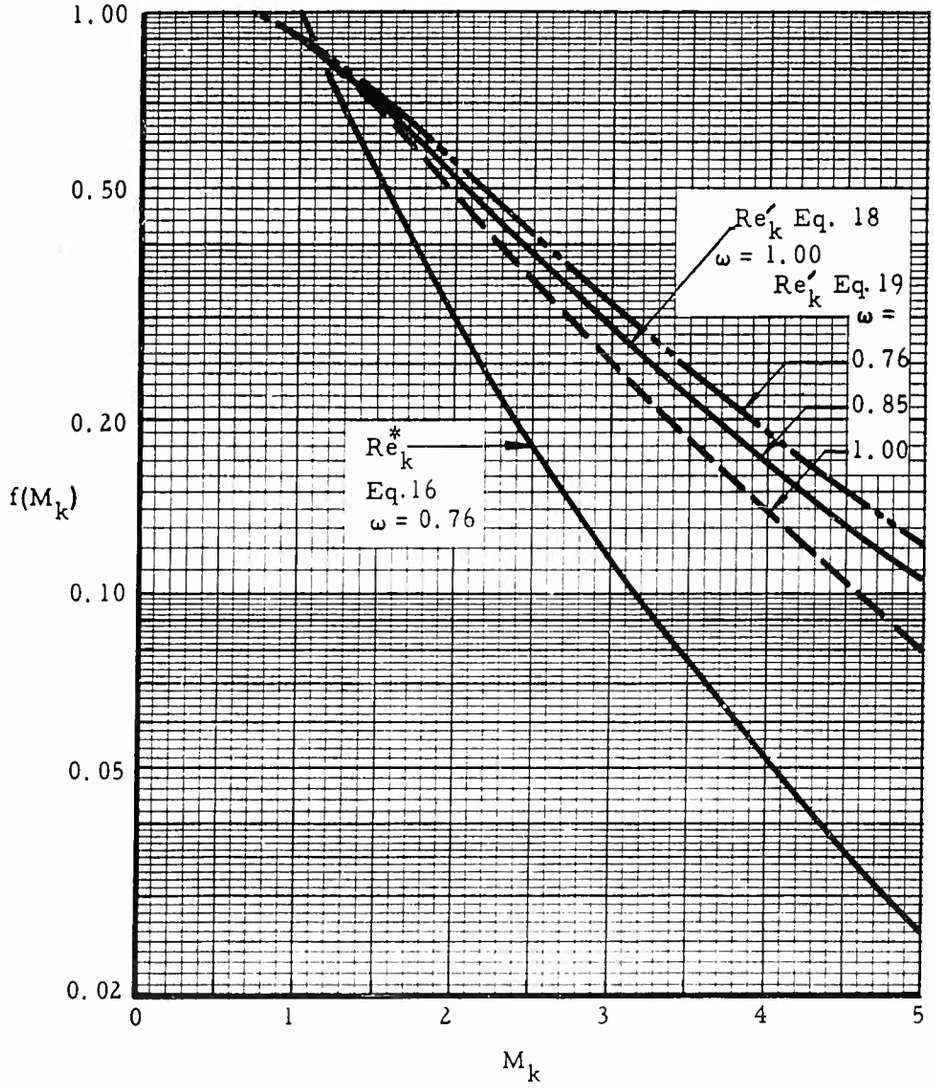

Fig. 30 Effective Reynolds numbers of roughness

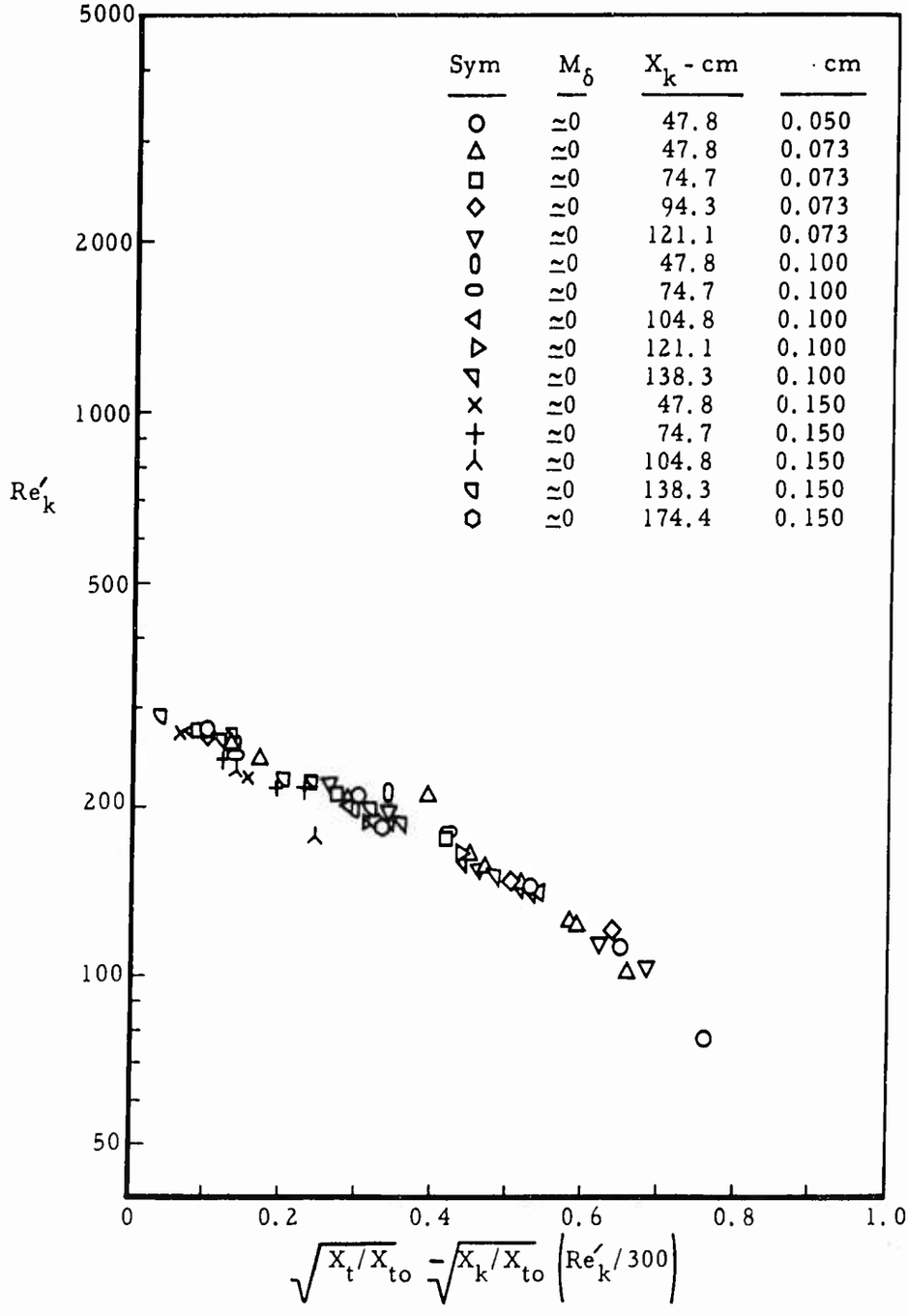

Fig. 31 Correlation of data for single wires on flat plates, $M_\delta \rightarrow 0$, Reference 29

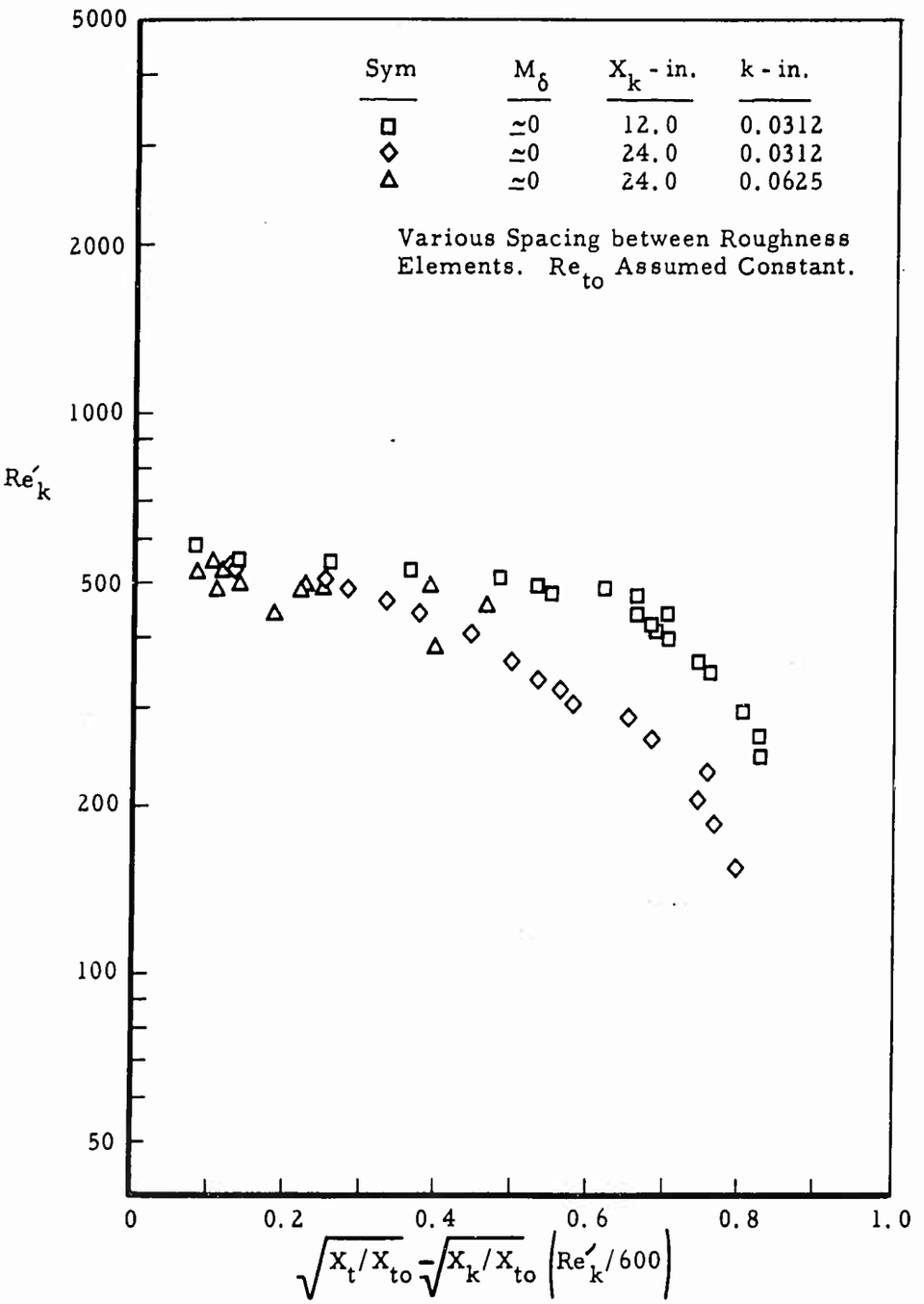

Fig. 32 Correlation of data for single row of spheres on flat plates, $M_\delta \rightarrow 0$, Reference 26

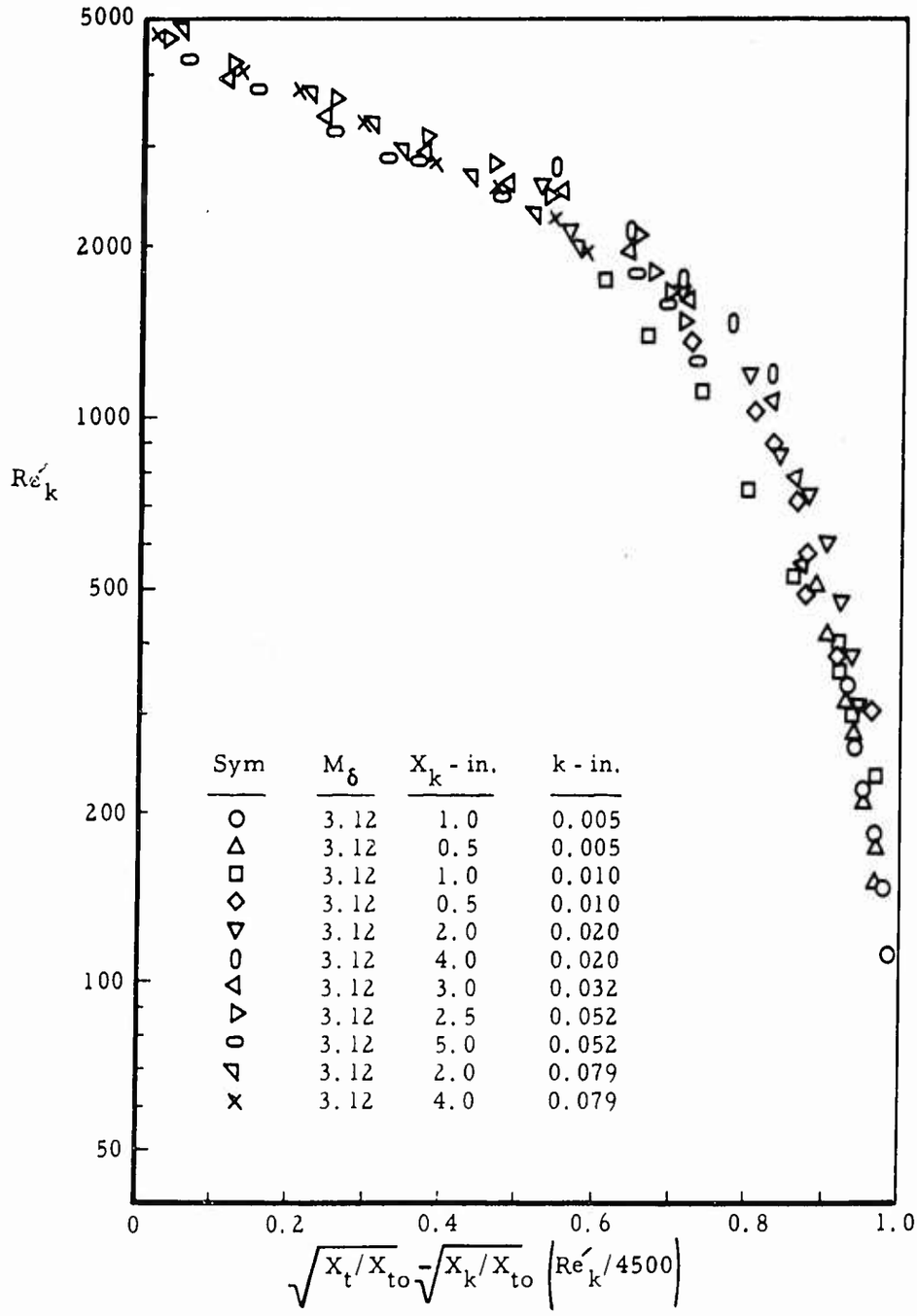

Fig.33 Correlation of data for single wires on hollow cylinders, M_δ = 3.12, Reference 36

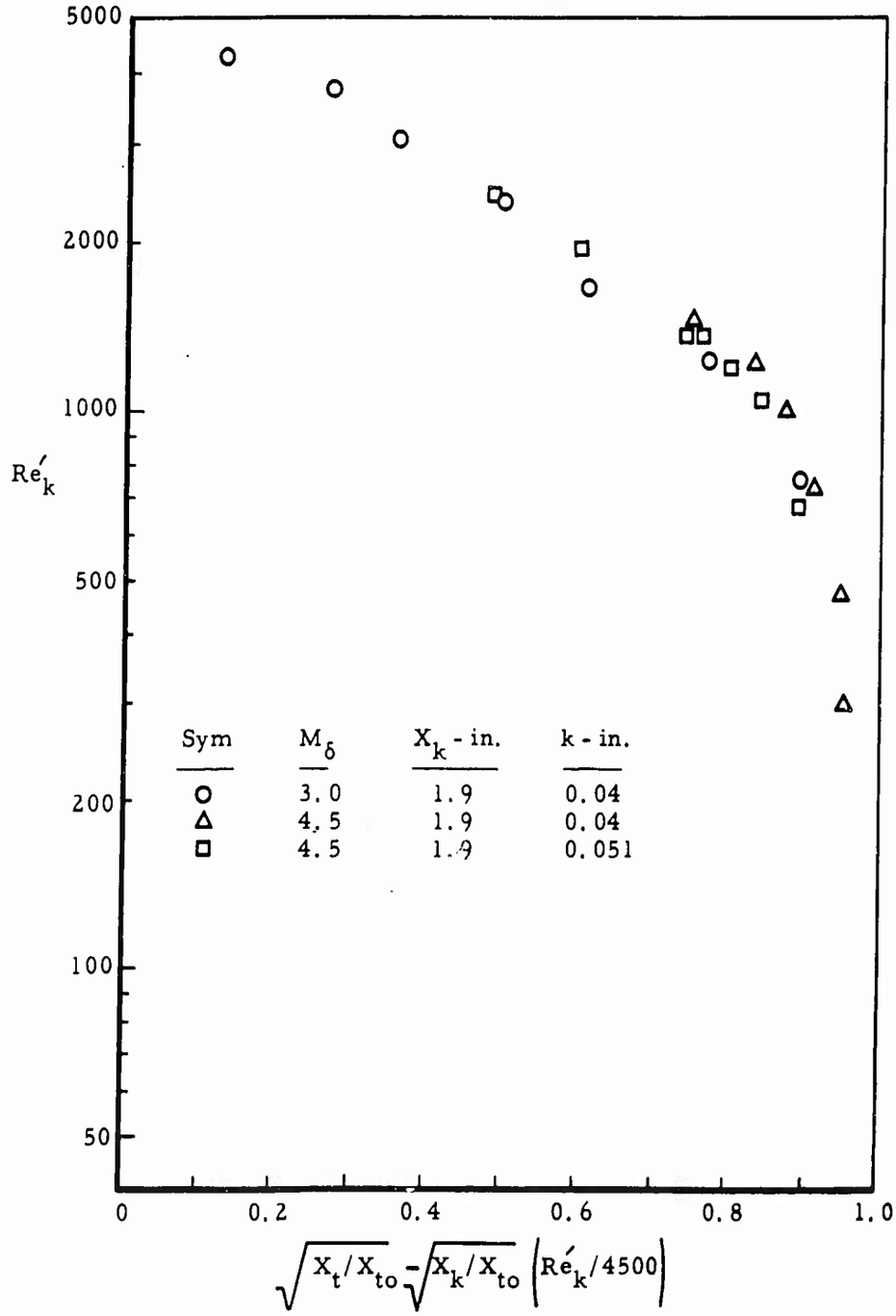

Fig. 34 Correlation of data for single wires on hollow cylinders, M_δ = 3.0 - 4.5, VKF data

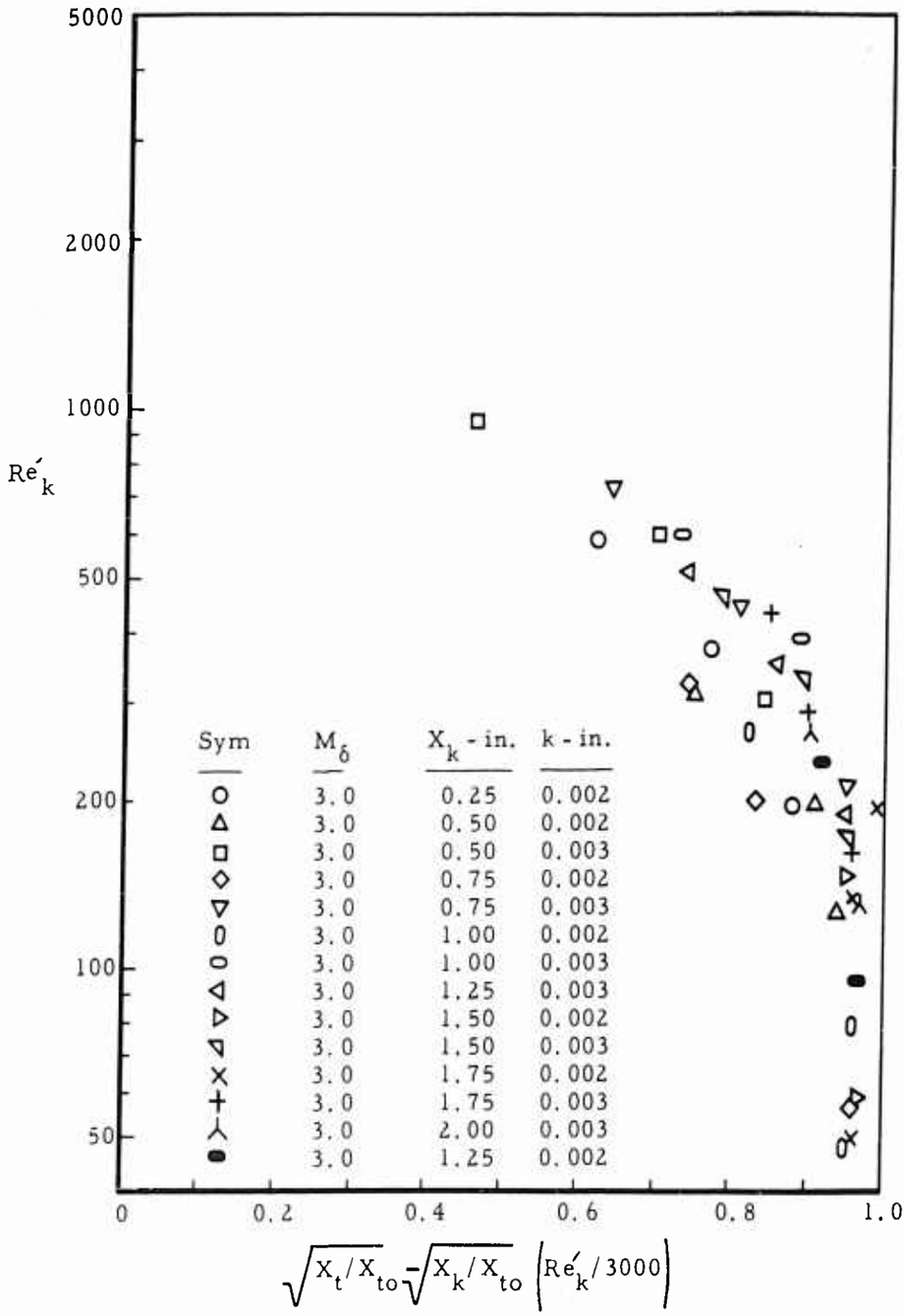

Fig. 35 Correlation of data for band of grit on flat plate, M_δ = 3.0, Reference 37 (Table 1a)

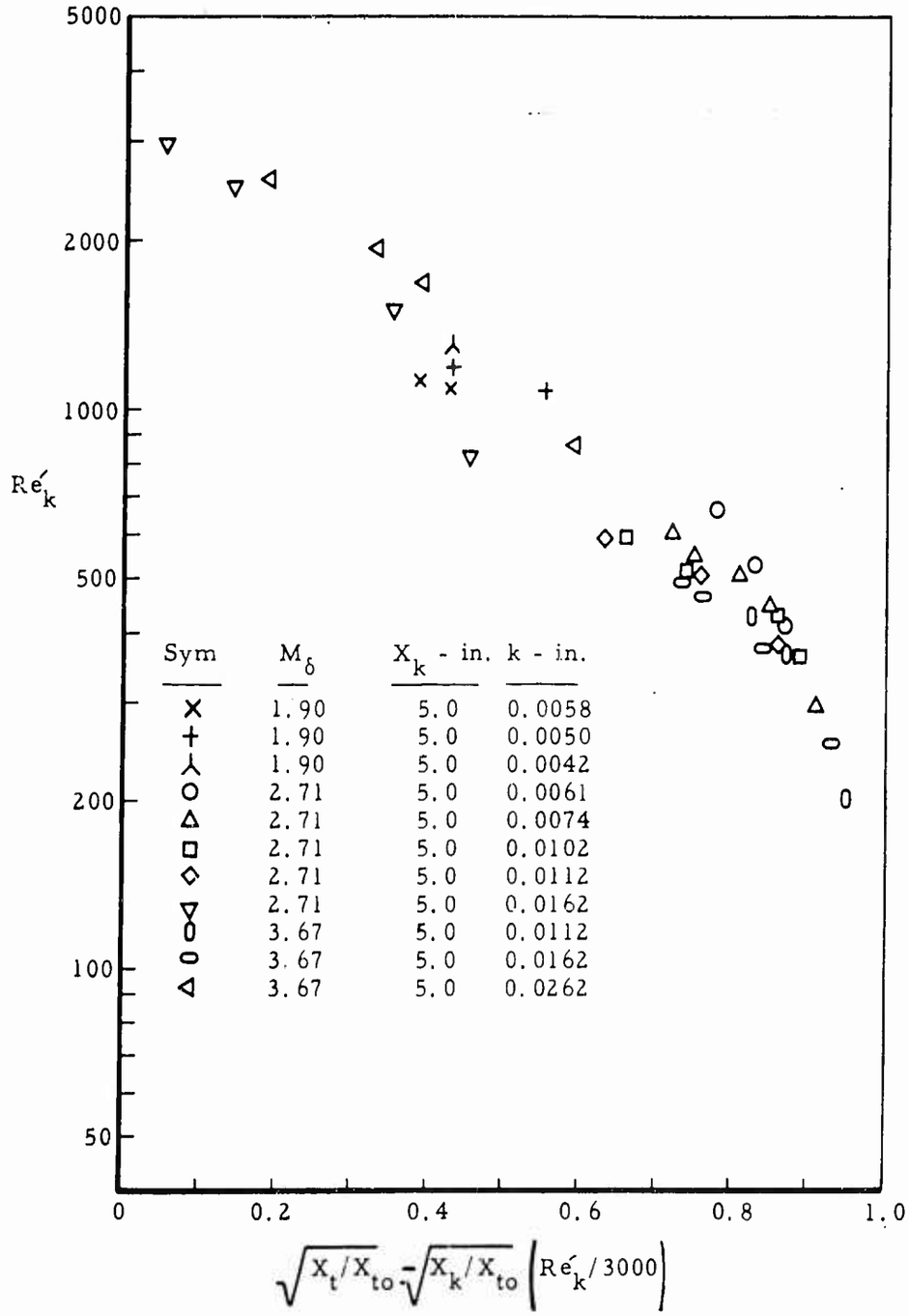

Fig.36 Correlation of data for single row of spheres on cones, M_δ = 1.9 - 3.67, Reference 24

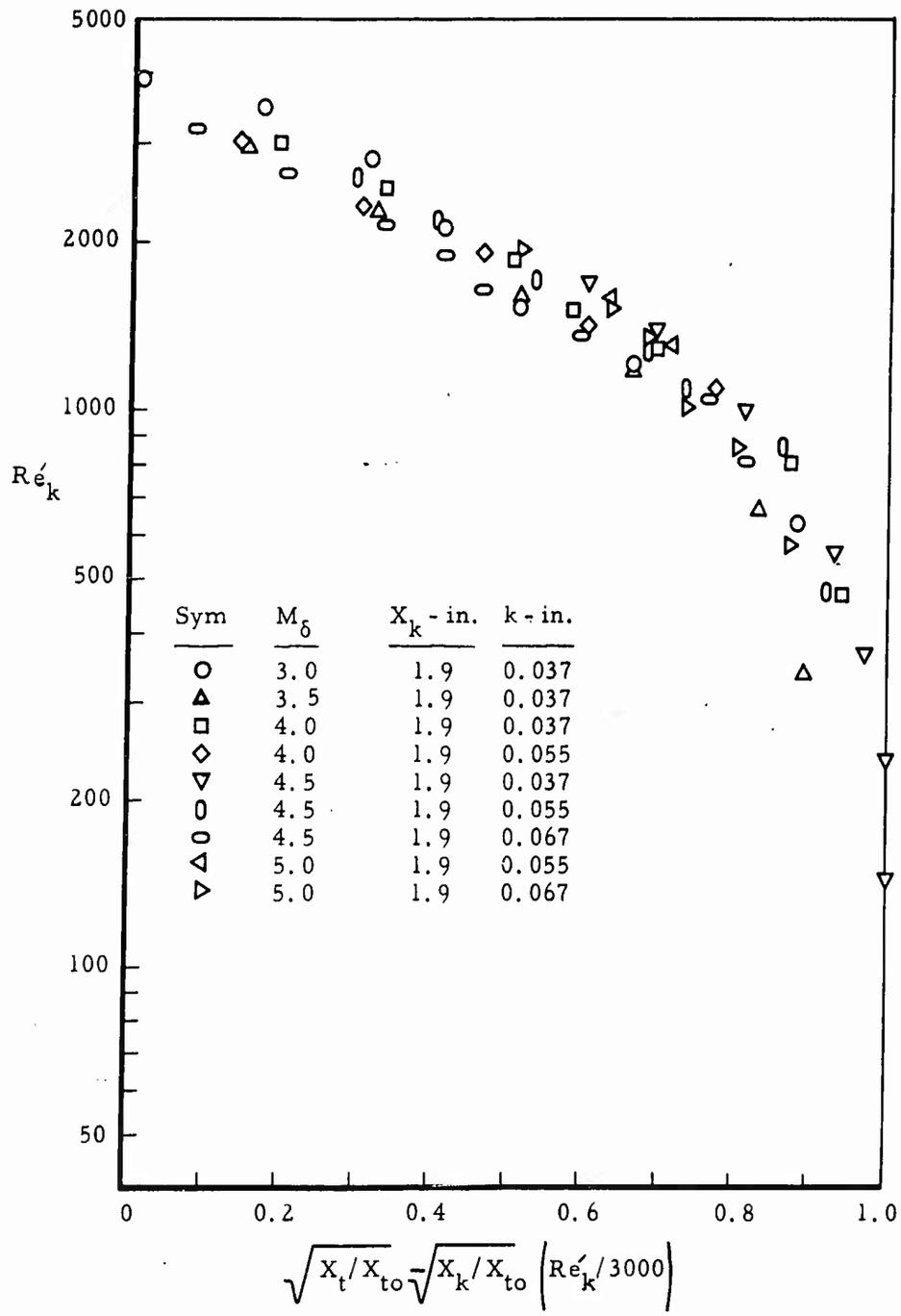

Fig. 37 Correlation of data for single row of spheres on hollow cylinders, M_δ = 3.0 - 5.0, VKF data

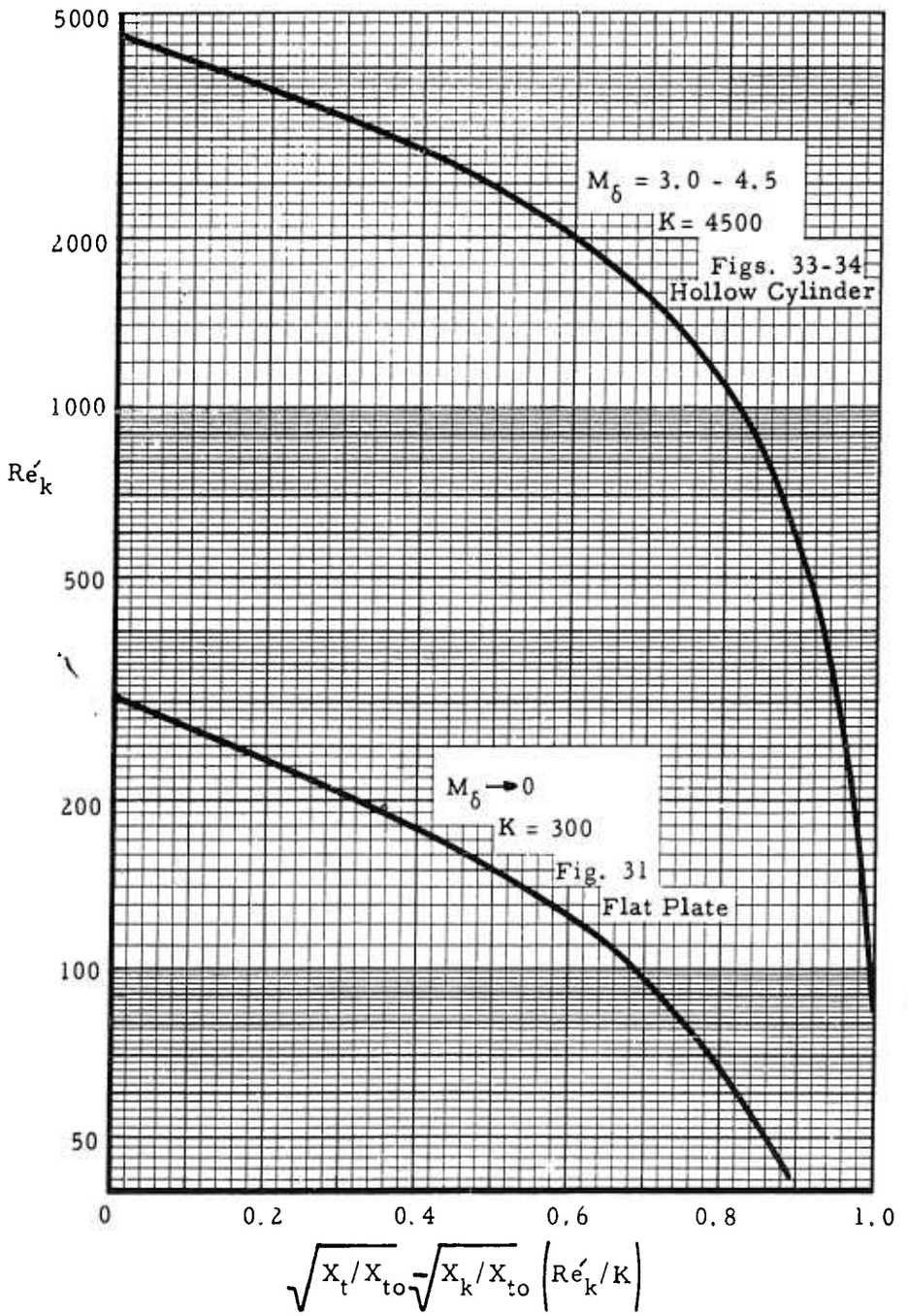

Fig.38 Faired correlation curves for single wires on bodies with zero pressure gradient

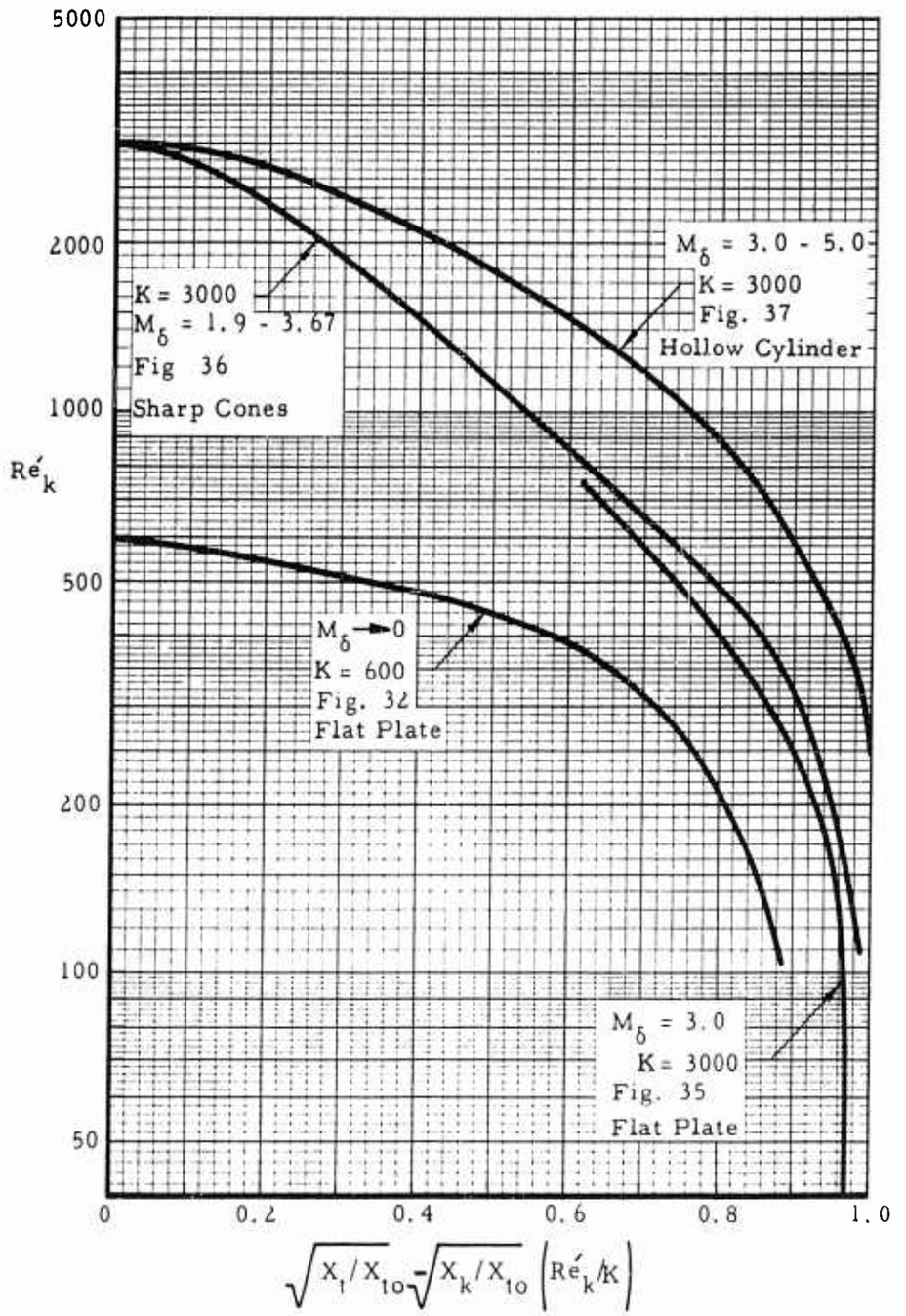

Fig. 39 Faired correlation curves for two types of three-dimensional elements (as noted) on bodies with zero pressure gradient

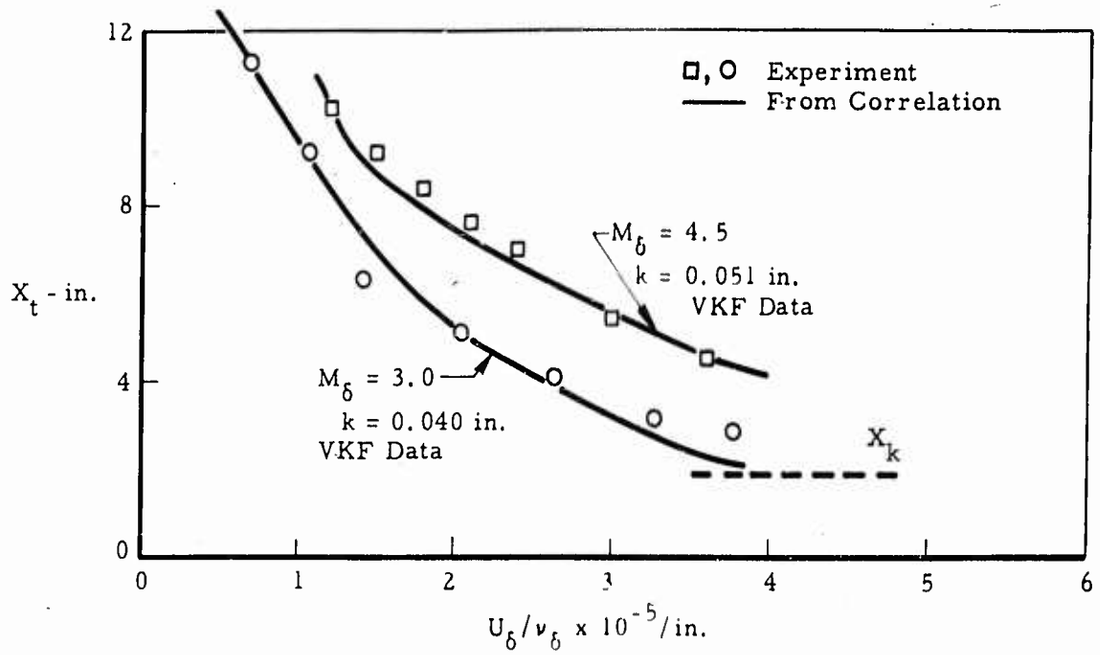

Fig. 40a Application of correlation-wires on cylinders

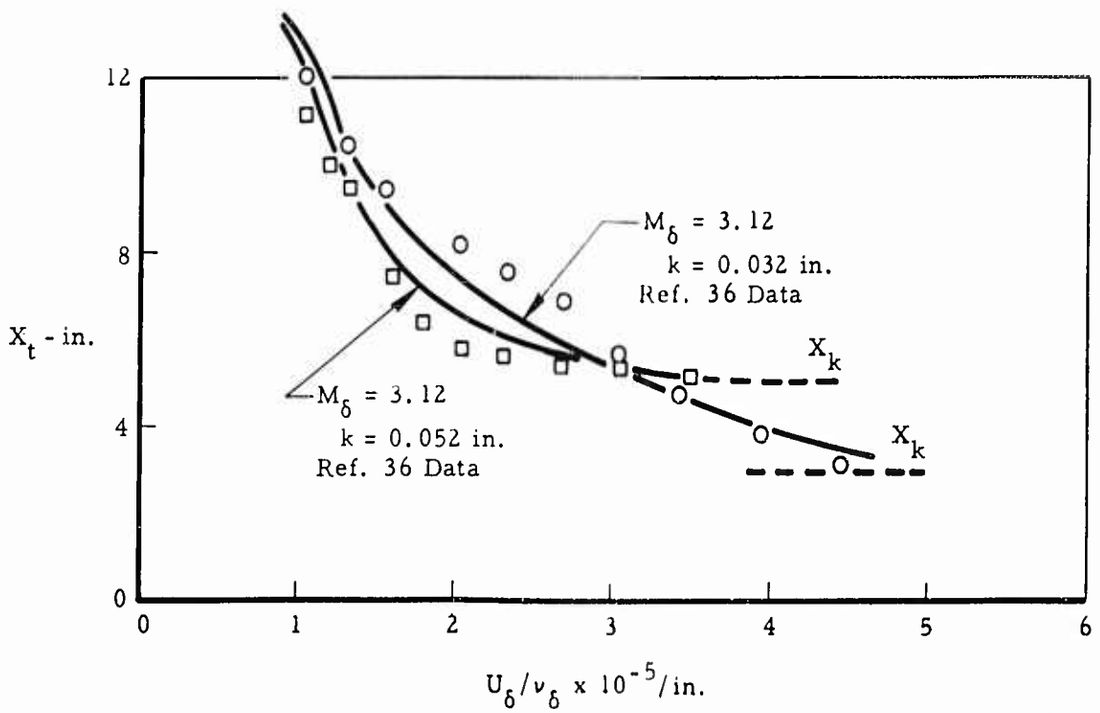

Fig. 40b Application of correlation-wires on cylinders

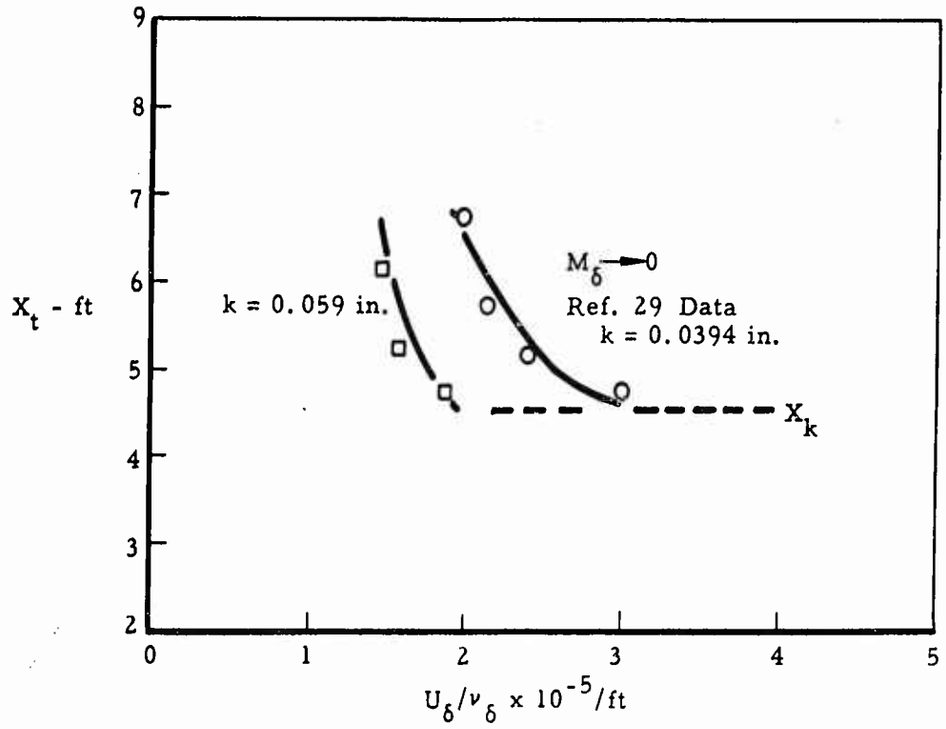

Fig. 40c Application of correlation-wires on plates

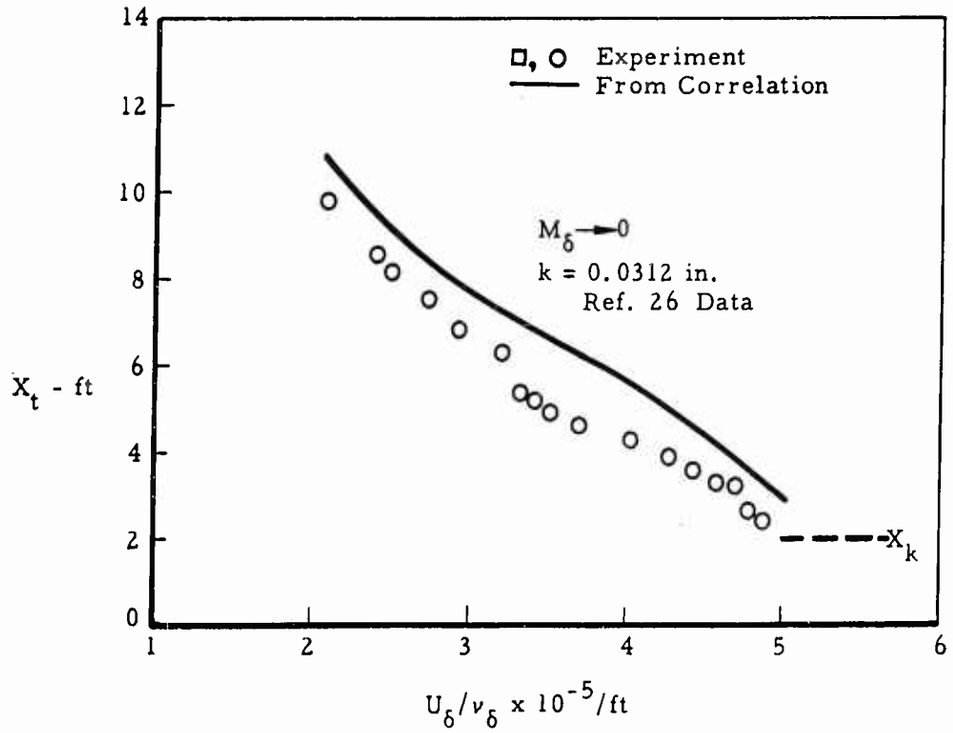

Fig. 41a Application of correlation-spheres on plates

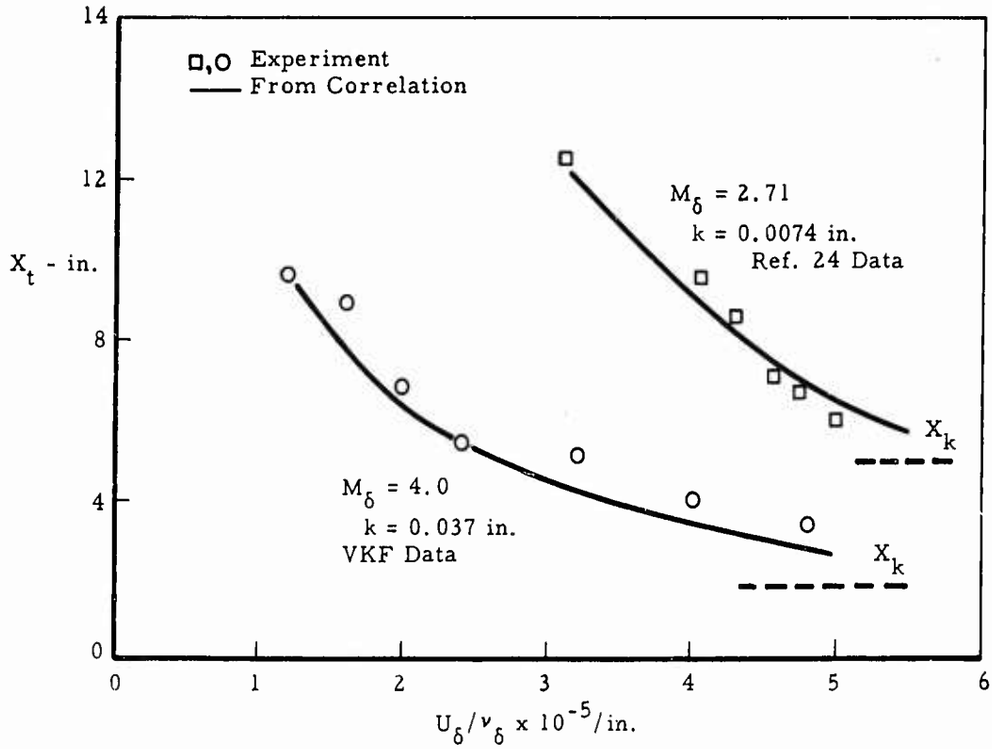

Fig. 41b Application of correlation-spheres on cylinders and cones

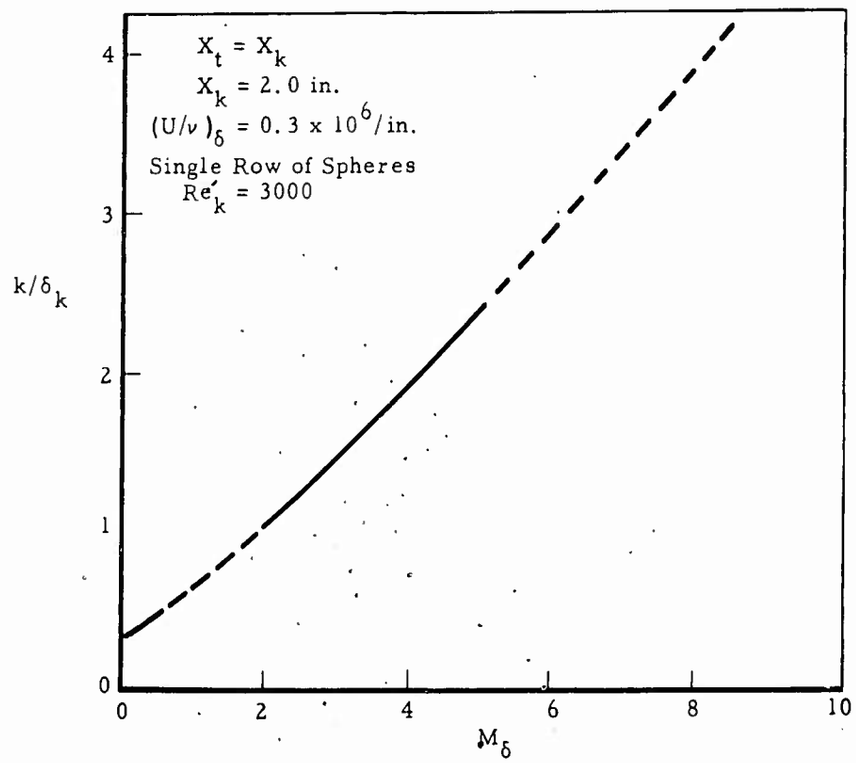

Fig. 42 An illustration of the increase in roughness size required at hypersonic speeds

DISTRIBUTION

Copies of AGARD publications may be obtained in the various countries at the addresses given below.

On peut se procurer des exemplaires des publications de l'AGARD aux adresses suivantes.

BELGIUM BELGIQUE	Centre National d'Etudes et de Recherches Aéronautiques 11, rue d'Egmont Bruxelles.
CANADA	Director of Scientific Information Services, Defence Research Board Department of National Defence 'A' Building Ottawa, Ontario.
DENMARK DANEMARK	Military Research Board Defence Staff Kastellet Copenhagen Ø.
FRANCE	O.N.E.R.A. (Direction) 25, avenue de la Division-Leclerc Châtillon-sous-Bagneux (Seine)
GERMANY ALLEMAGNE	Wissenschaftliche Gesellschaft für Luftfahrt Zentralstelle der Luftfahrtdokumentation Munchen 64, Flughafen Attn: Dr. H.J. Rautenberg
GREECE GRECE	Greek Nat. Def. Gen. Staff B. MEO Athens.
ICELAND ISLANDE	Director of Aviation C/o Flugrad Reykjavik Iceland
ITALY ITALIE	Centro Consultivo Studi e Ricerche Ministero Difesa - Aeronautica Rome.

LUXEMBURG LUXEMBOURG	Luxemburg Delegation to NATO Palais de Chaillot Paris 16.
NETHERLANDS PAYS BAS	Netherlands Delegation to AGARD 10 Kanaalstraat Delft, Holland.
NORWAY NORVEGE	Norway Defence Research Establishment Kjeller, Norway. Attn: Mr. O. Blichner
PORTUGAL	Subsecretariado da Estado da Aeronautica Av. da Liberdade 252 Lisbon. Atten: Lt. Col. Jose Pereira do Nascimento
TURKEY TURQUIE	M.M. Vekaleti Erkaniharbiyei Umumiye Riyaseti Ilmi Istisare Kurulu Mudurlugu Ankara, Turkey Attn: Brigadier General Fuat Ulug
UNITED KINGDOM ROYAUME UNI	Ministry of Aviation TIL, Room 009A First Avenue House High Holborn, London, W.C.1.
UNITED STATES ETATS UNIS	National Aeronautics and Space Administration 1512 H Street, N.W. Washington 25, D.C.

Printed by Technical Editing and Reproduction Ltd
95 Great Portland St. London, W.1.

AGARD Report 284
North Atlantic Treaty Organization, Advisory Group for Aeronautical Research and Development
AN EXPERIMENTAL TECHNIQUE TO MEASURE HEAT TRANSFER FLUXES AT HIGH SPEEDS: TURBULENT HEAT TRANSFER DATA ON A BLUNT BODY AT M = 3.98
L.Broglio and C.Buongiorno
1960
12 pages, incl. 6 refs., 6 figs.

This Report consists of two parts. In the first part is presented a technique for measuring heat transfer rates on a model and for fixing the temperature distribution at a given value. In the second part the technique is applied to the particular case of turbulent heat transfer on a blunt body at a Mach number of 3.98.

This Report is one in the Series 253-284 of papers presented at the Boundary Layer Research Meeting of the AGARD Fluid Dynamics Panel held from 25th to 29th April, 1960, in London, England

533.6.011.6:533.696
3b8b6:3c1a5c2

AGARD Report 284
North Atlantic Treaty Organization, Advisory Group for Aeronautical Research and Development
AN EXPERIMENTAL TECHNIQUE TO MEASURE HEAT TRANSFER FLUXES AT HIGH SPEEDS: TURBULENT HEAT TRANSFER DATA ON A BLUNT BODY AT M = 3.98
L.Broglio and C.Buongiorno
1960
12 pages, incl. 6 refs., 6 figs.

This Report consists of two parts. In the first part is presented a technique for measuring heat transfer rates on a model and for fixing the temperature distribution at a given value. In the second part the technique is applied to the particular case of turbulent heat transfer on a blunt body at a Mach number of 3.98.

This Report is one in the Series 253-284 of papers presented at the Boundary Layer Research Meeting of the AGARD Fluid Dynamics Panel held from 25th to 29th April, 1960, in London, England

533.6.011.6:533.696
3b8b6:3c1a5c2

AGARD Report 284
North Atlantic Treaty Organization, Advisory Group for Aeronautical Research and Development
AN EXPERIMENTAL TECHNIQUE TO MEASURE HEAT TRANSFER FLUXES AT HIGH SPEEDS: TURBULENT HEAT TRANSFER DATA ON A BLUNT BODY AT M = 3.98
L.Broglio and C.Buongiorno
1960
12 pages, incl. 6 refs., 6 figs.

This Report consists of two parts. In the first part is presented a technique for measuring heat transfer rates on a model and for fixing the temperature distribution at a given value. In the second part the technique is applied to the particular case of turbulent heat transfer on a blunt body at a Mach number of 3.98.

This Report is one in the Series 253-284 of papers presented at the Boundary Layer Research Meeting of the AGARD Fluid Dynamics Panel held from 25th to 29th April, 1960, in London, England

533.6.011.6:533.696
3b8b6:3c1a5c2

AGARD Report 284
North Atlantic Treaty Organization, Advisory Group for Aeronautical Research and Development
AN EXPERIMENTAL TECHNIQUE TO MEASURE HEAT TRANSFER FLUXES AT HIGH SPEEDS: TURBULENT HEAT TRANSFER DATA ON A BLUNT BODY AT M = 3.98
L.Broglio and C.Buongiorno
1960
12 pages, incl. 6 refs., 6 figs.

This Report consists of two parts. In the first part is presented a technique for measuring heat transfer rates on a model and for fixing the temperature distribution at a given value. In the second part the technique is applied to the particular case of turbulent heat transfer on a blunt body at a Mach number of 3.98.

This Report is one in the Series 253-284 of papers presented at the Boundary Layer Research Meeting of the AGARD Fluid Dynamics Panel held from 25th to 29th April, 1960, in London, England

533.6.011.6:533.696
3b8b6:3c1a5c2

AGARD Report 284
North Atlantic Treaty Organization, Advisory Group for Aeronautical Research and Development
AN EXPERIMENTAL TECHNIQUE TO MEASURE HEAT TRANSFER FLUXES AT HIGH SPEEDS: TURBULENT HEAT TRANSFER DATA ON A BLUNT BODY AT M = 3.98
L.Broglio and C.Buongiorno
1960
12 pages, incl. 6 refs., 6 figs.

This Report consists of two parts. In the first part is presented a technique for measuring heat transfer rates on a model and for fixing the temperature distribution at a given value. In the second part the technique is applied to the particular case of turbulent heat transfer on a blunt body at a Mach number of 3.98.

This Report is one in the Series 253-284 of papers presented at the Boundary Layer Research Meeting of the AGARD Fluid Dynamics Panel held from 25th to 29th April, 1960, in London, England

533.6.011.6:533.696
3b8b6:3c1a5c2

AGARD Report 284
North Atlantic Treaty Organization, Advisory Group for Aeronautical Research and Development
AN EXPERIMENTAL TECHNIQUE TO MEASURE HEAT TRANSFER FLUXES AT HIGH SPEEDS: TURBULENT HEAT TRANSFER DATA ON A BLUNT BODY AT M = 3.98
L.Broglio and C.Buongiorno
1960
12 pages, incl. 6 refs., 6 figs.

This Report consists of two parts. In the first part is presented a technique for measuring heat transfer rates on a model and for fixing the temperature distribution at a given value. In the second part the technique is applied to the particular case of turbulent heat transfer on a blunt body at a Mach number of 3.98.

This Report is one in the Series 253-284 of papers presented at the Boundary Layer Research Meeting of the AGARD Fluid Dynamics Panel held from 25th to 29th April, 1960, in London, England

533.6.011.6:533.696
3b8b6:3c1a5c2

AGARD Report 284
North Atlantic Treaty Organization, Advisory Group for Aeronautical Research and Development
AN EXPERIMENTAL TECHNIQUE TO MEASURE HEAT TRANSFER FLUXES AT HIGH SPEEDS: TURBULENT HEAT TRANSFER DATA ON A BLUNT BODY AT M = 3.98
L.Broglio and C.Buongiorno
1960
12 pages, incl. 6 refs., 6 figs.

This Report consists of two parts. In the first part is presented a technique for measuring heat transfer rates on a model and for fixing the temperature distribution at a given value. In the second part the technique is applied to the particular case of turbulent heat transfer on a blunt body at a Mach number of 3.98.

This Report is one in the Series 253-284 of papers presented at the Boundary Layer Research Meeting of the AGARD Fluid Dynamics Panel held from 25th to 29th April, 1960, in London, England

533.6.011.6:533.696
3b8b6:3c1a5c2